INL/MIS-21-62601-Revision-0

Release-to-Birth Ratios for AGR-5/6/7 Operating Cycles 162B168A

May 2021

Dawn M Scates

Changing the World's Energy Future

INL is a U.S. Department of Energy National Laboratory operated by Battelle Energy Alliance, LLC

INL/MIS-21-62601-Revision-0

Release-to-Birth Ratios for AGR-5/6/7 Operating Cycles 162B168A

Dawn M Scates

May 2021

Idaho National Laboratory
Idaho Falls, Idaho 83415

http://www.inl.gov

Prepared for the
U.S. Department of Energy
Under DOE Idaho Operations Office
Contract DE-AC07-05ID14517

Release-to-Birth Ratios for AGR-5/6/7 Operating Cycles 162B–168A

1. Effective Date	05/26/2021	**Professional Engineer's Stamp** **N/A** **See LWP-10010 for requirements** **Not Required**
2. Does this ECAR involve a Safety SSC?	No	
3. Safety SSC Determination Document ID	NA	
4. SSC ID	NA	
5. Project No.	23841	
6. Engineering Job (EJ) No.	NA	
7. Building	NA	
8. Site Area	NA	

9. Objective / Purpose

This engineering calculations and analysis report (ECAR) documents the release-to-birth ratios of the Advanced Gas Reactor (AGR) experiment, AGR-5/6/7, which was irradiated in the Advanced Test Reactor (ATR) Northeast Flux Trap from February 16, 2018 to July 22, 2020.

10. If revision, please state the reason and list sections and/or page being affected.

N/A

11. Conclusion / Recommendations

The AGR-5/6/7 experiment was irradiated from February 16, 2018 to July 22, 2020 in the northeast flux trap. All AGR-5/6/7 operating cycle release-to-birth ratios (R/B) and gross gamma (GG) data were reviewed for accuracy and completeness.

For all cycles evaluated in this report, there are no indications that the Fission Product Monitoring System (FPMS) failed to capture data reliably with the exception being at the end of Cycle 166A where experimental conditions involving Capsule1 lead to the total detector saturation for FPMS Station 1. During irradiation and at the end of each cycle, each FPM is put through an "On the Fly" energy calibration and a standard energy calibration test, and all data were reliably verified per test plans mentioned earlier in this document.

This ECAR detailed the calculational method used to determine the R/B for the 12 measured isotopes, Kr-85m, Kr-87, Kr-88, Kr-89, Kr-90, Xe-131m, Xe-133, Xe-135, Xe-135m, Xe-137, Xe-138, and Xe-139 of interest.

During the first five cycles (162B–165A), fission-gas isotope R/B ratios were stable in the 10^{-8}–10^{-6} range and no in-pile particle failures were observed based on the GG counts. During this time, the higher exposed kernel fraction and high-fuel particle temperatures in Capsule 1 led to the maximum R/B value of around 2×10^{-6} for Kr-85m.

The gas line issues in Capsule 1 occurred from the fourth cycle (164B) and were mitigated to minimize crosstalk between capsule gas lines. Capsule 1 fission product release measurements

were not possible during the last three cycles (166B, 167A, and 168A) because of the isolation of Capsule 1. Capsule 1 gas line issues caused fission gas leakage into Capsules 2–5 to various degrees over time starting from Cycle 166A. By the end of Cycle 166A, a significant number of in-pile failures occurred in Capsule 1, causing a substantial increase in fission gas activity and saturation of the FPMS HPGe detector and increased activity in the 1A primary that was picked up by the GG NaI(Tl) detectors . In addition, numerous particle failures were also observed in Capsule 3 and perhaps a few in Capsule 2 during Cycle 168A. No in-pile failures were observed in Capsules 4 and 5 and this is supported by the lack of distinct increases in activity as captured by the GG system. Increased and unstable R/Bs in Capsules 4 and 5 can be attributed to fission gas leakage from Capsule 1. R/Bs for all capsule from mid-cycle of Cycle 166A are considered suspect because of contamination from Capsule 1; however, it can be used as bounding conditions for fuel performance.

CONTENTS

APPENDIXES

ACRONYMS

AGR	Advanced Gas Reactor
ATR	Advanced Test Reactor
ECAR	Engineering Calculations and Analysis Report
EFPD	Effective Full-Power Day
FPM	Fission Product Monitoring
FPMS	Fission Product Monitoring System
GG	Gross Gamma
INL	Idaho National Laboratory
MCWO	Monte Carlo Coupled With ORIGEN
NDMAS	Nuclear Data Management and Analysis System
NEFT	Northeast Flux Trap
PALM	Powered Axial Locator Mechanism
PF	Packing Fraction
PCGAP	Personal Computer Gamma Analysis Package
R/B	Release-to-Birth ratio
SCRAM	Safety Control Rod Axe Man (Reactor Shutdown)
TRISO	TRi-structural ISOtropic
UCO-LEU	Uranium Oxycarbide Low Enriched Uranium

1.0 PROJECT ROLES AND RESPONSIBILITIES

Project Role	Name	Organization	Pages Covered (if applicable)
Performer	D. M. Scates	C620	-----
Checker[a]	M. Plummer	C220	-----
Independent Reviewer[b]	N/A	N/A	N/A
CUI Reviewer[c]	M. E. Davenport	C640	-----
Manager[d]	P. A Demkowicz	C600	-----
Requestor[ef]	M. E. Davenport	C640	-----
Nuclear Safety[f]	N/A	N/A	N/A
Document Owner[f]	P. A. Demkowicz	C600	-----
Reviewer[f]	M. T. Sharp	H330/C020	-----

Responsibilities:

a. Confirmation of completeness, mathematical accuracy, and correctness of data and appropriateness of assumptions.

b. Concurrence of method or approach. See definition, LWP-10106.

c. Concurrence with the document's markings in accordance with LWP-11202.

d. Concurrence of procedure compliance. Concurrence with method/approach and conclusion.

e. Authorizes the commencement of work of the engineering deliverable. See Appendix A.

f. Concurrence with the document's assumptions and input information. See definition of Acceptance, LWP-10200.

2.0 SCOPE AND BRIEF DESCRIPTION

The AGR-5/6/7 test was a fueled multiple-capsule experiment irradiated in the Advanced Test Reactor (ATR) at Idaho National Laboratory (INL) from February 6, 2018 to July 22, 2020. AGR-5/6/7 was the fourth and last experiment in the "AGR experiment" series that was performed and funded by the United States Department of Energy (DOE) as part of the INL Advanced Reactor Technologies (ART) program. This experiment's purpose was to qualify the reference fuel particle design under conditions representative of normal operation in an HTGR and to explore fuel performance at temperatures appreciably higher than expected during HTGR normal operation. This experiment's design was significantly different from the past AGR experiments. An important measure of the fuel performance in these tests is quantifying the fission products released over the duration of the experiment. Larger capsule volumes and an increase in the amount of fuel per capsule impacted how gaseous fission products, such as long- and short-lived isotopes of krypton and xenon, were transported to the Fission Product Monitoring System (FPMS). This affects the released activity calculations that were used in conjunction with birthrates as a metric of fuel performance.

The primary mission for AGR-5/6/7 is to support fuel qualification, accomplish fuel margin testing (i.e., AGR-7), and prove industrial scale fuel fabrication capabilities. AGR-7 (Capsule 3) was designed as a margin test of the uranium oxycarbide (UCO) fuel, and a dominant fuel performance parameter for this test is time at temperature. The primary objective of the AGR-5/6 test (Capsules 1, 2, 4, and 5) was to verify successful performance of the reference-design fuel under normal-operating conditions. AGR-5/6/7 was irradiated in the northeast flux trap (NEFT) position (Figure 1) in the ATR.

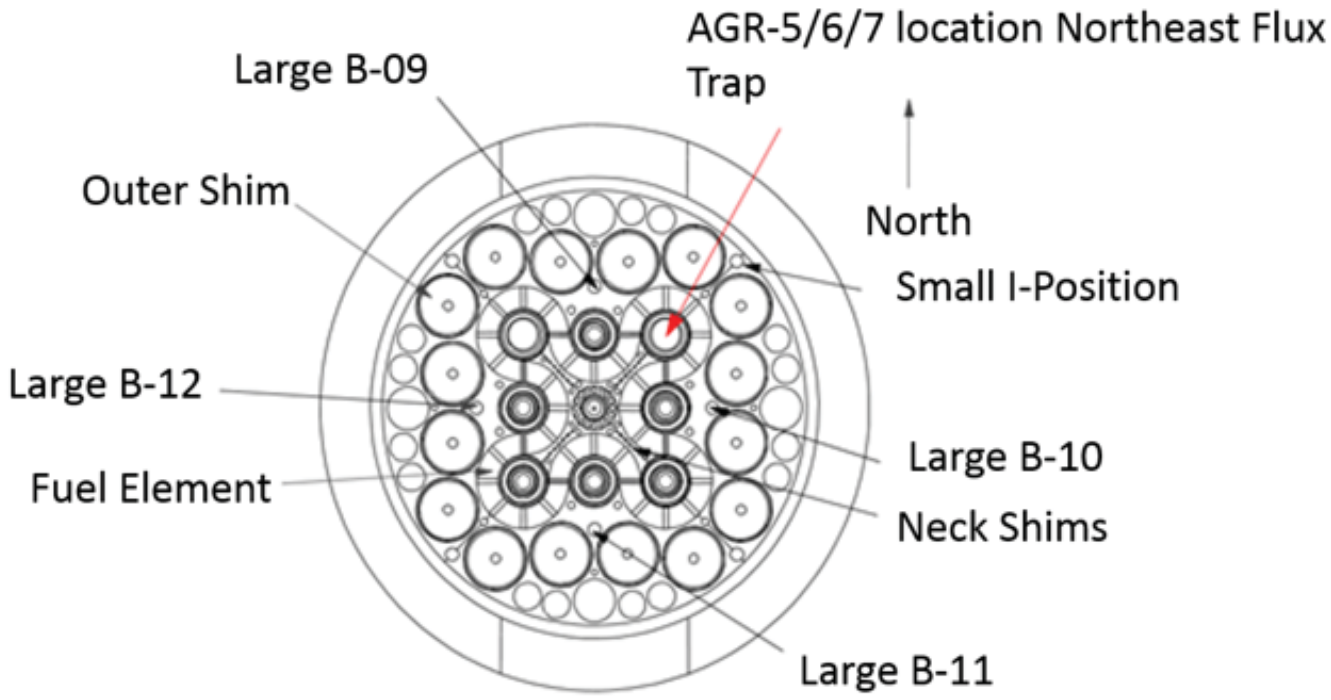

Figure 1. ATR core cross-section showing the AGR fuel irradiation locations [1].

The AGR-5/6/7 fuel was comprised of tri-structural isotropic (TRISO)-particle fuel in the form of cylindrical compacts that were nominally 25.0 mm in length and 12.3 mm in diameter. A total of 194 compacts were distributed within five capsules that each contained 35.7 grams U-235 and 230.3 grams total uranium content [1]. The compacts had nominal packing fractions (PF) of 25% in the inner capsules near the core center and 40% in the outer capsules at the core ends. The particles are Uranium Oxycarbide Low Enriched Uranium (UCO-LEU) fuel kernels with an enrichment level of 15.5 wt%. Individual fuel particles are comprised of fuel kernels that are covered with a layer of silicon carbide encased between two pyrolytic carbon layers to make up the TRISO-coated fuel particles. The fuel particles are over-coated with a mixture of graphite powder and thermo-set resin that are pressed into fuel compacts which are then sintered to remove the volatile compounds from the resin.

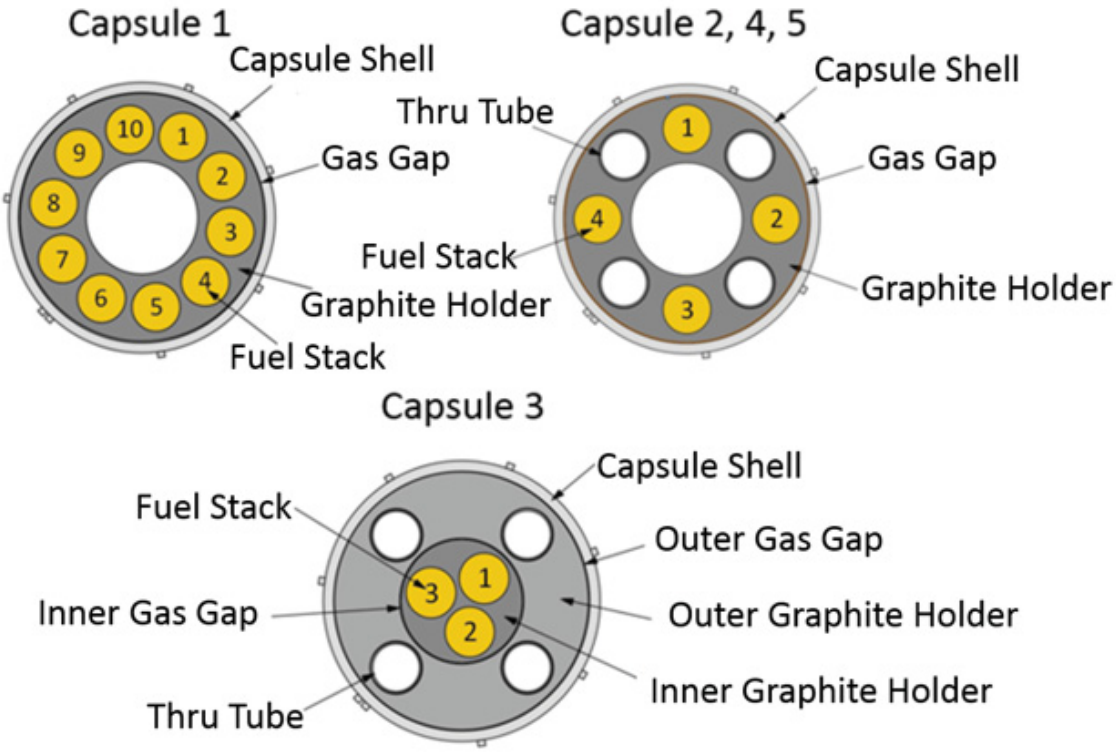

Figure 2. AGR-5/6/7 capsule cross-section for Capsules 1–5 [1].

Capsule 1 (bottom capsule in the test train) contained ten fuel stacks (90 compacts), a hollow center to reduce total energy deposition, and is nine inches long. Because of its position at the bottom of the capsule test train, Capsule 1 did not contain through-tubes, which allow gas lines and instrumentation from the lower capsules to be passed up and out of the test train. With no through-tubes, there was more room for fuel stacks, so; Capsule 1 contained the most fuel (60%) of the AGR-5/6 Capsules. By design, it was also maintained at the highest temperature [1].

Capsules 2, 4, and 5 had four fuel stacks each and contained hollow centers like Capsule 1 (see Figure 2). Capsule 2 contained 32 compacts and was eight inches in length; Capsules 4 and 5 contained 24 compacts each and were six inches in length. Capsule 3 is the AGR-7 margin test and contained three fuel stacks consisting of 24 compacts and was 8 inches in length. Capsule 3 contained a unique design feature in that the graphite holder was separated into two pieces, allowing the center mass to run hot while keeping the through-tubes relatively cool.

Each capsule has independent gas lines to route a helium/neon gas mixture to the capsule. This allows temperature control during irradiation by adjustment of the He/Ne mixture transports any released fission products to the corresponding FPMS. The FPMS is comprised of an HPGe detector for isotopic quantification and a NaI(Tl) gross gamma (GG) detector for instantaneous fuel performance information (see Figure 3).The GG detector is tuned to view the entire energy regime that is present for the HPGe spectrometer system, thus acting as an instantaneous count rate meter. If release rates from individual isotopes were to increase, this would be reflected in the GG data stream as either a gradual increase in count rate or a rapid increase in count rate (i.e., a spike”), where the count rate would decrease back towards baseline yet remain slightly elevated once the event has come to an equilibrium state. This event is usually indicative of a fuel failure or some other unknown phenomena occurring within the capsule [2]. It is important to state that accurate particle failure detection can be difficult to determine when multiple failures happen at once in a capsule and during a possible fission gas leakage into other capsules; therefore, the GG system is only used to find evidence on whether failures or other events occurred and will not be used to determine the number of failures. The data from the GG system are constantly paired to the HPGe as an independent crosscheck of fuel performance.

Figure 3. The FPMS in ATR-670, 1A primary. Each of the five AGR-5/6/7 Capsules has a corresponding FPMS. This system also contained two on-line spares.

The FPMS continuously measures the gamma activity of the sweep gas from each of the five capsules to provide an indicator of fuel irradiation performance. Spectrometer detector systems measure the concentrations of various krypton and xenon isotopes in the sweep gas from each capsule. Eight-hour counting intervals are used to measure the concentrations of Kr-85m, Kr-87, Kr-88, Kr-89, Kr-90, Xe-131m, Xe-133, Xe-135, Xe-135m, Xe-137, Xe-138, and Xe-139 [1]. These concentrations, along with gas flow data, are used to determine release rates. The release rates are paired with calculated birthrates to obtain the release-to-birth ratio (R/B) values, which are used as indicators of initial fuel quality and fuel performance during irradiation.

The release activities must be measured, and the release rates derived and paired with calculated birthrates to establish the initial fuel quality and fuel performance.

The FPMS post-processing program, FP_PostProc, is used to calculate the R/B values, interpolating birthrates between the provided values to obtain estimates at the times corresponding to spectra for which the reactor is at full power. It also averages the provided flows during the spectra, ignoring any incidental zero-flow values. The intent of this engineering calculations and analysis report (ECAR) is to present the R/B values, an estimated fuel failure count number, and a cycle-by-cycle GG representation for AGR-5/6/7operating Cycles 162B–168A.

3.0 DESIGN OR TECHNICAL PARAMETER INPUT AND SOURCES

N/A

4.0 RESULTS OF LITERATURE SEARCHES AND OTHER BACKGROUND DATA

N/A

5.0 ASSUMPTIONS

1. The FPMS must be operational.
2. Summary files from the FPMS must be available.
3. Comma delimitated text files need to be generated from FP_Examiner for use in FP_PostProc.
4. Flow data from the ATR-AGR experiment for the entire operating cycle must be supplied.
5. As-run birthrate input files must be provided.

6.0 COMPUTER CODE VALIDATION

A. Computer type, Operating System and Version: The FP_PostProc processing software runs on a Dell OptiPlex 7010/I73770, 32-bit PC running Microsoft Windows 7 Enterprise Service Pack 1.

B. Computer program name and revision: The birth ratio processing code name is FP_PostProc Version 04/11/2018.

C. Inputs: AGR outlet flow data is generated from the Nuclear Data Management and Analysis System (NDMAS) database. As-run birthrate input files are provided by ART physics staff, and activities are computed from the FPMS software.

D. Outputs (may refer to an appendix): All FPMS input and output data files are sent to the NDMAS server and are part of the program record.

E. Evidence of or reference to computer program validation: PLN-3551, Rev.2 “Fission Product Monitoring System Operability Test Plan for the AGR Experiment Series.”

F. Bases supporting application of the computer program to the specific physical problem: N/A.

7.0 DISCUSSION/ANALYSIS

7.1 Birthrate Computation

The AGR-5/6/7 test train was in the NEFT of the ATR core, and the test train consisted of five test capsules stacked vertically, one atop of the other. The five test capsules were situated axially within the ATR active core. Capsule 5 was located at the top of the test train capsule stack and consisted of a graphite annulus holder that held four vertical stacks of compacts and four vertical channels for through-tubes, all on a common radius from the capsule center. The four through-tubes contained gas lines and thermocouples. Each compact stack had six vertically stacked compacts for a total of 24 compacts in this capsule. Capsule 5 compacts had a particle packing fraction (PF) of approximately 38%. The compacts were held in place by graphite holders with drilled channels to accommodate the compacts. Surrounding the graphite holder was a helium-neon gas gap for capsule temperature control, and beyond the gas gap was a stainless-steel capsule wall or pressure containment boundary. Outside the capsule wall was the ATR coolant and then a neutron filter.

Capsule 4 is basically the same as Capsule 5, except Capsule 4 had a particle PF of approximately 25%. The lower PF was needed to reduce compact fission rates for temperature control.

Capsule 3 had a cylindrical solid inner graphite rod surrounded by an outer graphite annulus. Capsule 3 contained a total of 24 compacts and had a PF of approximately 25%. As stated earlier, Capsule 3 was designed as a margin test of the UCO fuel and contained a unique design feature in that the graphite holder was separated into two pieces, allowing the center mass to run hot while keeping the through-tubes relatively cool.

Capsule 2 was similar to Capsules 4 and 5, except each compact stack had eight vertically stacked compacts (i.e., eight levels), instead of six, for a total of 32 compacts in this capsule and, like Capsule 4 and 5, Capsule 2 had a PF of approximately 25%.

Capsule 1 was unique relative to the other capsules, but had one characteristic in common with Capsules 2, 4, and 5. All four of these capsules had an annular graphite holder with a central hole filled with helium-neon gas, which is the same gas composition as in the gas gap between the outside of the graphite holder and the capsule wall. Capsule 1 contained 90 compacts in this capsule and had a PF of approximately 38%. There were no thru-tube holes in the graphite holder.

The AGR-5/6/7 experiment was irradiated over nine ATR power cycles. Table 1 presents the as-run AGR-5/6/7 irradiation schedule. Six of the nine cycles were regular cycles, and the other three were powered axial locator mechanism (PALM) cycles. The table data includes the number of irradiation cycles, ATR identification cycle number, type of cycle (regular or PALM), and the cycle length (effective full-power days, EFPD), the number of birthrate time steps, the birthrate date range and the date that the birthrates were received by the FPMS team.

Table 1. AGR-5/6/7 as-run irradiation and birthrate submittal schedule.

Cycle Number	ATR Cycle	ATR Cycle Type	Cycle Length (EFPD)	Number of Birthrate Time Steps	Birthrate Date Range	Date Received via e-mail
1	162B	Regular	38.83	42	2/16/18–3/29/18	June 7, 2018
2	163A	PALM	8.49	10	4/29/18–5/8/18	July 13, 2018
3	164A	Regular	55.61	61	6/10/18–8/17/18	October 23, 2018
4	164B	Regular	64.29	69	9/18/18–1/17/19	February 25, 2019
5	165A	PALM	13.82	17	2/28/19–6/18/19	August 29, 2019
6	166A	Regular	62.41	66	7/25/19–10/6/19	October 28, 2019
7	166B	Regular	61.2	63	11/9/19–01/10/20	February 24, 2020
8	167A	PALM	9.8	12	2/27/20–3/4/20	April 13, 2020
9	168A	Regular	61.22	68	4/13/20–7/22/20	August 31, 2020

For the physics calculations of the birthrates, the high-resolution calculations that estimated birthrates were computed daily. ATR cycle lengths during AGR-5/6/7 ranged from approximately 8–65 days. Daily isotopic birthrates are computed using the JMOCUP ORIGEN2.2 [3] code system which is similar to Monte Carlo Coupled With ORIGEN (MCWO) but fully automated.

By definition, birthrate is the rate of production for a specific isotope. Birthrate is different than isotopic inventory in that the production of an atom is considered a birth, even if it is immediately lost to transmutation or decay. To calculate birthrates using ORIGEN2.2, the depletion of isotopes through transmutation and decay needs to be turned off. This was accomplished by creating modified decay and activation libraries for each isotope of interest. In addition, in the isotope-specific decay libraries, the half-life of the isotope was set to zero to have ORIGEN2.2 treat the isotope as a stable isotope, turning off the decay for the isotope. In the isotope-specific activation library, the absorption cross sections were set to zero to turn off transmutation for the isotope. With decay and transmutation turned off for the specific isotope, the change in inventory for the isotope divided by the irradiation time resulted in the birthrate [4]

7.2 Release Activity Computation

The performance of nuclear fuel is typically evaluated using R/Bs—the ratio of the released activity (R) of an isotope from the fuel to the predicted birthrate of the isotope because of irradiation conditions (birth activity [B]). The gamma-ray spectrum measurements from the high-purity germanium detectors in each FPMS were used to measure the activity at the detector and then compute the release activities of several different isotopes of krypton and xenon (Table 2). The acquired spectra were automatically analyzed using the INL-developed Personal Computer Gamma Analysis Package (PCGAP) gamma-ray spectral analysis code [5,6] and were stored electronically. At the end of each irradiation cycle, the

FPMS-measured activities were corrected to account for decay that occurred during transport from the capsules to the detectors. Transport times were calculated from outlet gas flow rates recorded by the automated experiment data control system of ATR and the capsule-specific volumes through which samples flow to reach the respective monitoring stations. In the AGR-1 and AGR-2 experiments the transport volume from the outlet of the capsule to the respective FPMS were determined using standard leadout flow/transport testing Ne-23 protocols. For AGR-3/4 the leadout flow/transport testing Ne-23 protocols were augmented with the remaining fission gas isotopes to determine the transport volumes. It is believed the increased capsule volumes in AGR-3/4 were the primary reason the remaining fission gas isotopes were necessary in the transport volume calculations. For AGR-5/6/7 the capsule volumes became even larger. The increase capsule volumes cloud the transport volume calculations in multiple ways, including unknown gas flow patterns through the capsule voids and diffusion through the large graphite samples. The methodology for this computation can be found in Appendix A and the transport volume fit parameters can be found in Appendix B.

Table 2. Isotopes of interest for R/B calculations.

Isotope		
Kr-85m	Xe-131m	Xe-135m
Kr-87	Xe-133	Xe-137
Kr-88	Xe-135	Xe-138
Kr-89	—	Xe-139
Kr-90	—	—

Release activities were measured with the FPMS, and fission product birthrates were estimated using MCWO. The activities measured from the spectra collected by the FPMS, adjusted if necessary by the “OnTheFly” program [7], and corrected for decay during transport were converted to released atoms per second at the capsule. The proper correction for the measured activity is calculated for equilibrium conditions for the different components illustrated in the simplified flow system in Figure 4.

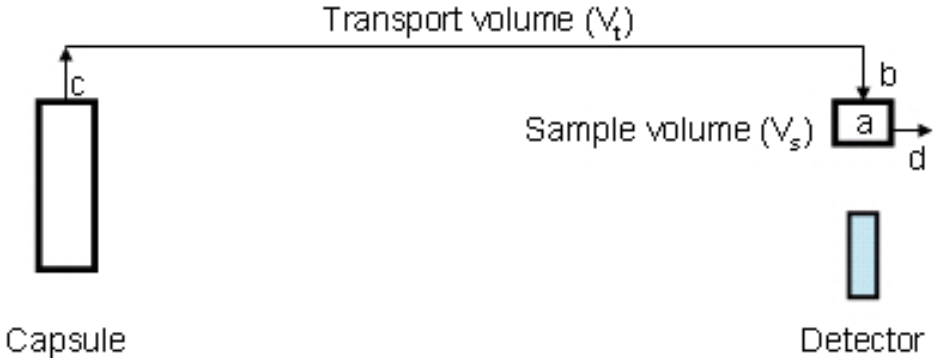

Figure 4. A simplified single capsule flow graphic to aid in flow correction calculations.

At equilibrium, when the rate of change of the number of atoms of an isotope of interest in the sample volume, 'a,' is zero, one can derive:

$$R_c = \frac{A_a \cdot e^{\frac{\lambda \cdot V_t}{f}}}{1 - e^{\frac{-\lambda \cdot V_S}{f}}} \quad (1)$$

where:

R_c = Release rate (atom/sec) of isotope at the capsule exit (c)

A_a = Activity (Bq) of isotope in sample volume a, measured with FPMS detectors

λ = Decay constant of isotope (sec^{-1})

V_T = Transport volume (mL) between (c) and (b)

V_s = Sample volume (mL) (a)

f = Capsule-specific flow (mL/sec).

The flow rate is taken as the average of all values with times during the spectrum acquisition. The activities (*A*) provided by the INL-developed PCGAP analysis are corrected for random summing and detector efficiency. The relationship between A_a, the activity of the isotope in the sample volume (Bq/sample), and A_v, the activity of the isotope entering the sample volume per Bq/cc, can be found in Appendix C. The first exponential involving the transport volume (V_t) accounts for decay before reaching the sample volume, while the remaining factor (V_s) accounts for the decay while passing through the sample volume. This equation is valid if the isotope involved remains entrained in the effluent gas and travels through the gas lines and sample volume at the flow rate, and the flow rate is fairly constant. Any isotope trapped prior to exiting the sample volume or large variations in the flow rate during acquisition would compromise the calculation.

The estimated uncertainty in R_c can be determined from standard error propagation techniques to be:

$$\sigma_{R_c}^2 = \left[\left(\frac{R_c}{A_a}\right)^2 \cdot \sigma_{A_a}^2\right] + \left[\left(\frac{R_c \cdot \lambda}{f}\right)^2 \cdot \sigma_{V_t}^2\right] + \left[\left(\frac{R_C \cdot \lambda \cdot e^{\frac{-\lambda \cdot V_S}{f}}}{f \cdot \left(1 - e^{\frac{-\lambda \cdot V_S}{f}}\right)}\right)^2 \cdot \sigma_{V_S}^2\right] \quad (2)$$

or in terms of relative errors:

$$\left(\frac{\sigma_{R_C}}{R_C}\right)^2 = \left[\left(\frac{\sigma_{A_a}}{A_a}\right)^2\right] + \left[\left(\frac{V_t \cdot \lambda}{f}\right)^2 \cdot \left(\frac{\sigma_{V_t}}{V_t}\right)^2\right] + \left[\left(\frac{V_S \cdot \lambda \cdot e^{\frac{-\lambda \cdot V_S}{f}}}{f \cdot \left(1 - e^{\frac{-\lambda \cdot V_S}{f}}\right)}\right)^2 \cdot \left(\frac{\sigma_{V_S}}{V_S}\right)^2\right] \quad (3)$$

To speed up the calculation of these ratios and to ensure accuracy, a semiautomatic processing code called FP_PostProc was developed. This program accesses the summary file of each spectral analysis to extract the required results for activity at the detector at a given time.

7.3 FP_PostProc Program

The FP_PostProc Program was developed to compute R/B ratios for selected isotopes. As input, the software loads the capsule summary file generated by FP Examiner, capsule-specific flow information, and birthrate information. The isotope activities and effluent flow rate are used to compute the release rate from the fuel compacts, corrected for decay during transport to the spectrometer sample volume and accounting for effluent residence time in the sample volume. This calculation assumes a steady-state condition that is valid if the reactor is stable and none of the fuel particles have recently failed. For this ECAR, the reactor average daily and four-point birthrates were provided. The FP PostProc analysis interpolates between the four-point times, or between the mid-day times, to obtain birthrate values for each of the spectrum times, using these to compute a R/B ratio for each nuclide for all spectra.

The relationship between the capsule release rate and the activity in the detector sample volume was determined during a leadout flow experiment and during normal run spectra from cycles 164A and 164B. These transport volumes are listed in Table 3.

Table 3. AGR-5/6/7 transport volumes determined using data obtained during a leadout flow experiment performed at the beginning of 2018 and from cycle 164A and 164B experimental data for the AGR-5/6/7 experiment.

AGR-5/6/7 Transport Volumes (CC)	
Capsule 1	240 ± 13
Capsule 2	282 ± 13
Capsule 3	317 ± 07
Capsule 4	293 ± 04
Capsule 5	282 ± 23

To couple the birthrate data with the FP_PostProc software, the birthrate values for a capsule represent a volume integral over all the compacts within the capsule and are presented in units of atoms/sec. The birthrate file lists values for each of the six capsules at a set number of times distributed over the irradiation cycle. The FP_PostProc software interpolates between these points to obtain estimates at the times corresponding to spectra for which the reactor is at full power.

The desired R/B ratio for the desired isotope is then calculated as:

$$\frac{R}{B}(t) = \frac{R_c(t)}{B(t)} \tag{4}$$

with a percent uncertainty (%σ) given by:

$$\%\sigma = \sqrt{\left(\frac{\sigma_{R_C}}{R_C}\right)^2 + \left(\frac{\sigma_B}{B}\right)^2} \cdot 100 \quad (5)$$

The activities in the summary file are in units of microcuries in the sample volume, which can be converted to decays-per-second in the sample volume by multiplying by 3.7×10^4. Once the FP_PostProc Program has loaded the activity summary file and the capsule-specific flow information, the release rates are calculated as:

$$R = 3.17\ x\ 10^4 \frac{A \cdot e^{\frac{\lambda \cdot V_t}{f}}}{1 - e^{\frac{-\lambda \cdot V_S}{f}}} \quad (6)$$

where:

A = the activity in microcuries in the sample volume V_S

λ = the nuclide decay constant

f = the capsule outlet flow rate

V_T = the transport volume from the capsule to the sample volume and where the volumes, decay constants, and flow rates are in consistent units.

As described above, the flow rate is the average of all values with times during the spectrum acquisition. The activities (A) provided by the standard PCGAP analysis are corrected for random summing and detector efficiency. The first exponential involving the transport volume (V_T) accounts for the decay before reaching the sample volume, while the remaining factor (V_S) accounts for the decay while passing through the sample volume. This equation is valid if the isotope involved remains entrained in the effluent gas, travels through the gas lines and sample volume at the flow rate, and the flow rate is fairly constant. Any trapping of the isotope prior to exiting the sample volume or large variations in the flow rate during acquisition would invalidate this calculation.

The birthrate data file is provided by reactor physics personnel. The analysis methodology MCWO is used to calculate the birthrates of the 12 fission product isotopes listed in Table 2 for each capsule. The values for a capsule represent a volume integral over all the compacts within the capsule and are presented as atoms/sec. The birthrate file lists values for each of the six capsules at a set number of times distributed over the irradiation cycle. The FP_PostProc software interpolates between these points to obtain estimates at the times corresponding to spectra when the reactor is at full power. An example of a daily birthrate file can be found in Appendix D.

To identify spectra times when the reactor is at full power, the list of dates at the start of the file includes the reactor startup times in addition to the full power and reactor shutdown (scram) times. The FP_PostProc Program uses decay constants from the constants.txt text file (Appendix F). It requires the user to specify a transport volume text file because these are different for the various in-pile experiments such as AGR-5/6/7 and are used to calculate release rates for the 12 isotopes listed in Table 2.

When the release activity has been computed, the software uses the average birthrate of each isotope within the capsule in atoms/sec to compute and generate an interpolated R/B output file. Example outputs for the release activity and R/B ratio files can be found in the Appendix E. These .txt files are easily imported into Excel and/or other data management systems and can be further processed at the request of AGR project management. Prior to generation of R/B ratio files, all operational buttons in the FP_PostProc software must be functional. If a feature is not operational, an error will display. If just the birthrate file is omitted, this version still computes release rates.

At the end of every irradiation cycle, the AGR-5/6/7 project staff reports the R/B values for the radioactive fission gases listed in Table 2 and all test parameters relating to the FPMS are captured in registered laboratory notebooks [8].

7.4 Experiment Performance

The R/B results reported in this transmittal are computed as the measured release activity at the associated FPMS detector corrected for decay during transport using the average flow rate over the spectral acquisition period and the previously determined transport volumes, divided by the provided/interpolated birthrate over the same period. FP_PostProc Version 04/11/18 was used to process these data over the course of the 2-year experiment. AGR-5/6/7 reactor physics personnel provided as-run fission product birthrates for Kr-85m, Kr-87, Kr-88, Kr-89, and Kr-90 and Xe-131m, Xe-133, Xe-135, Xe-135m, Xe-137, Xe-138, and Xe-139. These isotopes are useful because the half-life for each isotope is short enough to enable the inventory to reach equilibrium within the fuel. A summary of the measured R/B and their uncertainty statistics for the krypton and xenon isotopes of interest is captured in the conclusion section of this document. During the first five cycles (i.e., 162B-165A), fission-gas isotope R/B ratios were stable in the 10^{-8}–10^{-6} range and no in-pile particle failures were observed based on the GG counts. During this time, the higher exposed kernel fraction and high-fuel particle temperatures in Capsule 1 led to the maximum R/B value of around 2×10^{-6} for Kr-85m.

Helium/neon gas flows recorded during Cycle 166A and forward may not adequately represent the gas flow mixture through the associated capsule due to Capsule 1's outlet line clogs and breaks leading to contamination of the gas in the leadout and fission gas in leakage into Capsules 2–5 [1]. Therefore, the reported values from the FPMs will serve as trending/bounding information and not as quantifiable capsule isotopic data. A comprehensive summary table of the measured R/B and their uncertainty statistics for the krypton and xenon isotopes of interest for cycles 162B through 168A can be found in Appendix H.

7.5 Cycle 162B

Leadout flow testing for AGR-5/6/7 began on February 16–26, 2018. The purpose of a leadout flow test is to determine the minimum leadout flow required to prevent capsule crosstalk. This process is performed at the beginning of each new AGR experiment. Through this testing, it was determined that the initial leadout flow for the AGR-5/6/7 experiment would be set to 10 sccm helium to prevent capsule crosstalk. After leadout flow testing was completed, the neon transport measurements were executed. This test helps the fission product monitor team determine gas transport through the experiment and to determine the AGR-5/6/7 transport volumes used in computing the release activity [1]. Once preliminary

testing was completed, the experiment was brought to temperature on February 27, 2018 (see Figures Figure 5–8). Note that for the leadout flow testing experiment, the FPMS run times were set to 20 minutes, a routine FPMS measurement is set to a runtime of 8 hours. The R/B values are stable in all capsules throughout Cycle 162B and correspond well to changes in fuel temperatures. The R/B values on average for krypton are on the order of 1E-06 and 1E-07 for xenon, and the northeast lobe power was at 14 MW for 14 days and 15 MW for 25 days. The isotopes presented in Figure 5–7 have moderate half-lives that are sufficiently short to enable to each isotope to reach equilibrium in the capsule yet long enough to provide measurable and quantifiable signals at the FPMS detectors. For releases of isotopes that have short half-lives such as Kr-90 (32.3 s) and Xe-139 (39.7 s) or long half-lives such as Xe-131m (11.9 days), the uncertainty of the values is usually greater than 30%. The reason for the high uncertainty for the short/long-lived isotopes is that there is either insufficient flow to carry the fission gas to the FPMS or not enough of the isotope present for sufficient detectability. Isotopes Xe-131m and Xe-139 in Figure 6capture this detail as is illustrated by the sporadic data points and by review of the spectra for the given time period. The GG data presented in Figure 8 also nicely details the gas changes to each capsule during the leadout flow experiment from February 16–26, 2018 and then independently reflects the stable isotopic release rate shown in Figures Figure 5–7.

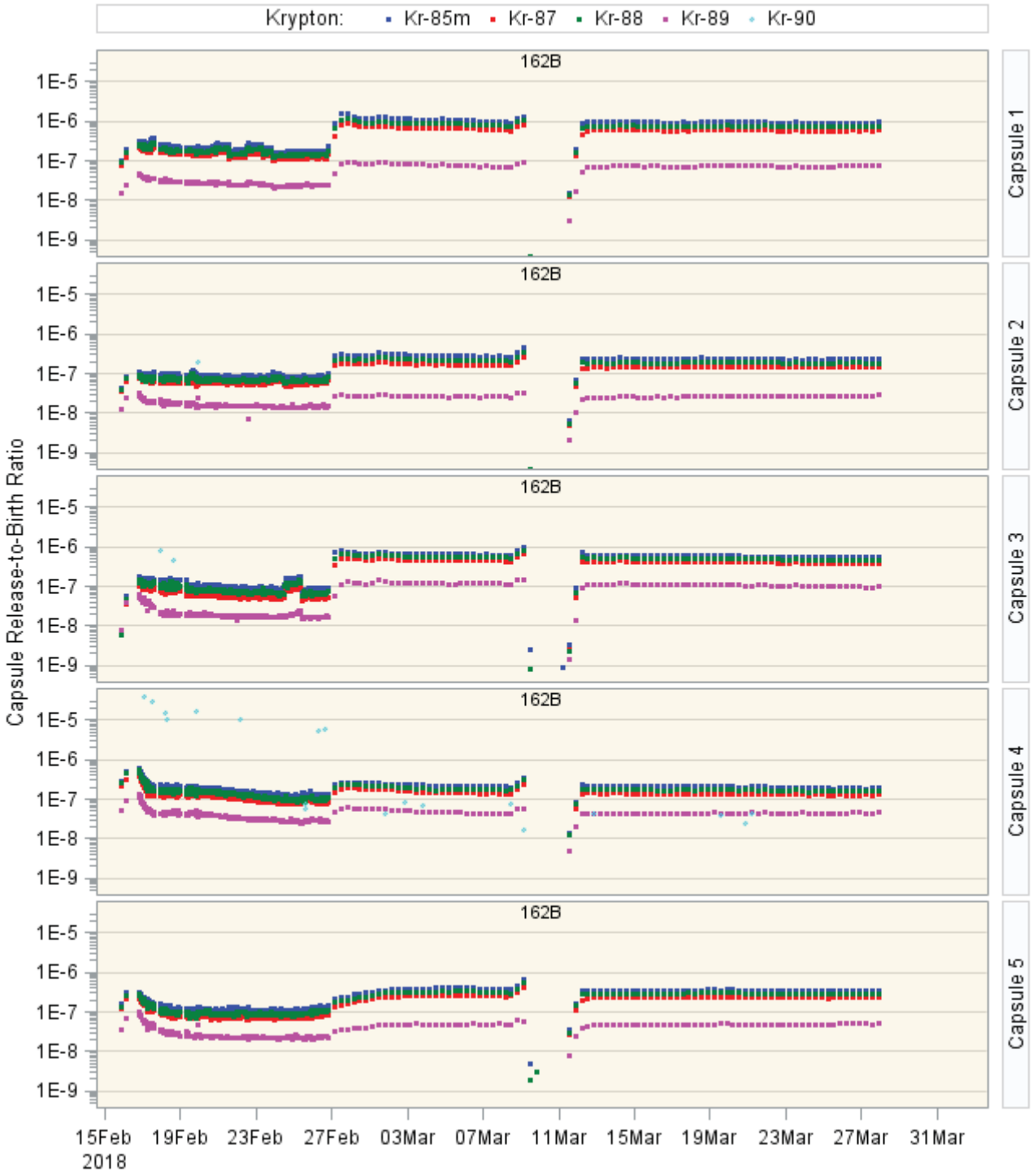

Figure 5. Cycle 162B release-to-birth ratios for selected krypton isotopes for AGR-5/6/7 Capsules 1–5.

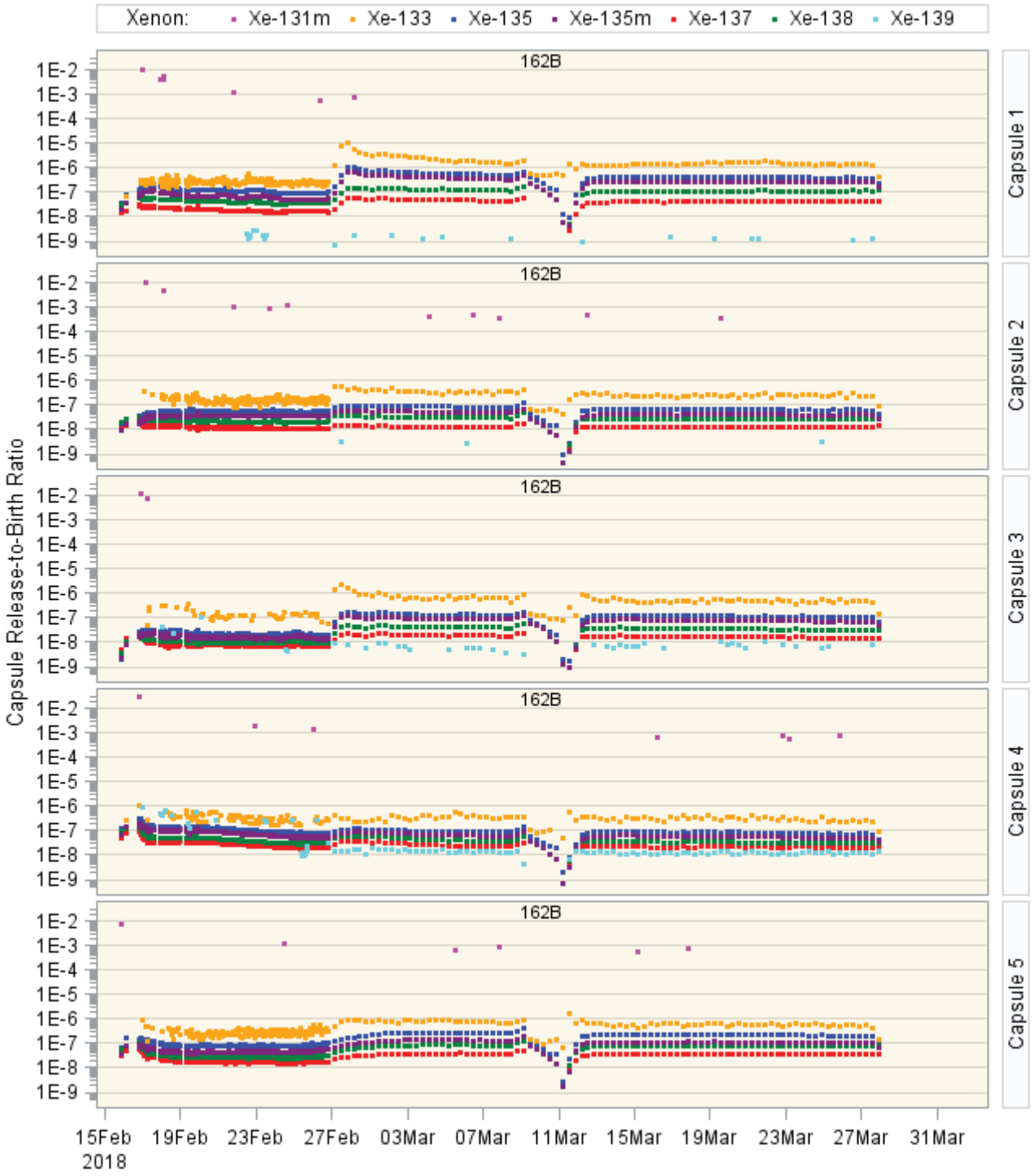

Figure 6. Cycle 162B release-to-birth ratios for selected xenon isotopes for AGR-5/6/7 Capsules 1–5.

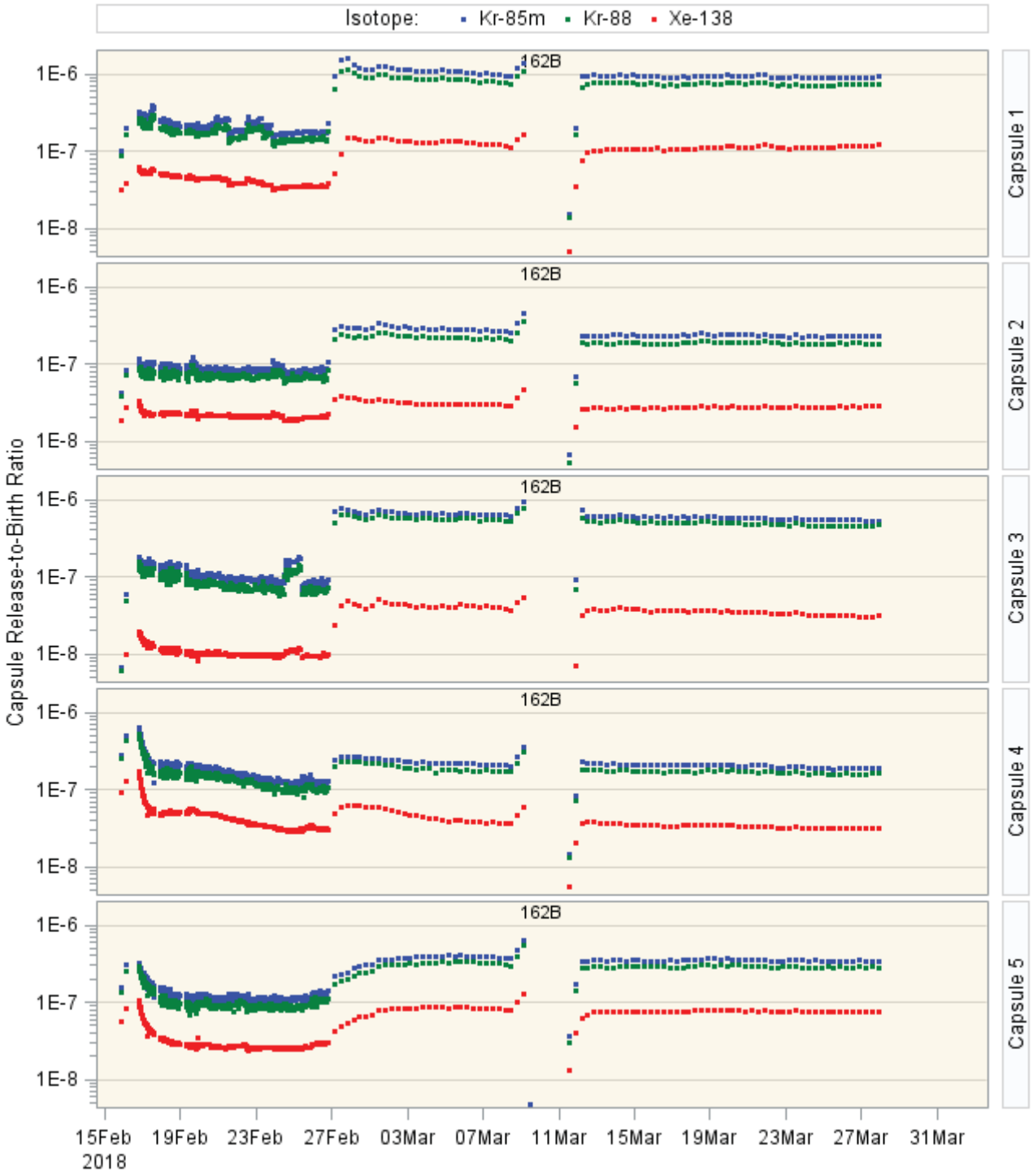

Figure 7. Cycle 162B release-to-birth ratios for selected krypton and xenon isotopes for AGR-5/6/7 Capsules 1–5 where equilibrium is believed to have been reached within the capsule based on half-life.

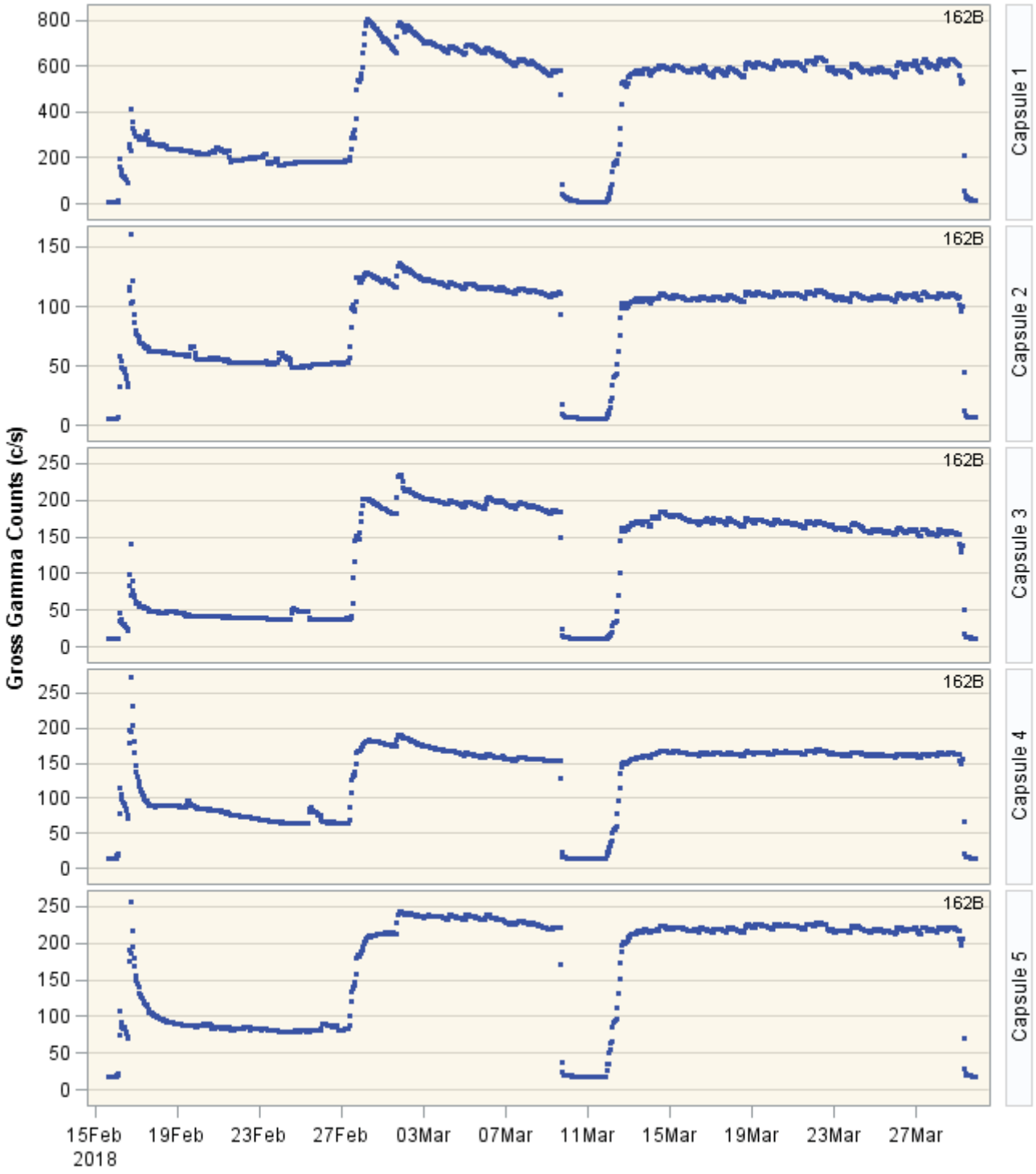

Figure 8. Cycle 162B GG release rate data AGR-5/6/7 Capsules 1–5.

7.6 Cycle 163A

Irradiation for Cycle 163B began on April 29, 2018 and ran through May 8, 2018. This 9-day cycle was irradiated at mostly at 5 MW with an increase during the end of the irradiation cycle to 20 MW, captured in Figures Figure 9–12. The R/B values on average is 1E-07 for krypton and 1E-08 for xenon because of low-neutron rate for this cycle [9]. Figure 12shows the corresponding GG data for Capsules 1–5 where the counts per second are comparatively low and, in some instances, barely higher than cubicle background. The increase from 5 MW to 20 MW is drastically captured in Figure 12, where the spare GG detectors show an increase in the room count rate of 10–20 counts per second.

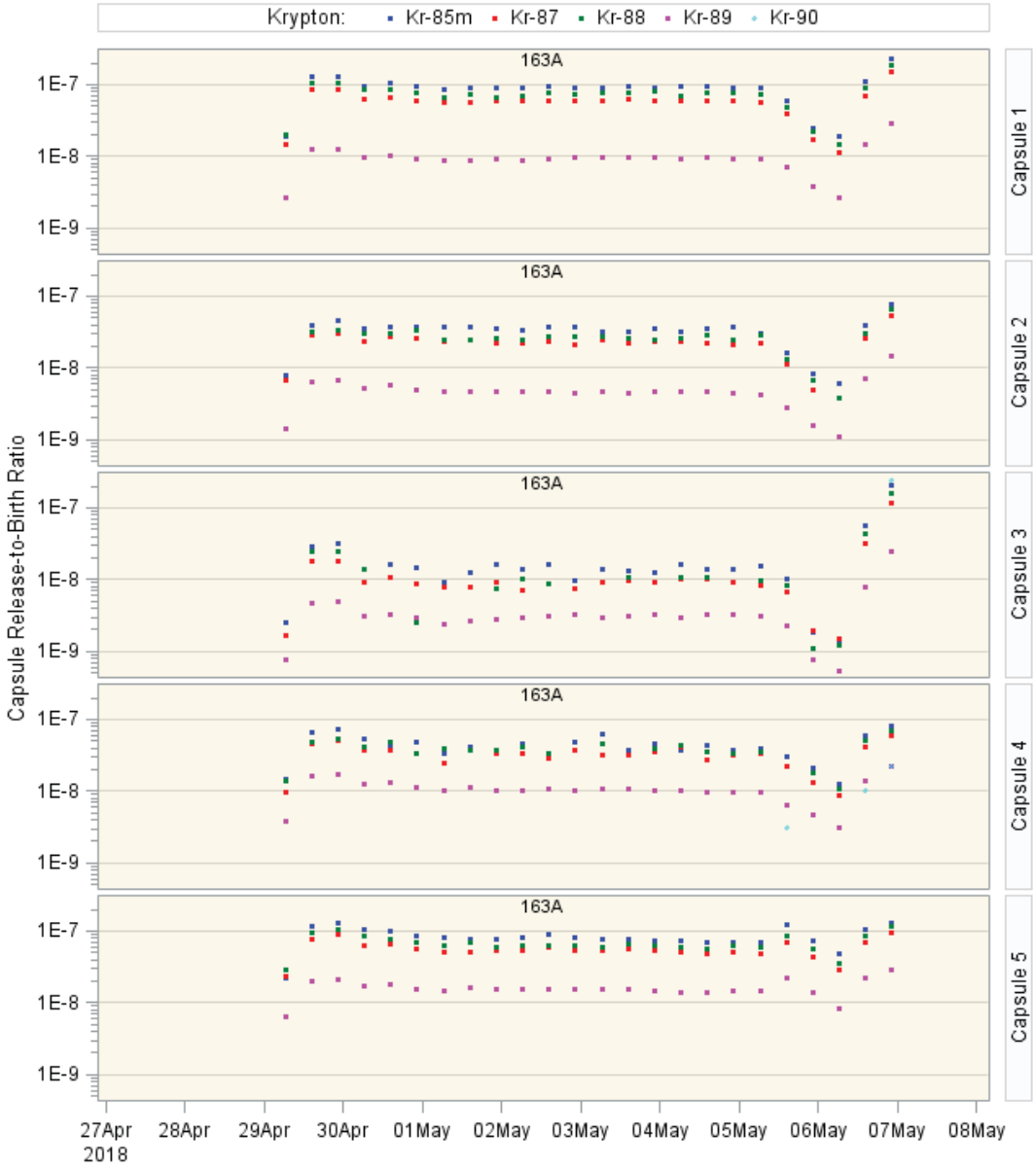

Figure 9. Cycle 163A release-to-birth ratios for selected krypton isotopes for AGR-5/6/7 Capsules 1–5.

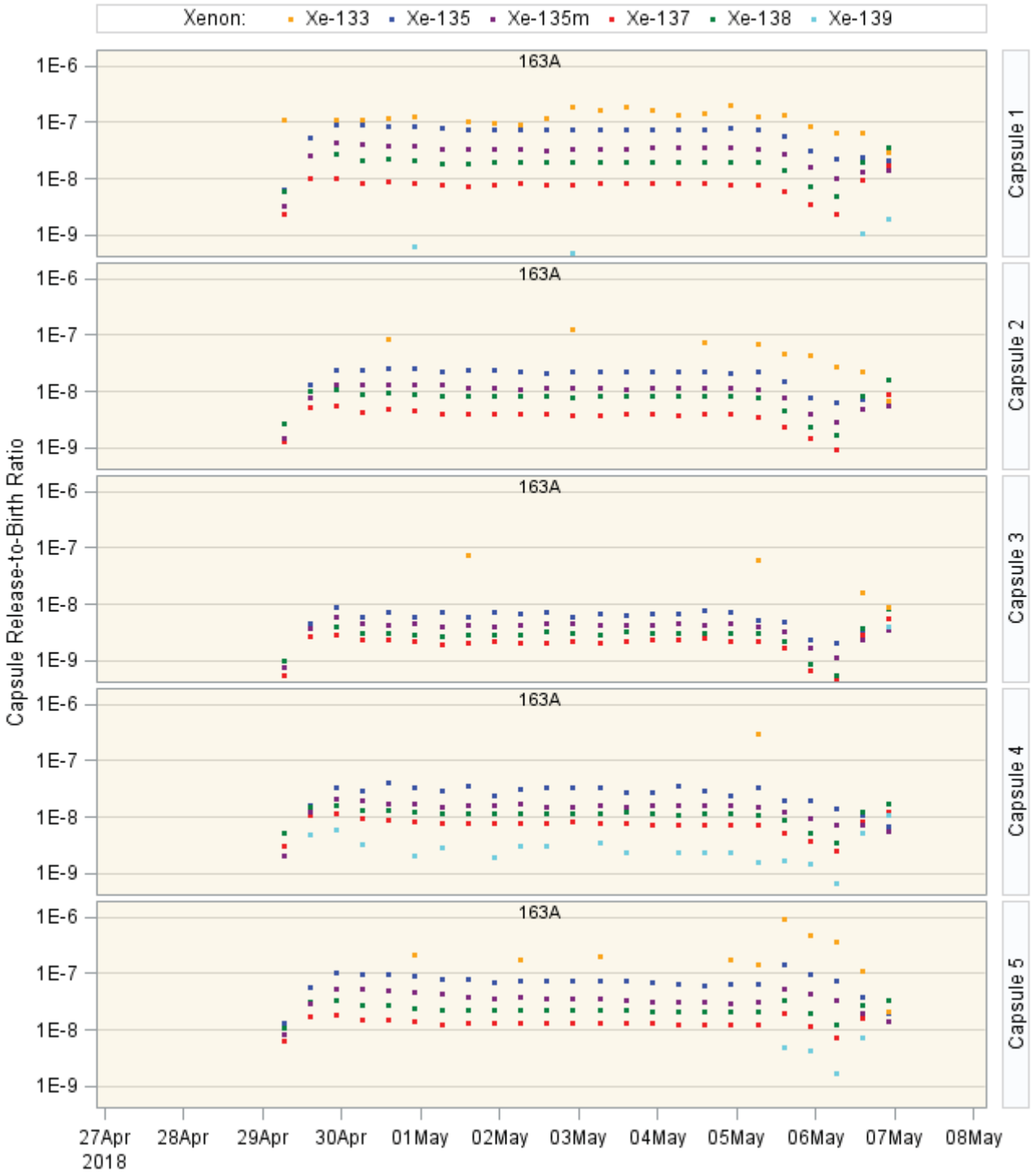

Figure 10. Cycle 163A release-to-birth ratios for selected xenon isotopes for AGR-5/6/7 Capsules 1–5.

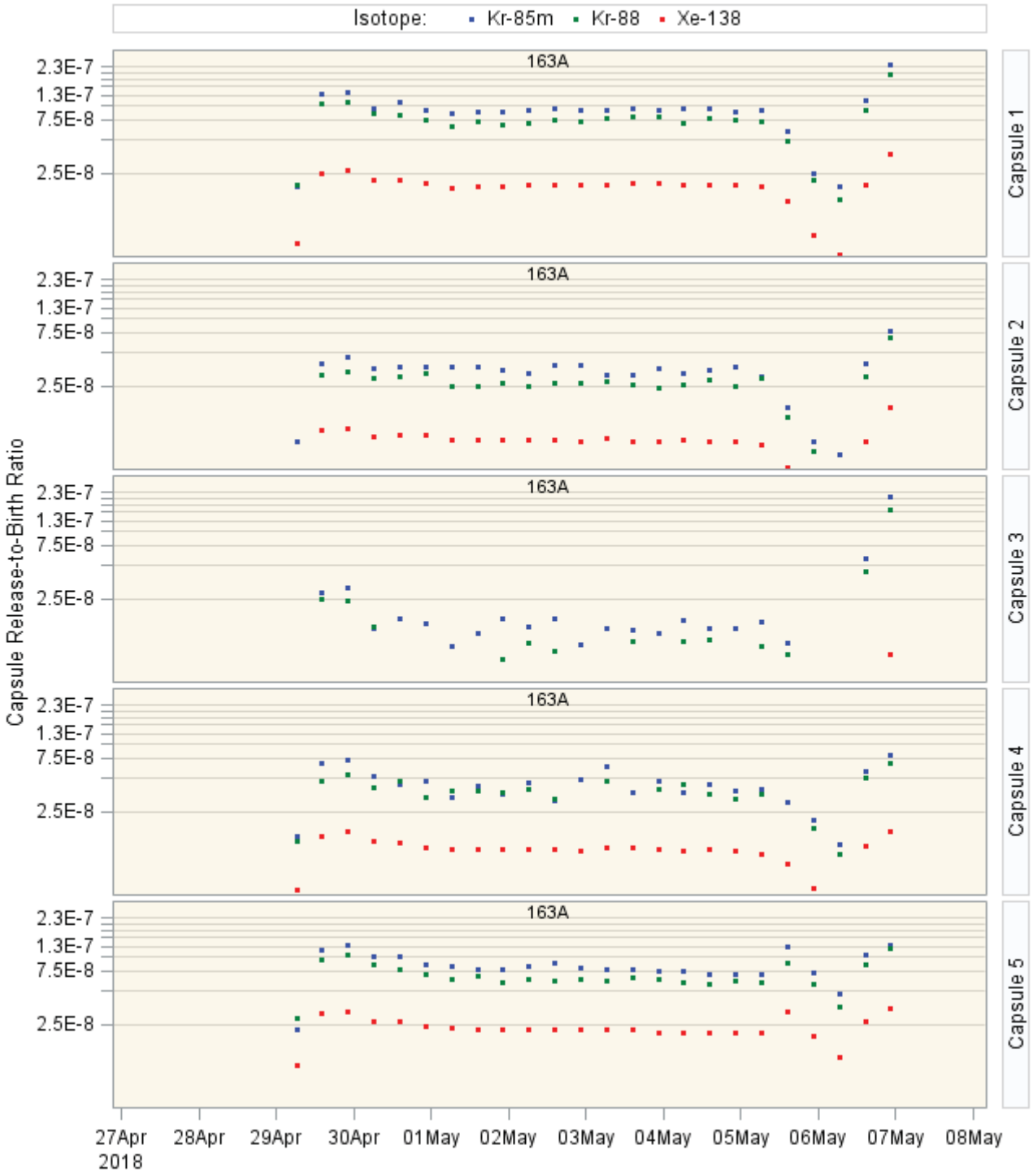

Figure 11. Cycle 163A release-to-birth ratios for selected krypton and xenon isotopes for AGR-5/6/7 Capsules 1–5 where equilibrium is believed to have been reached within the capsule based on half-life.

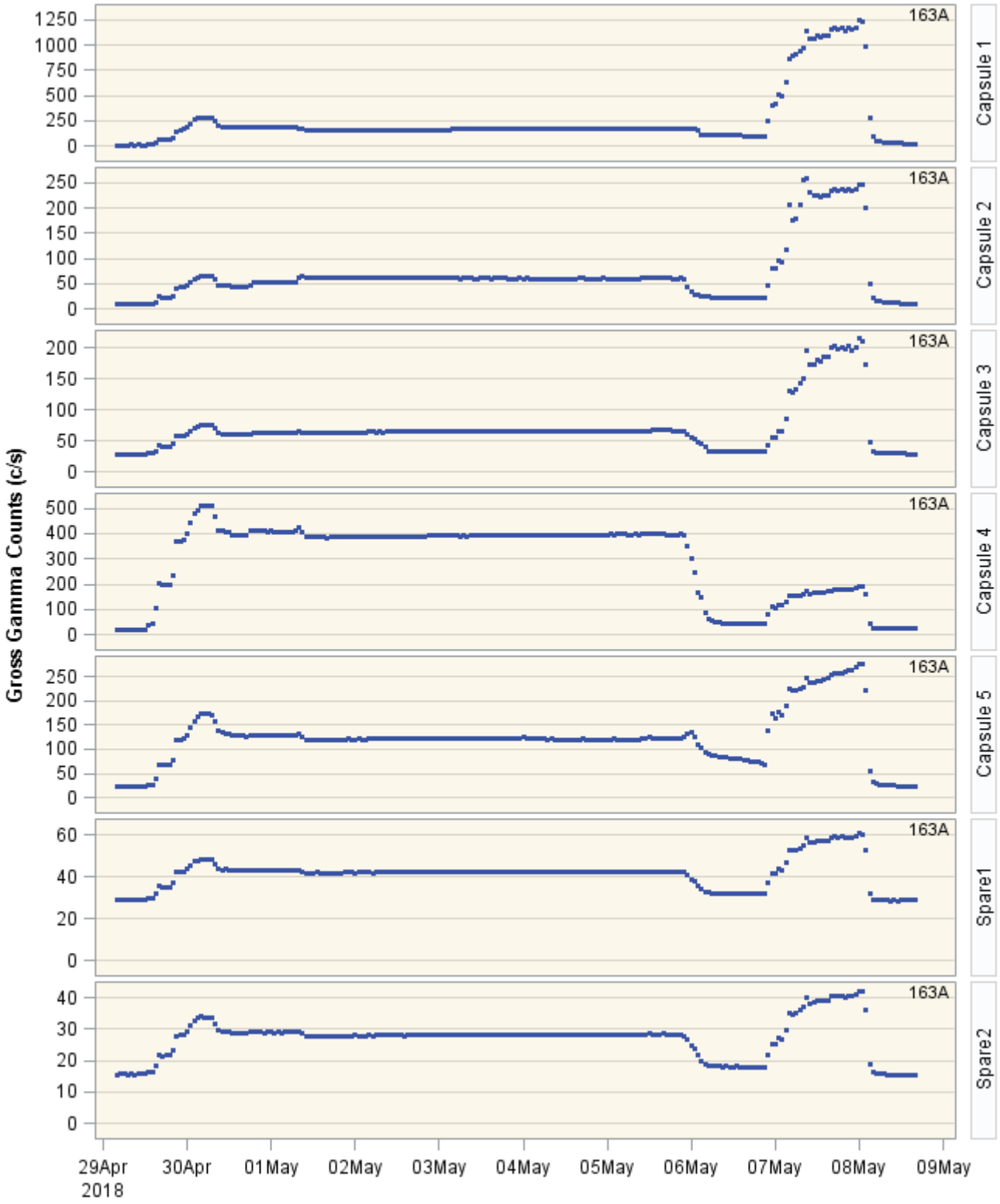

Figure 12. Cycle 163A GG release rate data AGR-5/6/7 Capsules 1–5.

7.7 Cycle 164A

Irradiation for Cycle 164A began on June 10, 2018 and ran through August 17, 2018 with reactor SCRAMs occurring on June 23–July 4, 2018 and July 30–August 2, 2018. This 68-day cycle was irradiated at a northeast lobe power of 16 MW. The R/B values on average is 1E-06 for krypton and 1E-07 for xenon [9]. Figure 16shows the corresponding GG data for Capsules 1–5 where the counts per second are consistent with the releases detailed in Figures 13–15. During Cycle 164A, it was noticed that the outlet flows were all greater than the inlet flows for Capsule 2–5. The decision was made to balance the flows with the intent to tighten down (i.e., throttle) the Capsule 4 needle valve (which was about 13 sccm greater than the inlet flow) until a flow rate in the Capsule 5 outlet was a few sccm above its inlet flow. This event is easily seen in Figure 16and is circled in red. This effort directly impacted the shorter-lived krypton and xenon isotopes which was expected and can be seen in Figure 13–15.

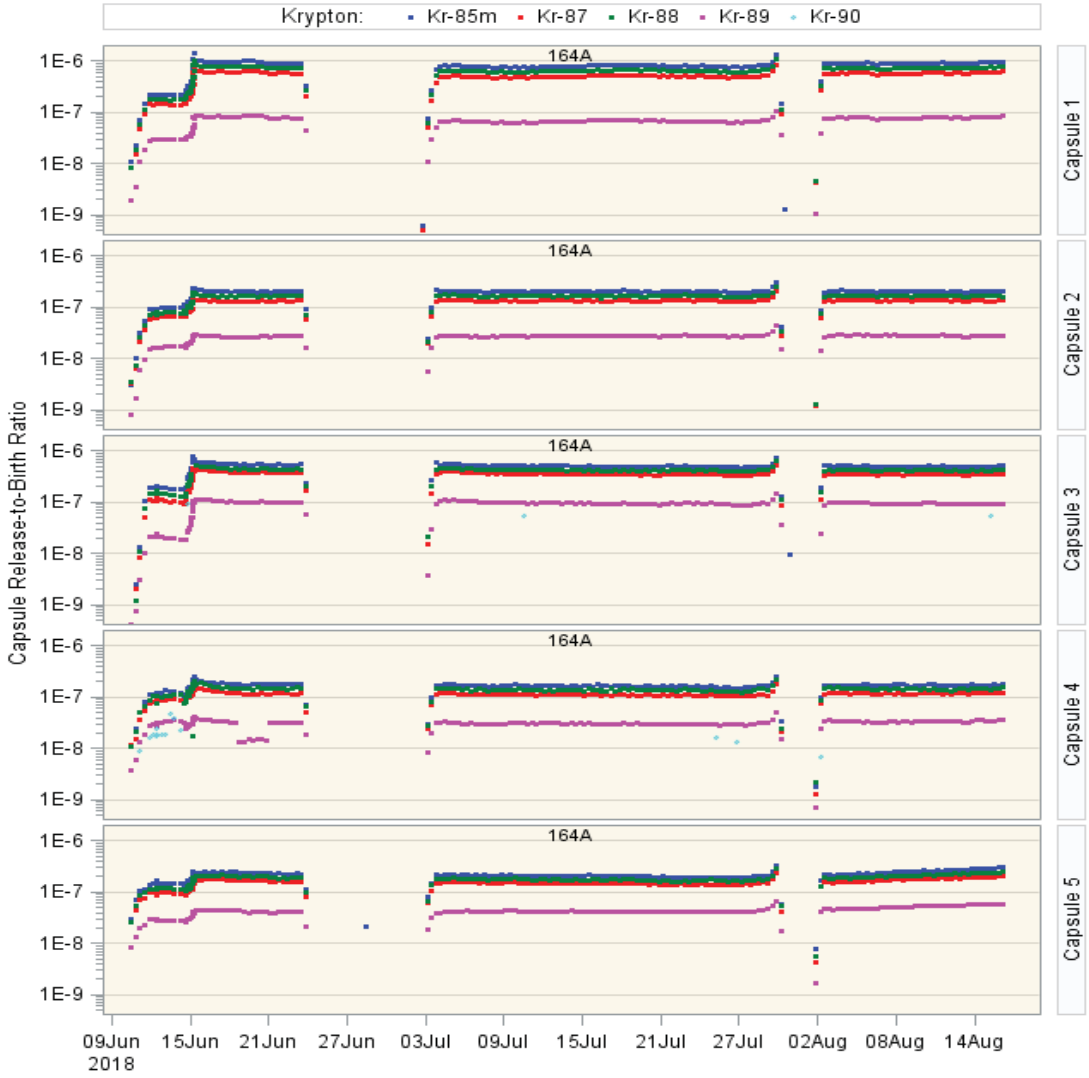

Figure 13. Cycle 164A release-to-birth ratios for selected krypton isotopes for AGR-5/6/7 Capsules 1-5.

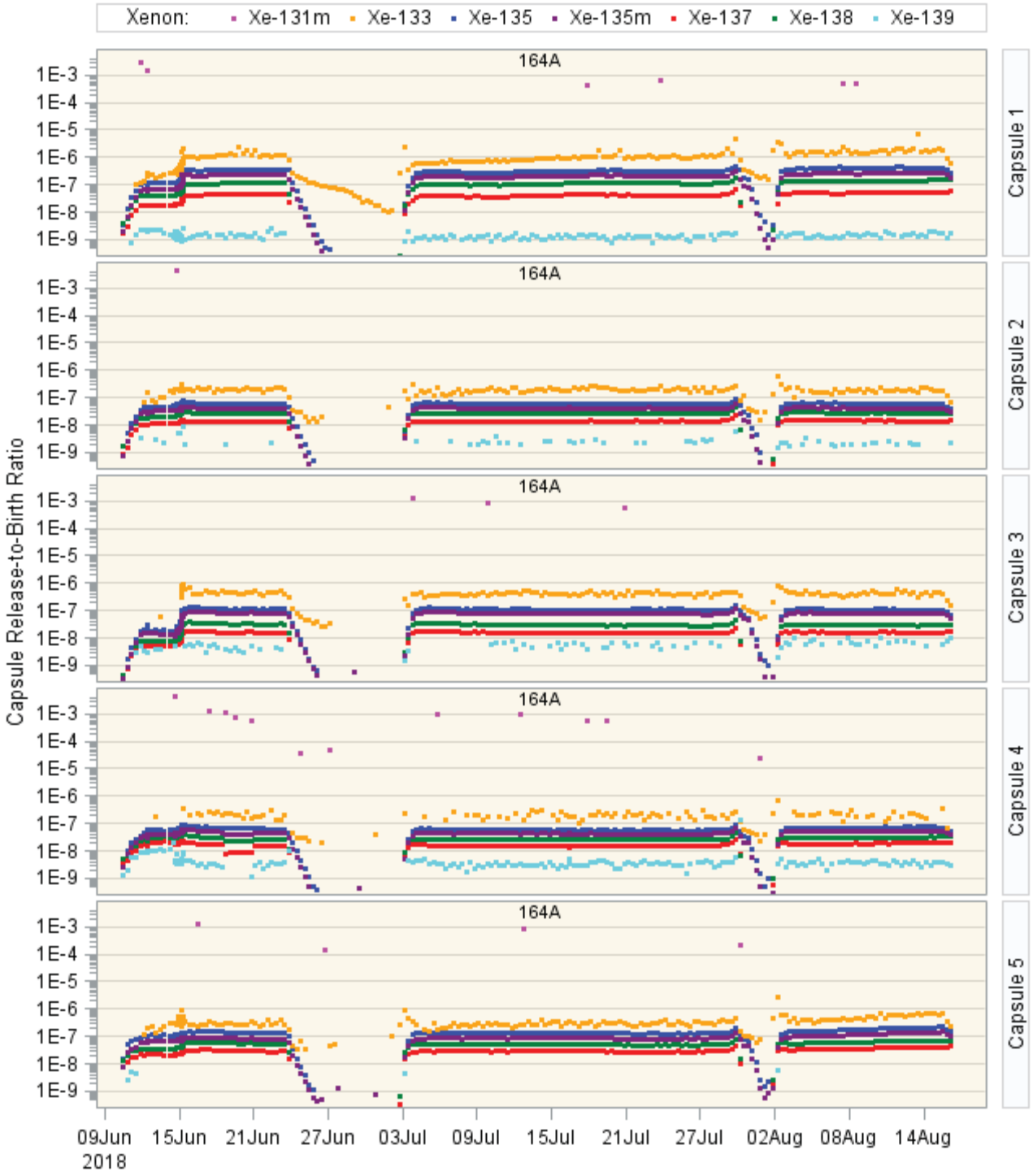

Figure 14. Cycle 164A release-to-birth ratios for selected xenon isotopes for AGR-5/6/7 Capsules 1-5.

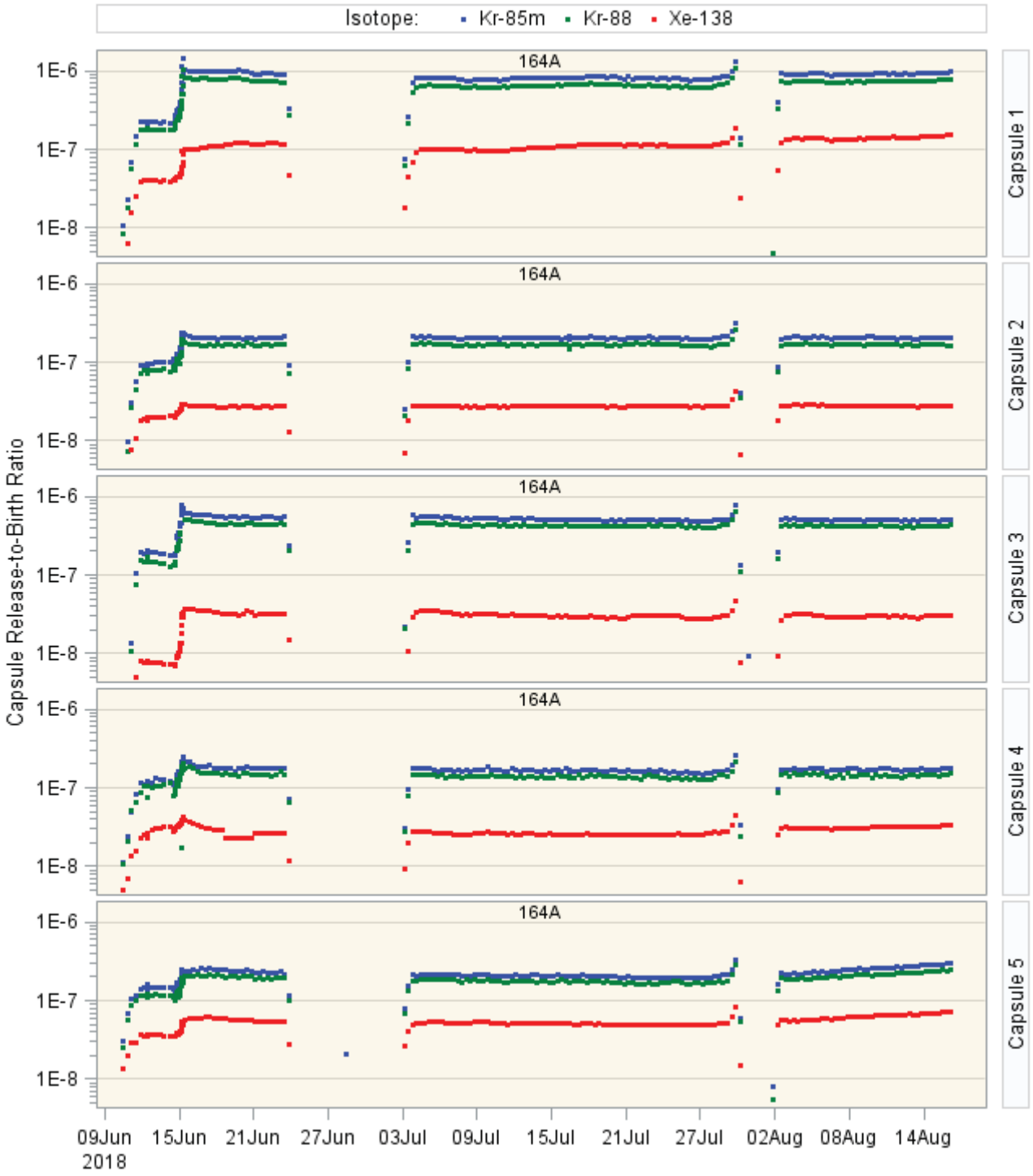

Figure 15. Cycle 164A release-to-birth ratios for selected krypton and xenon isotopes for AGR-5/6/7 Capsules 1–5 where equilibrium is believed to have been reached within the capsule based on half-life.

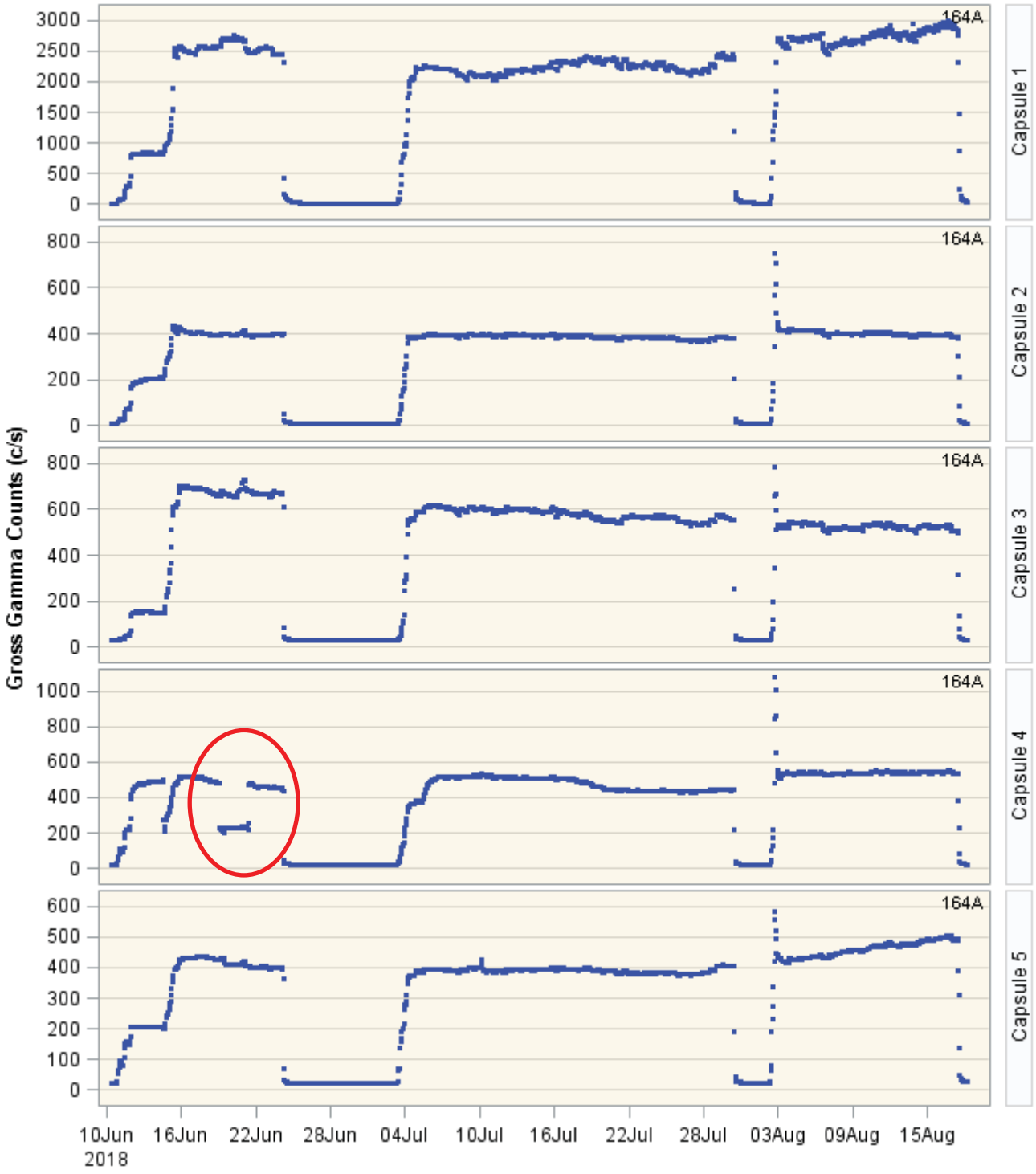

Figure 16. Cycle 164A GG release rate data AGR-5/6/7 Capsules 1–5. The outlet valve of Capsule 4 was throttled from June 19–June 21, 2018 (circled in red) in an attempt to rebalance capsule outlet flows.

7.8 Cycle 164B

Irradiation for Cycle 164B began on September 18, 2018 and ran through January 17, 2019 with reactor SCRAMs occurring on October 15–24, 2018 and November 4–December 22, 2018. Of this cycle, 27 days were irradiated at a northeast lobe power of 17 MW, and 37 days were at 16 MW. The R/B values on average is 1E-06 for krypton and 1E-07 for xenon [9]. Figure 20shows the corresponding GG data for Capsules 1–5 with the corresponding GG data for Capsules 1–5. Figures Figure 17–19 details that the counts per second are consistent with the releases and the capsule specific relief valves being adjusted towards the end of Cycle 164B. An example of this adjustment is circled in purple on Figure 20. At the beginning of Cycle 164B, the inlet pressure of Capsule 1 began to rise significantly between September 18 and October 2, 2018. Capsule 1 was isolated for about 2 weeks at the beginning of October but then was restarted at a reduced rate to prevent the capsule pressure from rising too high. This activity is observed in Figure 17–20. It was suspected that a blockage formed on the outlet side of Capsule 1. A detailed explanation of the line blockage is captured in ECAR-5114, Rev.0. The isotopic inventory buildup from the impending blockage was sufficient to be observed on the two spare GG systems and slightly on the remaining GG systems. The count rate from the resumption of Capsule 1 flow on the spare GG systems yielded a 75-cps rate increase above system background, whereas the rate for capsule one at that time was around 7,000 cps. The effluent lines come from the 1A secondary cubicle into the 1A primary cubicle in between FPMS Stations 5 and 6 which is why the effluent from Capsule 1 is observed on the aforenoted GG systems. It is important to note that the signal being picked up from the spare GG detectors is from the elevated room rate and not from the effluent line that is shielded and runs in front of the NaI(Tl) detector.

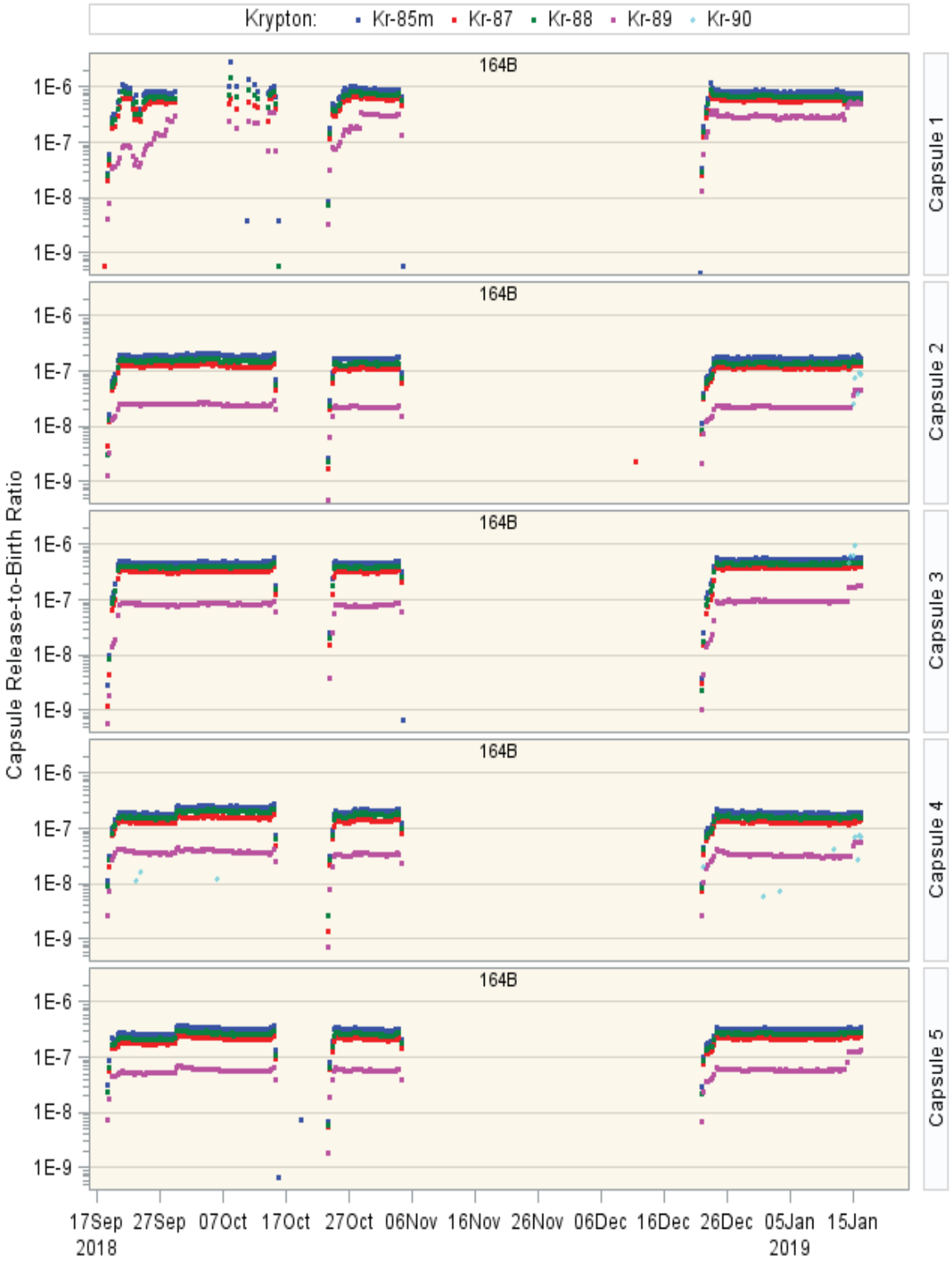

Figure 17. Cycle 164B release-to-birth ratios for selected krypton isotopes for AGR-5/6/7 Capsules 1–5.

Figure 18. Cycle 164B release-to-birth ratios for selected xenon isotopes for AGR-5/6/7 Capsules 1–5. The trailing Xe-133 in this figure is from isotopic decay. The half-life for Xe-133 is 5.24 days.

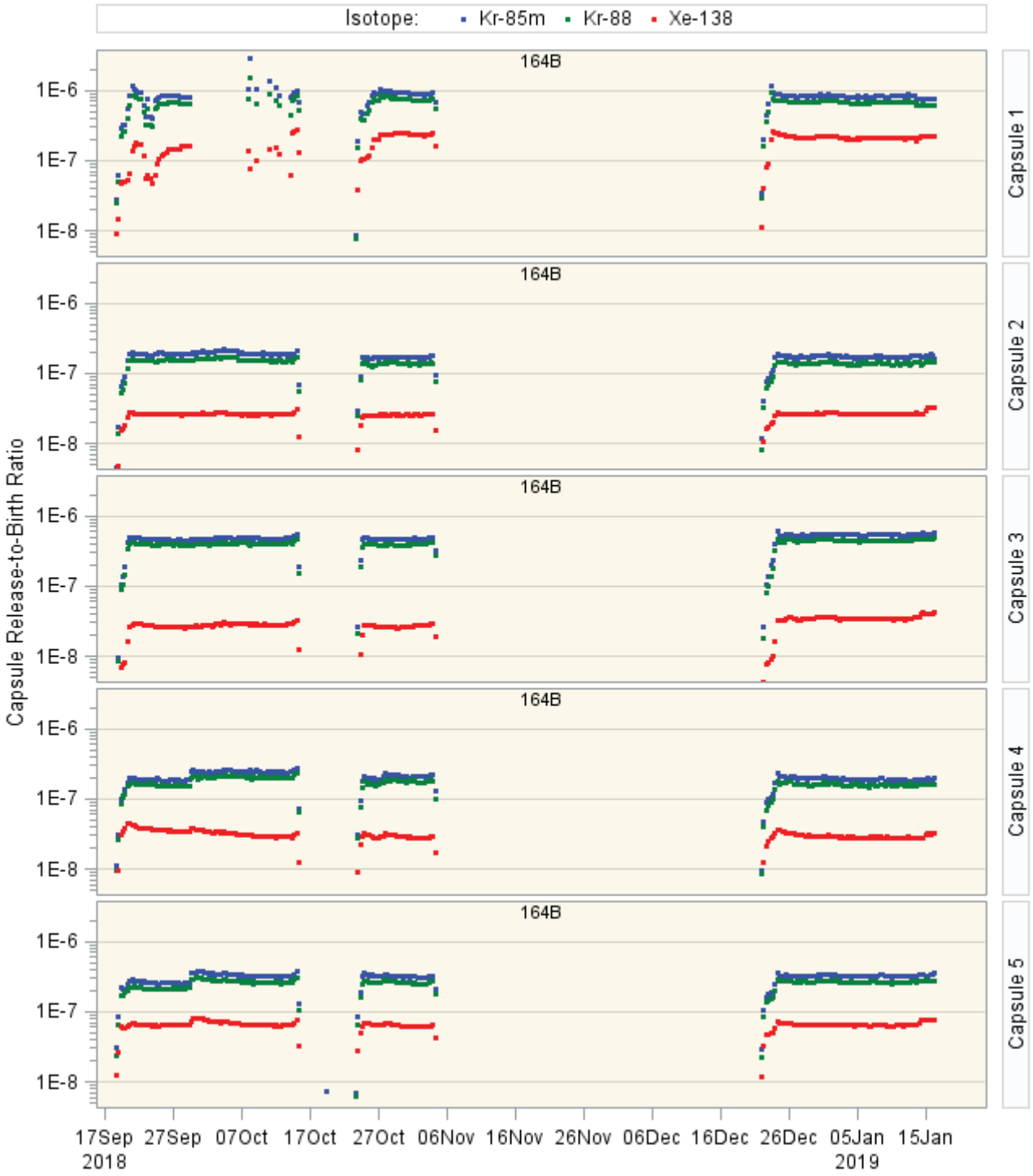

Figure 19. Cycle 164B release-to-birth ratios for selected krypton and xenon isotopes for AGR-5/6/7 Capsules 1–5 where equilibrium is believed to have been reached within the capsule based on half-life.

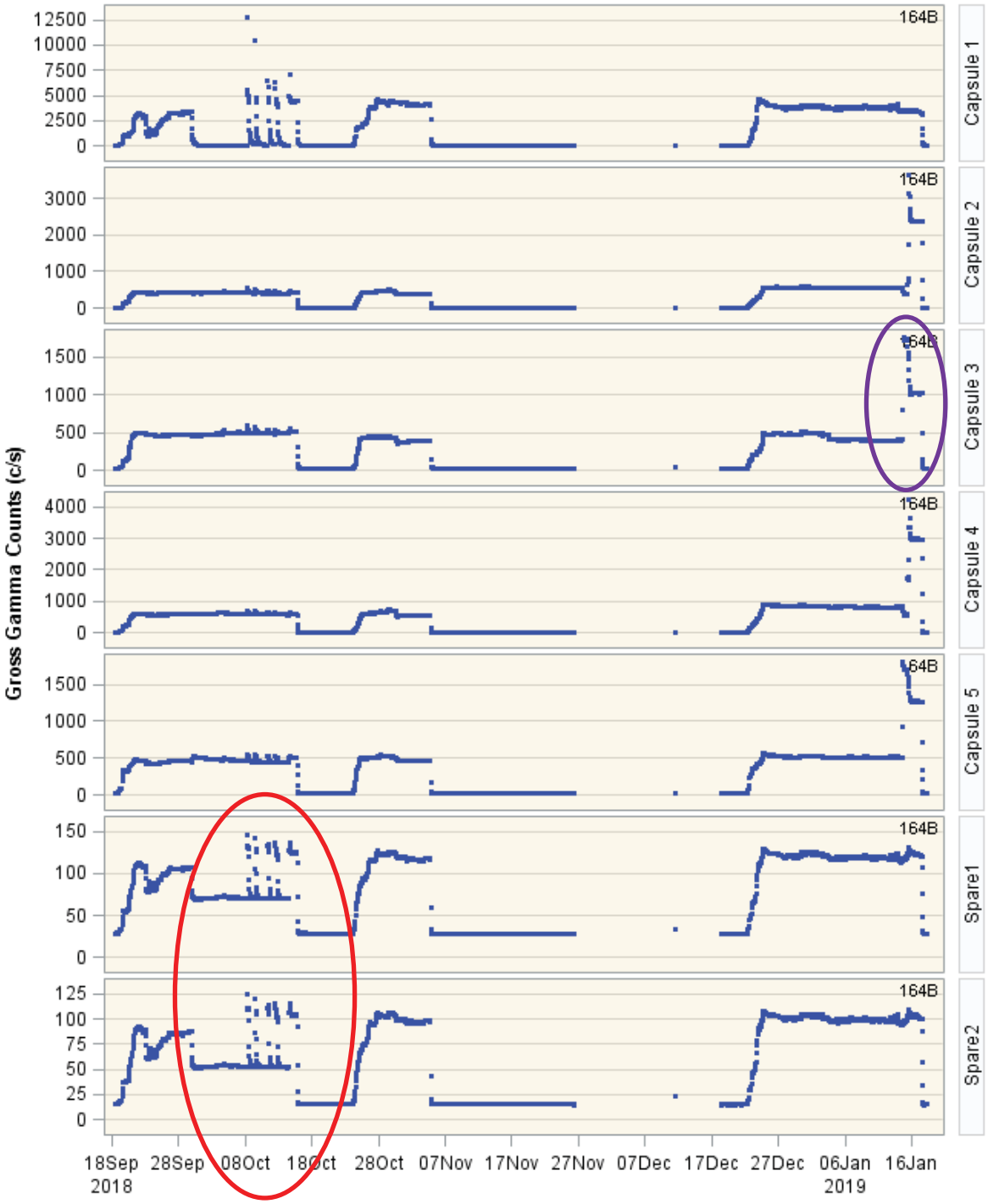

Figure 20. Cycle 164B GG release rate data AGR-5/6/7 Capsules 1–5 and Spare 1 and 2. The red circle on Figure 20 indicate inventory buildup and release from Capsule1 when flow was restored. Upon examination of isotopic data and GG data the primary contributor to this stored inventory is Xe-133. Towards the end of Cycle 164B, all capsule relief valves were adjusted and reset. This event is captured in the purple circle and can easily be seen in Capsule 2–5 data on this figure.

7.9 Cycle 165A

Irradiation for Cycle 165A began on February 28, 2019 and ran through June 18, 2019 with a reactor SCRAM occurring for most of the cycle dating from March 3 to June 8, 2019. Of this cycle, 13 days were irradiated at a northeast lobe power of 19 MW. The R/B values on average for krypton is on the order of 1E-06 and 1E-07 for xenon [10]. Figure 24shows the corresponding GG data for Capsules 1–5 where the counts per second are consistent with the releases detailed in Figure 21–23. During the last portion of cycle, 165A flow was increased to Capsule 2–5 enabling the shorter-lived Kr-89 and Kr-90 to be observable at the FPMS. At the beginning of cycle 165A, a crack in the Capsule 1 outlet line opened downstream of the plug that was formed during Cycle 164B. After Cycle 165A was complete, the inlet and outlet lines for Capsule 1 were switched to ensure that the Capsule 1 outlet flow reached the fission product monitor predictably. Up to the end of Cycle 165A, the GG averages are low and stable which was a good indication that in-pile particle failures were unlikely. Stable release to birthrate values for all capsules further confirm the GG data.

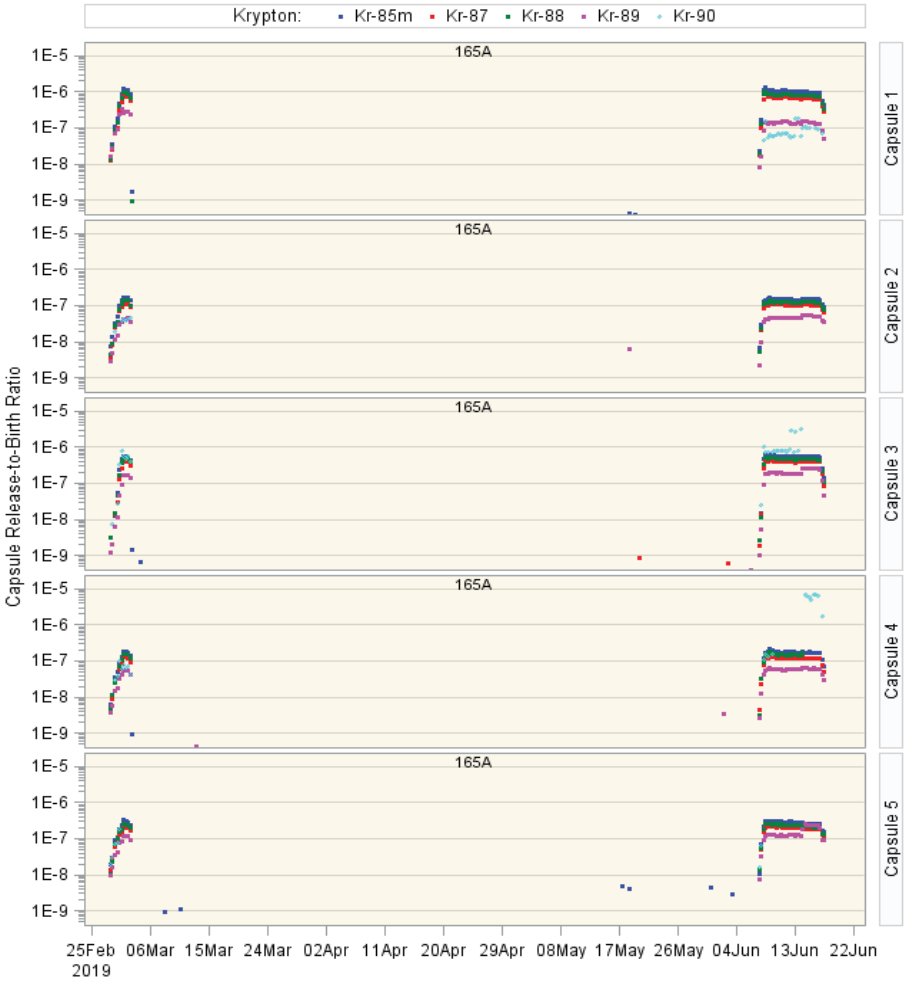

Figure 21. Cycle 165A release-to-birth ratios for selected krypton isotopes for AGR-5/6/7 Capsules 1–5.

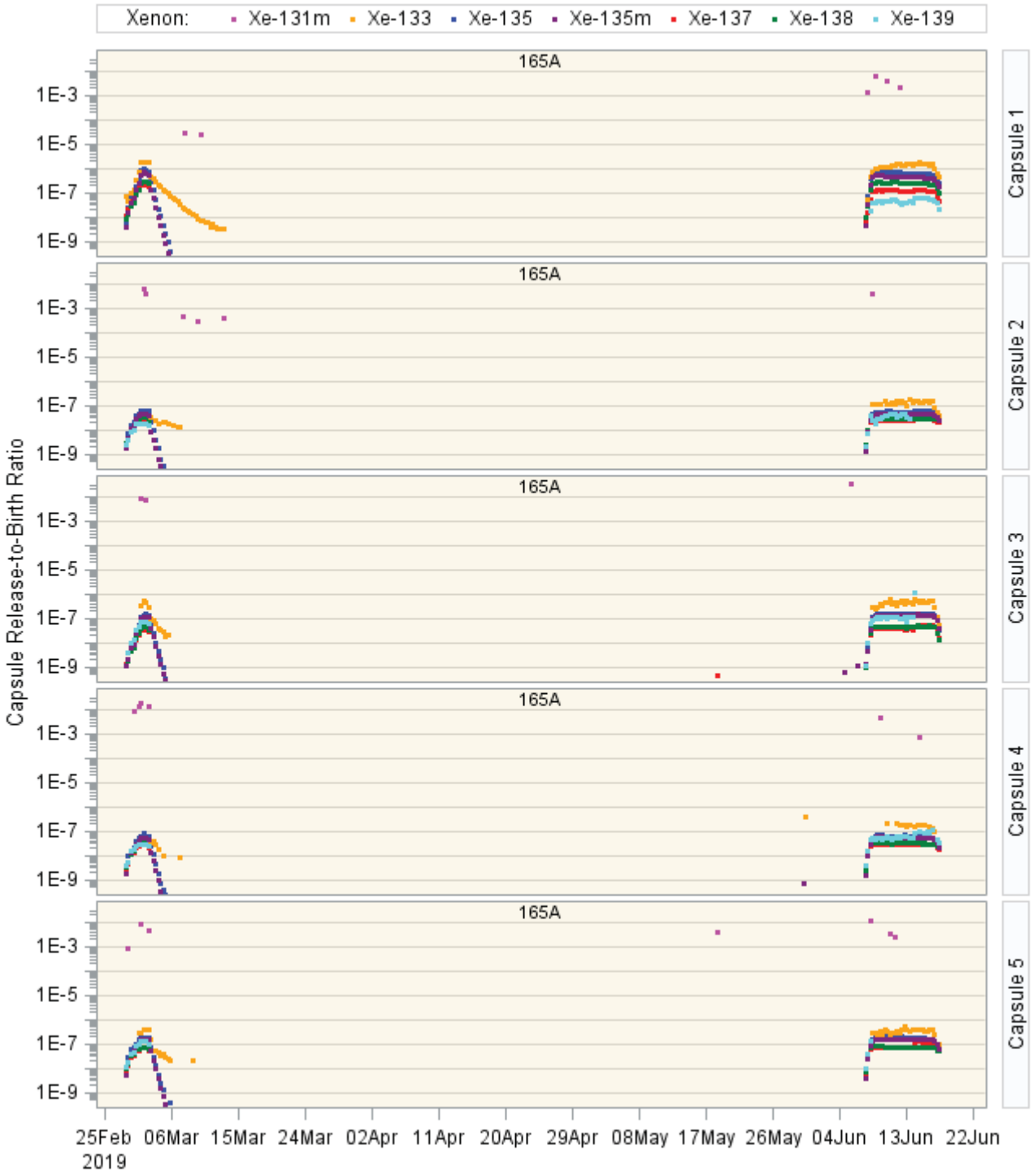

Figure 22. Cycle 165A release-to-birth ratios for selected xenon isotopes for AGR-5/6/7 Capsules 1–5.

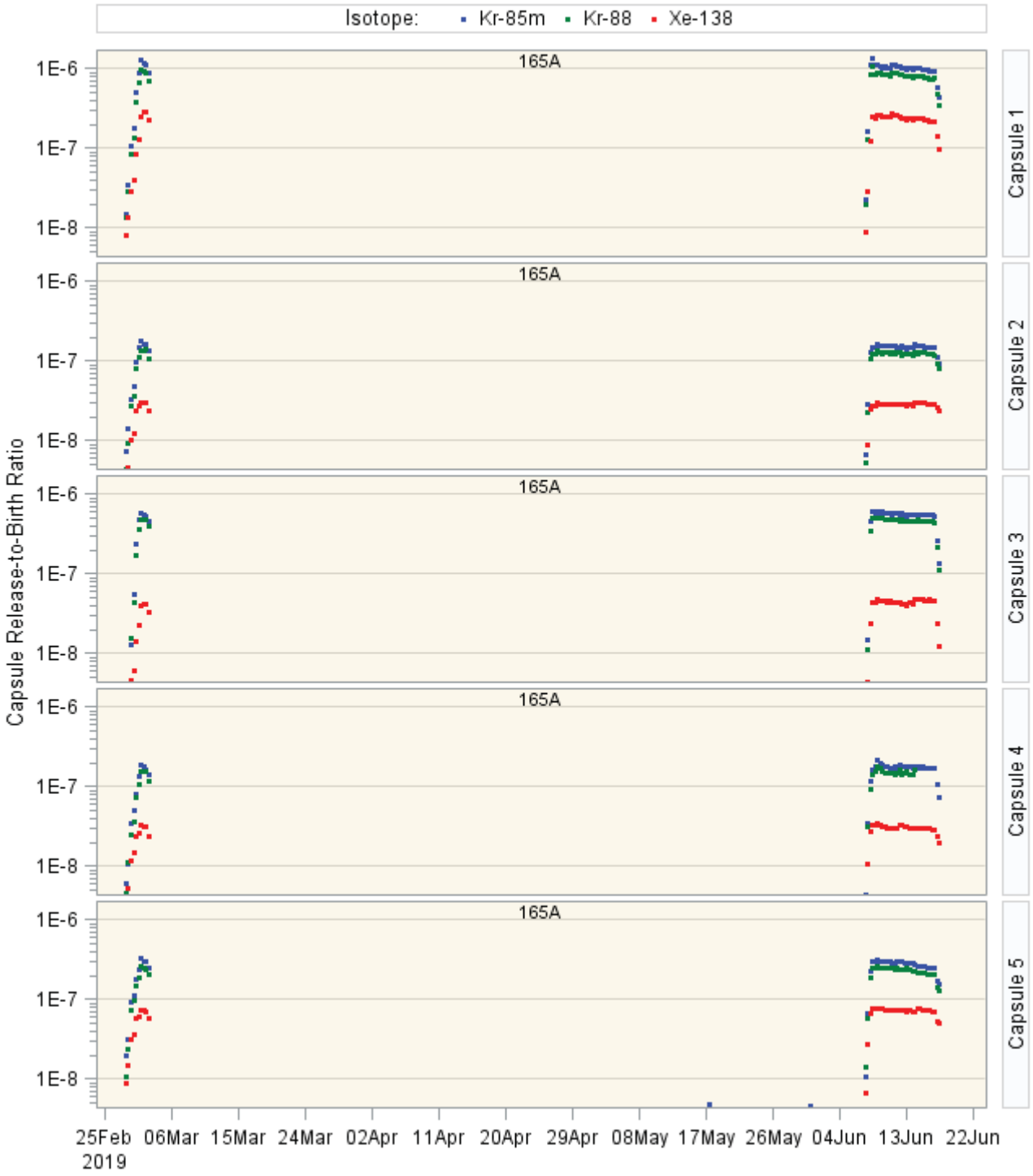

Figure 23. Cycle 165A release-to-birth ratios for selected krypton and xenon isotopes for AGR-5/6/7 Capsules 1–5 where equilibrium is believed to have been reached within the capsule based on half-life.

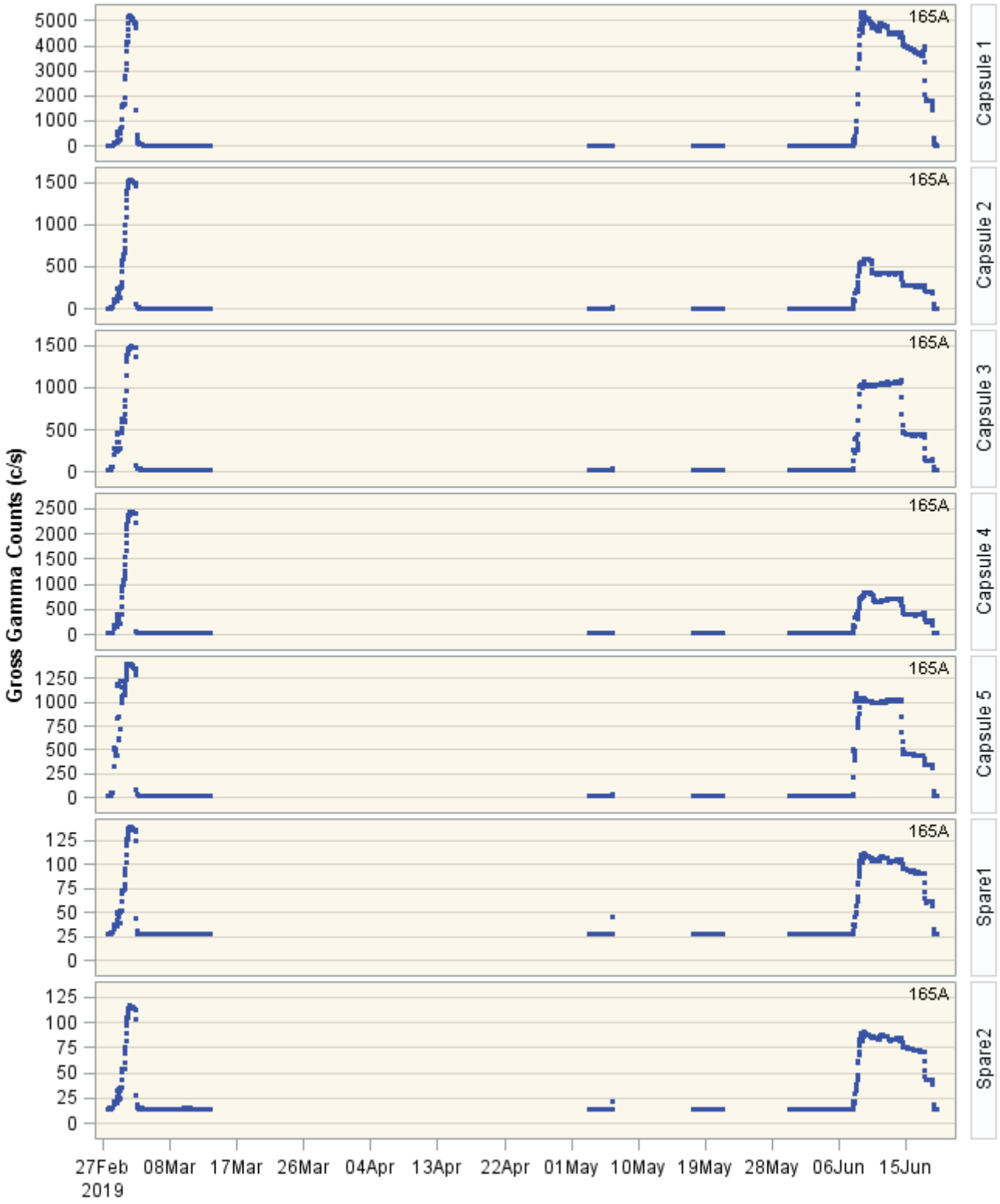

Figure 24. Cycle 165A GG release rate data AGR-5/6/7 Capsules 1–5 and Spare 1 and 2.

7.10 Cycle 166A

Irradiation for Cycle 166A began on July 24, 2019 and ran through October 6, 2019 with a reactor SCRAM occurring from September 5–17, 2019. Of this cycle, 63 days were irradiated at a northeast lobe power of 17 MW. With a large amount of dilution gas entering the Capsule 1 exhaust line from the leadout through the crack that was formed during Cycle 165A, it was difficult to interpret the fission gas measurements from Capsule 1. At the conclusion of Cycle 165A the inlet and outlet lines for Capsule 1 were switched to ensure that the Capsule 1 outlet flow reached the fission product monitor predictably. It was also postulated that the line switch might improve the plug situation. It was noted that the plug seemed to ablate when Capsule 1 was in a no-flow condition. A detailed explanation of the reasoning and the process is contained in ECAR-5114. After the lines were swapped, Capsule 1 performed as expected for a short period of time from July 27 through August 15, 2019. Then evidence of a second series of plugs and cracks was observed. Ultimately, Capsule 1 was completely plugged. During Cycle 166A, indications of fuel particle failures were observed in Capsule 1. By the end of Cycle 166A, the GG continued to monitor fuel activity, while the HPGe detector was saturated the deadtime for the NaI detector is unknown because of its configuration as a gross rate meter.

Fission product leakage is apparent in the GG data by observing the long-lived isotopes such as Xe-133 and Xe-135 into the other capsules. Xe-133 is the primary isotope that contributes to the “spike” in the GG system and is a major contributor to the GG count rate.

Figure 25 details the failures that were observed starting on August 4, 2019. Starting around August 16, 2019, a new clog developed in Capsule 1 causing line pressure, so flow became intermittent to avoid exceeding pressure limits. From August 29–31, 2019, there were no additional particle failures observed, illustrated in Figure 26. Upon resumption from a SCRAM that ended on September 17, 2019, no particle failures were observed on Capsule 1 from September 18–24, 2019 as shown in Figure 27.

Capsule 1 gas flow was suspended from September 23–30, 2019, when gas flow was re-established, a large number of GG spikes were observed for Capsule 1 between September 30–October 4. These spikes and subsequent increase in averages indicate that multiple failures had occurred in Capsule 1 (see Figure 28). Starting on August 4, 2019 through October 3, 2019 Xe-133, activity indicates that more than 1000 particle failures may have occurred. Data from the germanium detectors became unreliable after October 3 because of the increased detector deadtime which led to complete saturation.

As a result of the crack in Capsule 1, some of the accumulated fission gas in Capsule 1 diffused out via the crack in the gas line and contaminated gas in the leadout. Then, the contaminated gas in the leadout flowed through the other four capsules, resulting in various amounts of Capsule 1 fission gas being leaked to the other four capsules during this cycle. The same trend became apparent for Capsules 4 and 5 near the end of Cycle 165A. However, the fluctuating behavior is much less apparent for Capsule 3; instead, the R/B for all isotopes were gradually increasing during that time. Figure 29-32 captures all the events from Cycle 166A. Upon examination of isotopic data from Capsule 3 effluent and review of GG data, the increase in Capsule 3 activity is possible from heating and heavy metal fission product release (see Figure 33) and no particle failures were observed for any other capsule for this cycle.

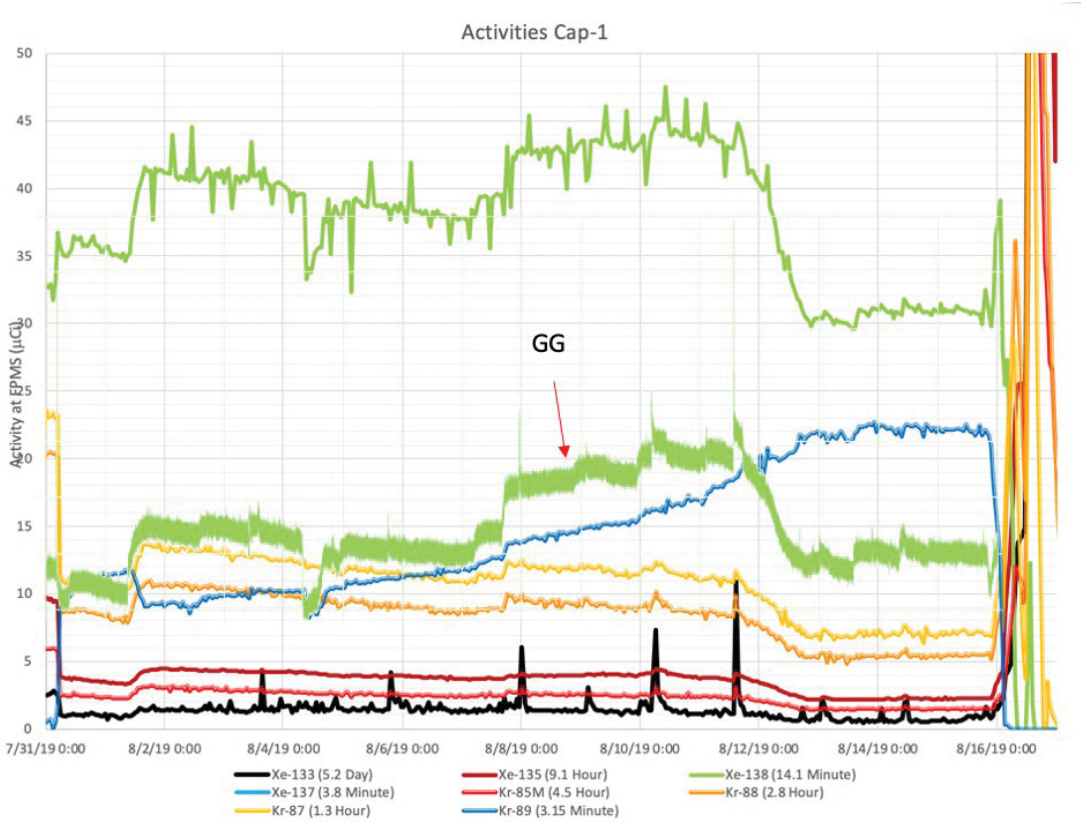

Figure 25. Gross gamma activity compared to HPGe isotopic data. “Spikes” in GG data correlate to increases in reported Xe-133 isotopic data.

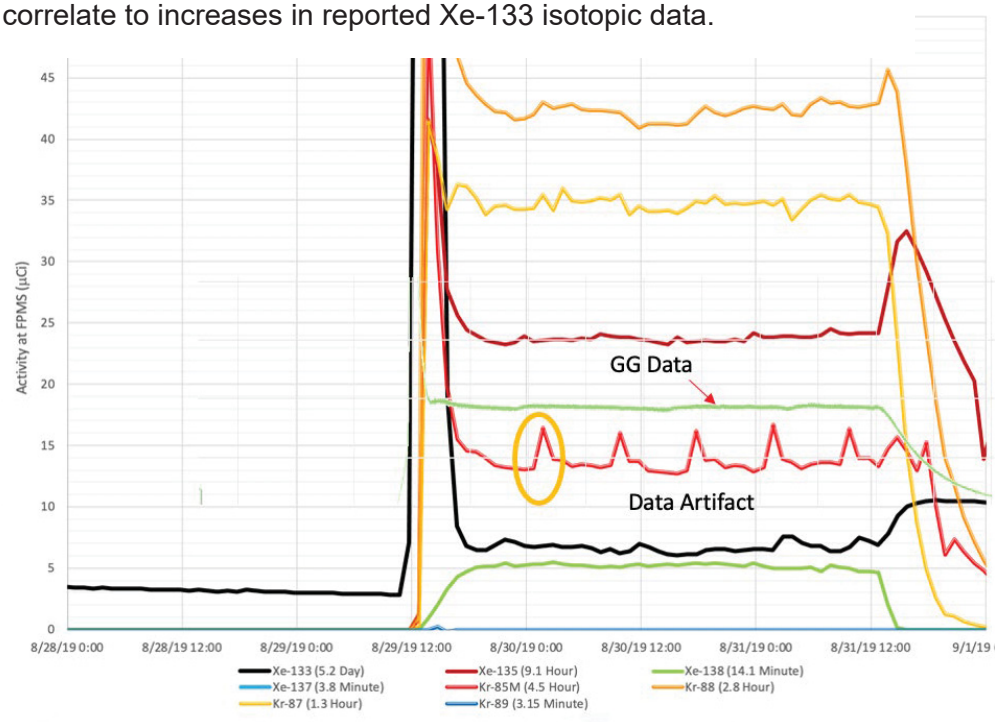

Figure 26. Isotopic and GG data from Capsule 1, Cycle 166A. No observed failures from August 29 to August 31, 2019.

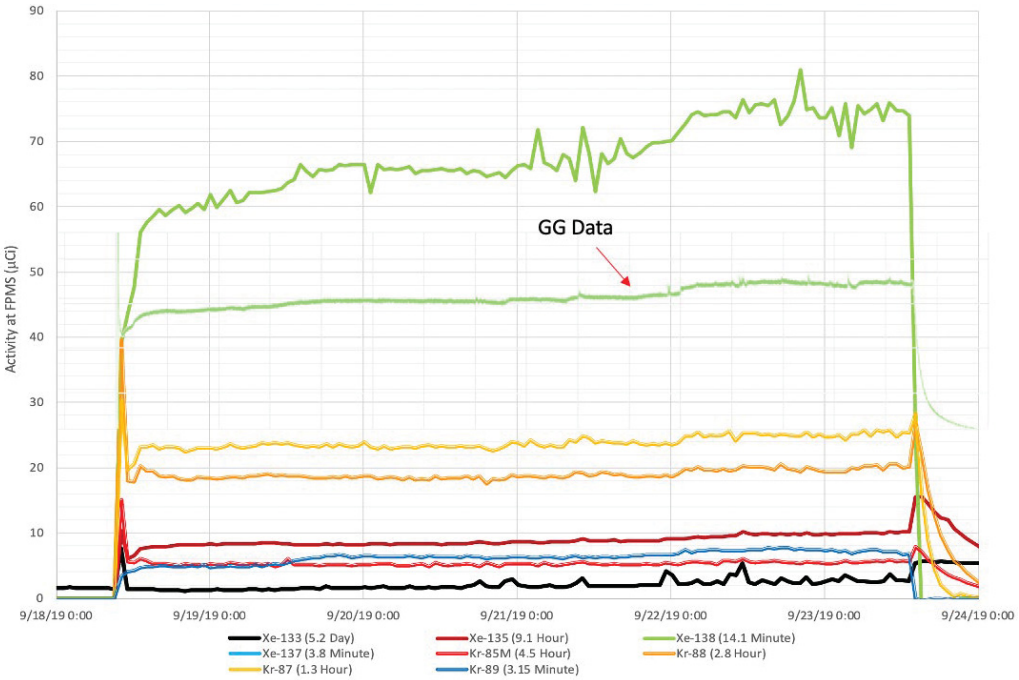

Figure 27. Isotopic and GG data from Capsule 1, Cycle 166A. No failures observed from September 18 to September 24, 2019.

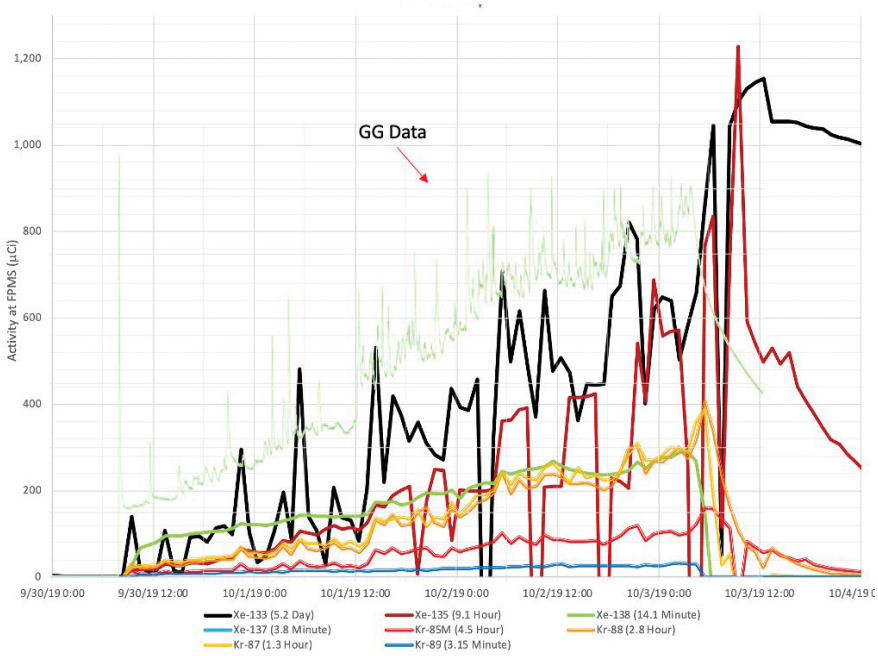

Figure 28. A large number of spikes is evident for Capsule 1 between September 30 and October 4, 2019 when Capsule 1 outlet flow resumed by the end of this cycle. These spikes and subsequent increase in averages indicate possible multiple failures had occurred in Capsule 1. From August 4 to October 3, 2019, Xe-133 activity indicates that more than 1,000 particle failures may have occurred. Data from the germanium detectors became unreliable after October 3 because of the increased detector deadtime which led to complete saturation.

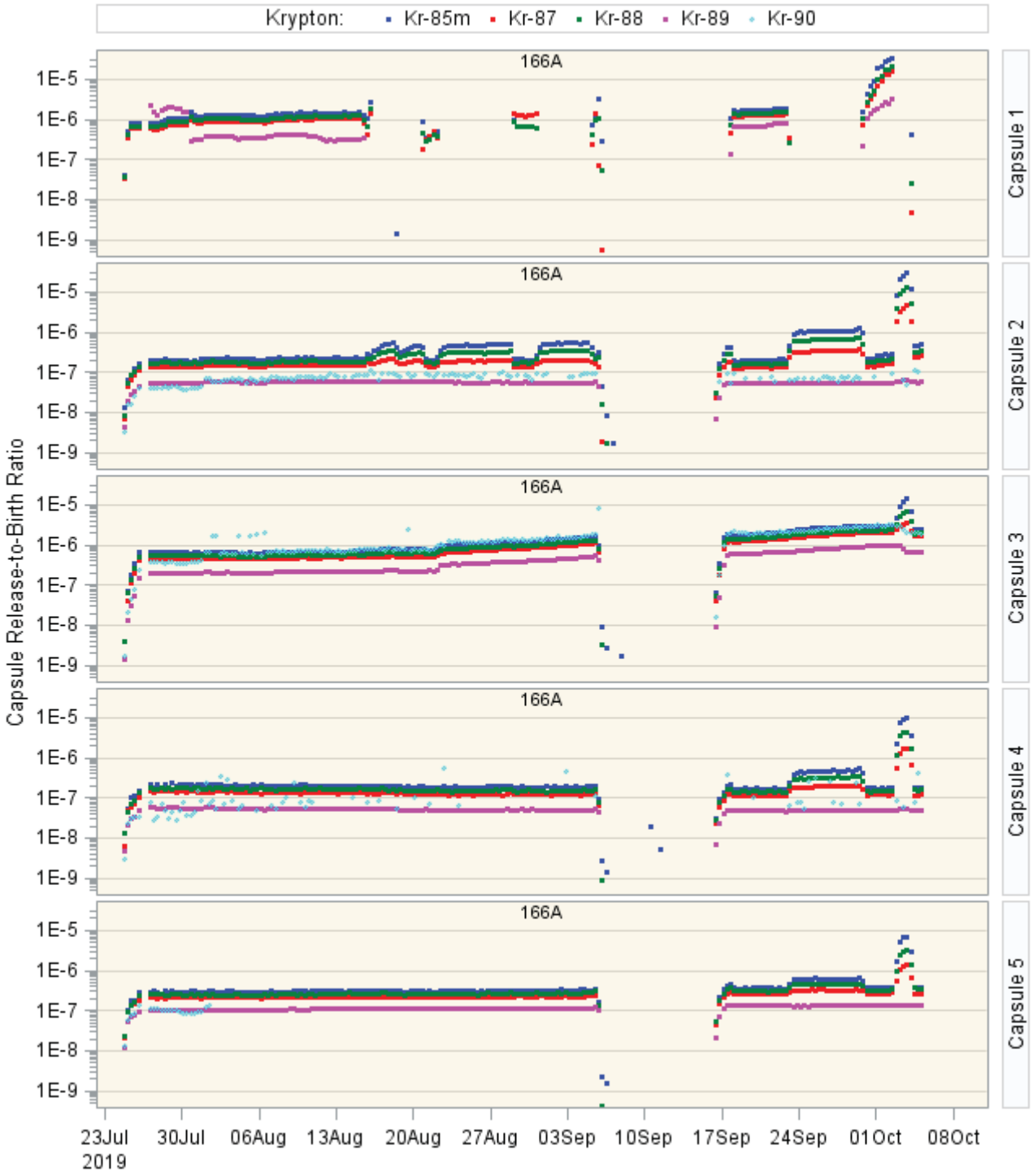

Figure 29. Cycle 166A release-to-birth ratios for selected krypton isotopes for AGR-5/6/7 Capsules 1–5.

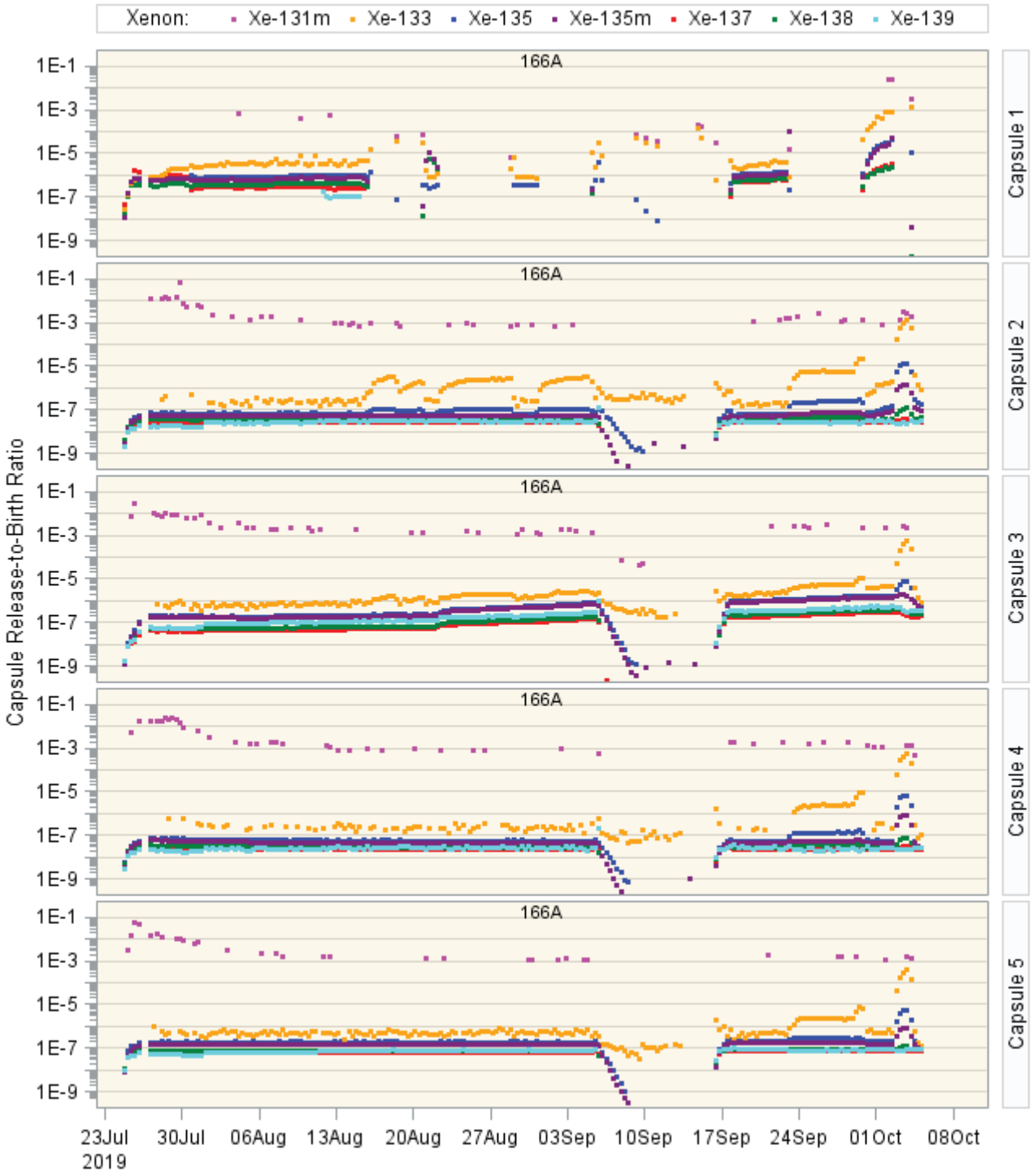

Figure 30. Cycle 166A release-to-birth ratios for selected xenon isotopes for AGR-5/6/7 Capsules 1–5.

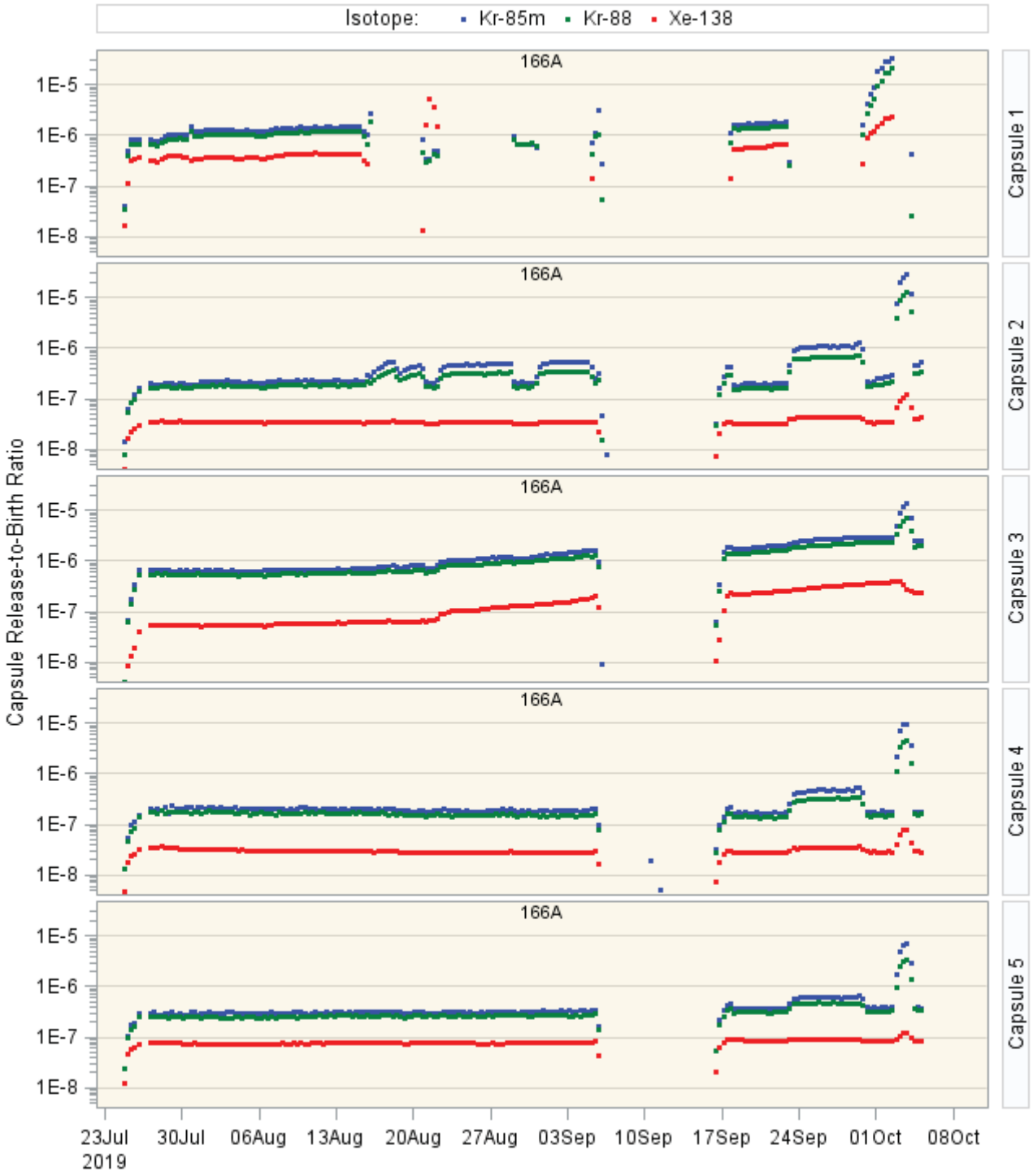

Figure 31. Cycle 166A release-to-birth ratios for selected krypton and xenon isotopes for AGR-5/6/7 Capsules 1–5 where equilibrium is believed to have been reached within the capsule based on half-life.

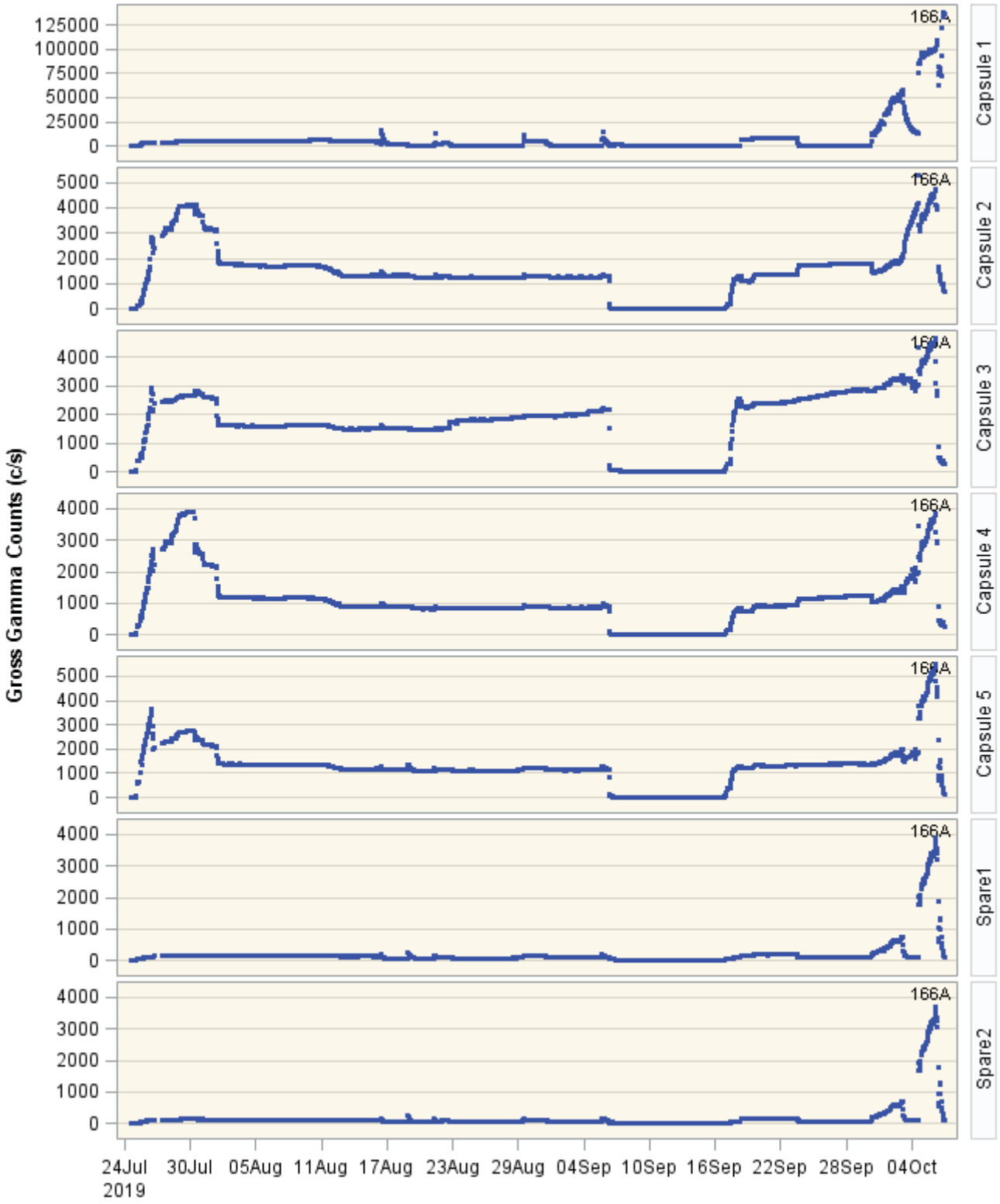

Figure 32. Cycle 166A GG release rate data AGR-5/6/7 Capsules 1–5 and Spare 1 and 2.

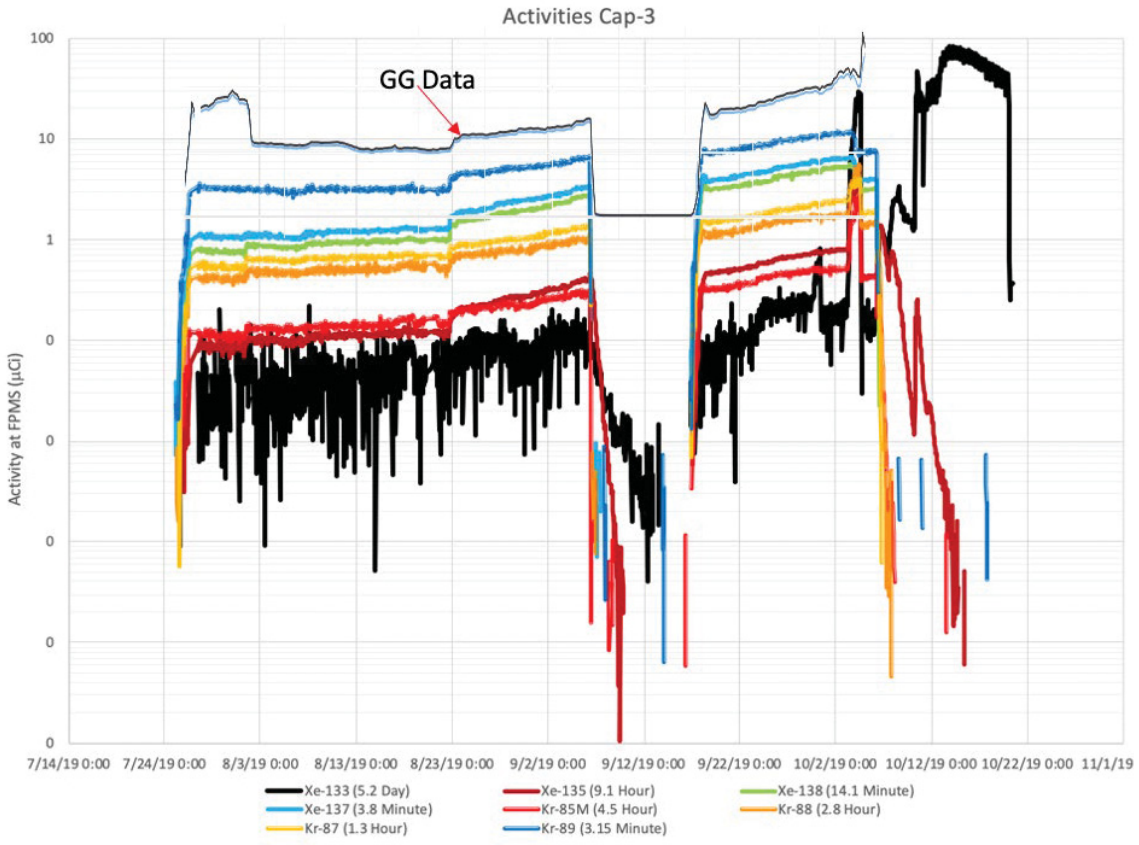

Figure 33. Activity increases in Capsule 3 as indicated by the R/B, GG, and 1-hour incremental data. No failures were observed in Capsule 3 for Cycle 166A, there was an increase in rate possibly from increase in heating and HM fission product release.

7.11 Cycle 166B

Irradiation for Cycle 166B began on November 9, 2019 and ran through January 10, 2020. This 62-day cycle was irradiated in the northeast lobe at 17 MW. At the end of ATR Cycle 166A, Capsule 1 fission gas suddenly increased to the facility alarm level at the ATR stack monitor. This event caused concern because of the excessive fission gas activity present at the stack monitor. As a precaution, gas flows were suspended for the whole test train during the first half of Cycle 166B, and the Capsule 1 gas line was isolated during the entire cycle. During the same period, the leadout outlet valve was opened, allowing Capsule 1 fission gas to discharge through the leadout to FPMS station (i.e., FPMS6 or Spare 1) to limit fission gas leakage to other capsules.

As a result, R/B data were collected only for Capsules 2–5 during the second half of 166B and no release data for Capsule 1 were collected. However, the fission gas leakages into Capsules 2, 4, and 5 are still observable by elevated R/B for longer-lived isotopes during that time.

The R/B for Kr-89 and Xe-137 (Figure 35–37) increased at much smaller fraction relative to R/B during earlier cycles for Capsules 2, 4, and 5. This is because the impact of fission gas leakage is smaller for shorter isotopes due to decay over the transport time from Capsule 1 to other capsules, especially the top Capsules 4 and 5. For Capsule 3, the R/B for all isotopes, except Xe-131m and Xe-133, are slightly higher than levels at the end of the previous cycle. This indicated only insignificant fission gas leakage from Capsule 1. Since there is a possibility of particle failure in Capsule 3 due to the fuel's

high-temperature (operating well beyond the normal conditions of a high-temperature gas reactor), isotopic information and GG data were reviewed. Figure 34captures the isotopic activities plotted with the GG data which showed no significant indication of a particle failure. The R/B values on average is 1E-05 for krypton and 1E-07 to 1E-04 for xenon. These values are not necessarily indicative of fuel failure in the capsule but of contamination from Capsule 1 from the leadout. It is recommended that R/B data from Cycle 166A be used as a bounding condition because the in-leakage from the leadout cannot be avoided. Figure 38shows the corresponding GG data for Capsules 1–5 with the two FPMS spares, which captures the entire operating cycle of Cycle 166B where the leadout outlet valve was opened. This allowed Capsule 1 fission gas to discharge through the leadout to Spare 1 with an initial count rate of over 30,000 counts per second. Because the initial stored inventory in the leadout from Capsule 1 leakage, this count rate was high. This event is observed in all the in-cubicle effluent lines due to the way the effluent lines are routed into the 1A primary. The GG for Capsule 1 still shows some activity that is slightly above background which is caused by isotopic plate out in the gas lines and is observable by watching the isotopic decay. A closer inspection of the GG data (see Figure 39) shows that the data agree with the data represented in Figure 34–38. It is important to note again that this is due to elevated activity from Capsule 1 in-cubicle crosstalk from the effluent lines that run along the cubicle wall and are picked up by each GG NaI detector. This increase in room activity was not observed in the heavier shielded HPGe spectrometer systems.

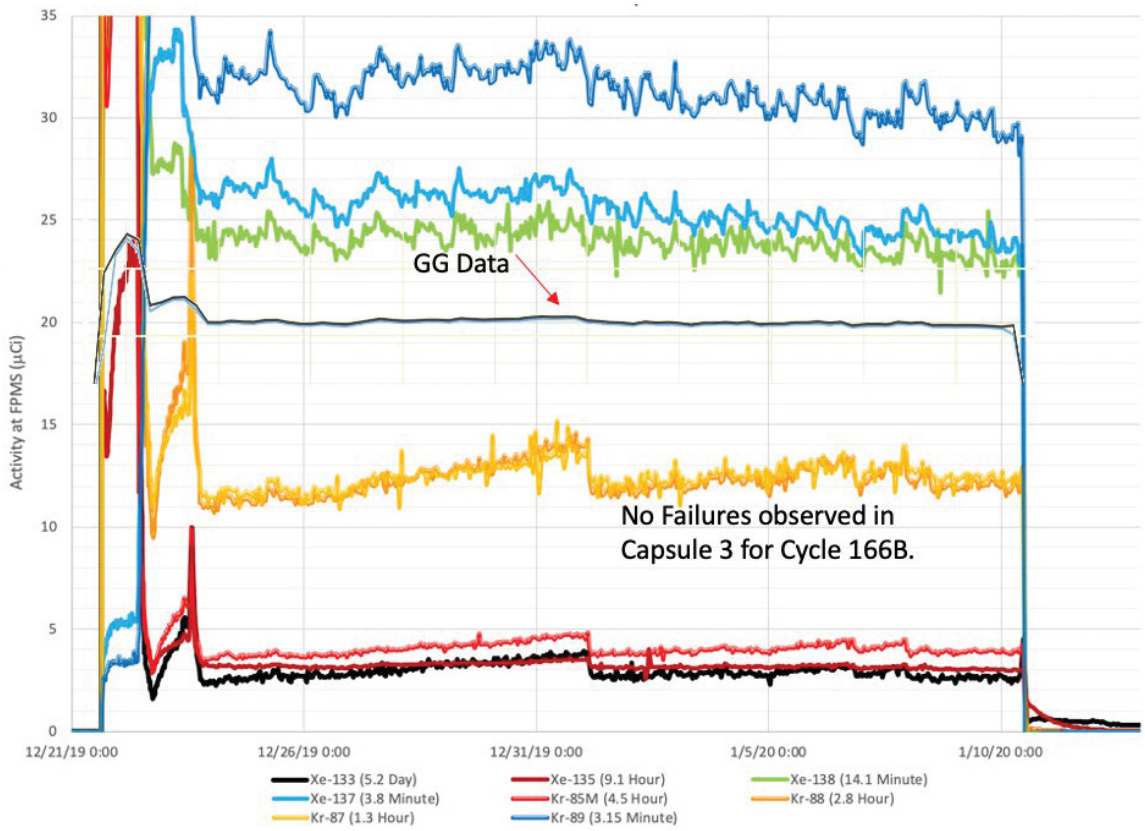

Figure 34. Cycle 166B, Capsule 3 comparison of isotopic and GG data demonstrating no identifiable particle failures.

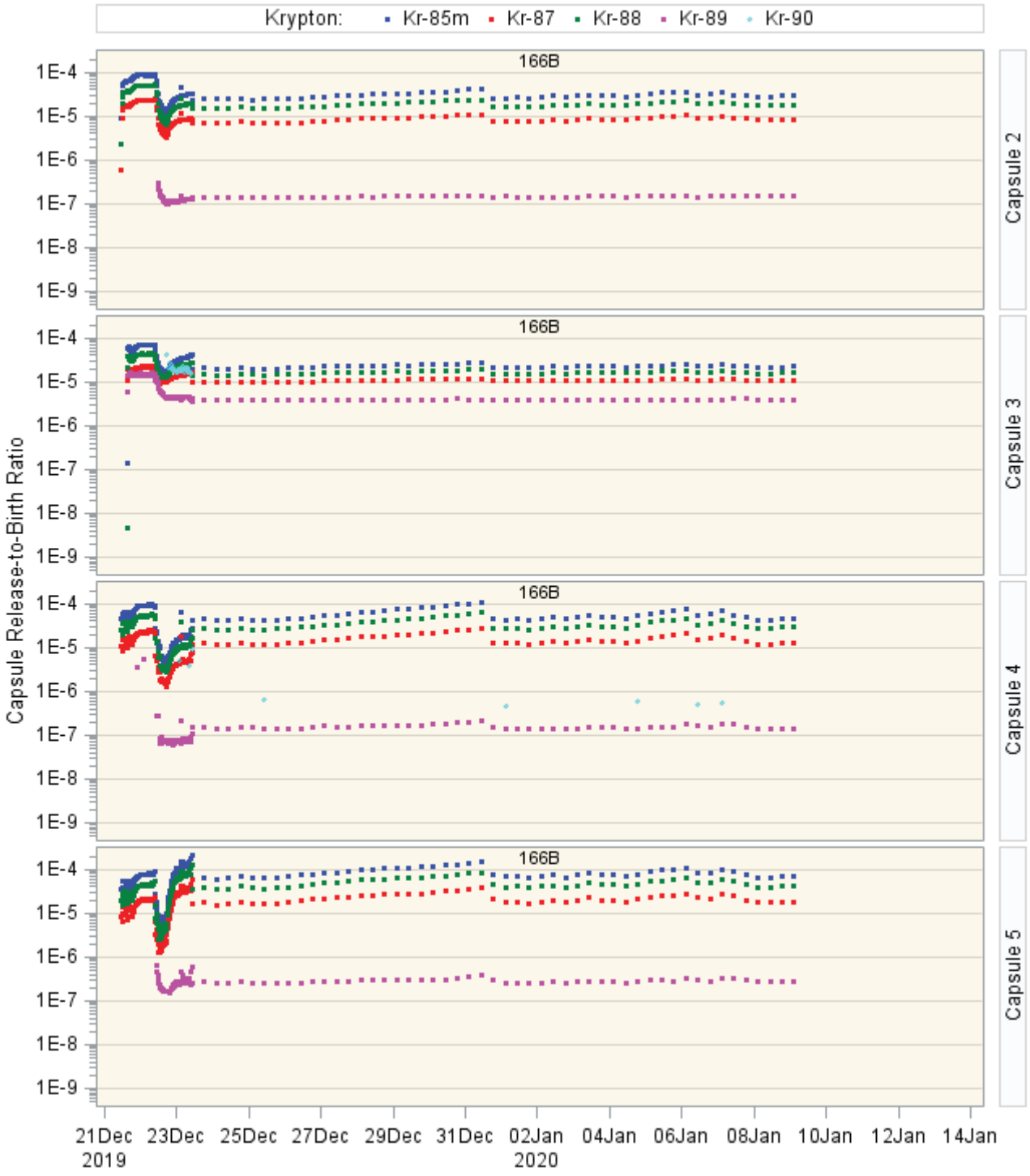

Figure 35. Cycle 166B release-to-birth ratios for selected krypton isotopes for AGR-5/6/7 Capsules 1–5.

Figure 36. Cycle 166B release-to-birth ratios for selected xenon isotopes for AGR-5/6/7 Capsules 1–5.

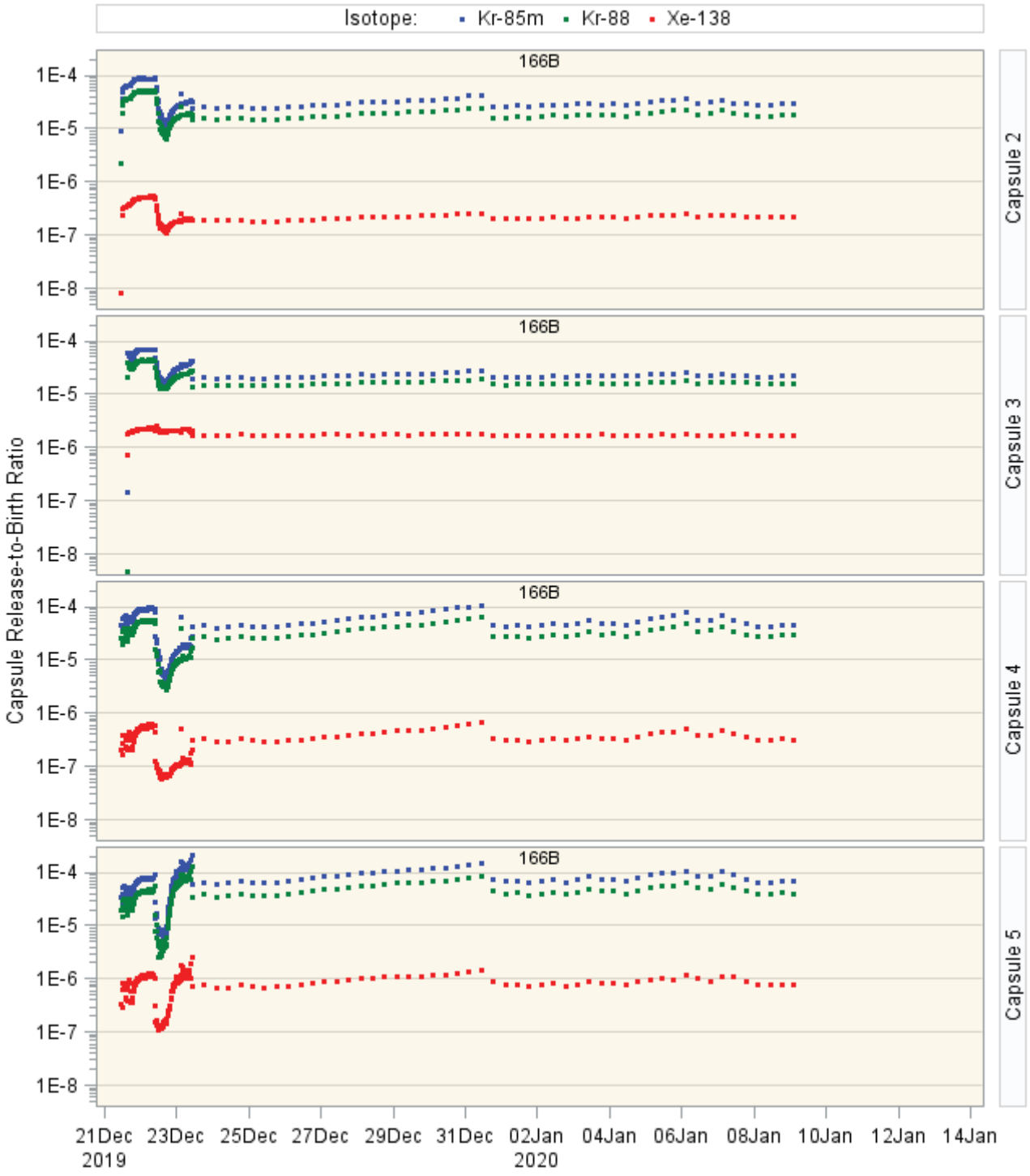

Figure 37. Cycle 166B release-to-birth ratios for selected krypton and xenon isotopes for AGR-5/6/7 Capsules 1–5 where equilibrium is believed to have been reached within the capsule based on half-life.

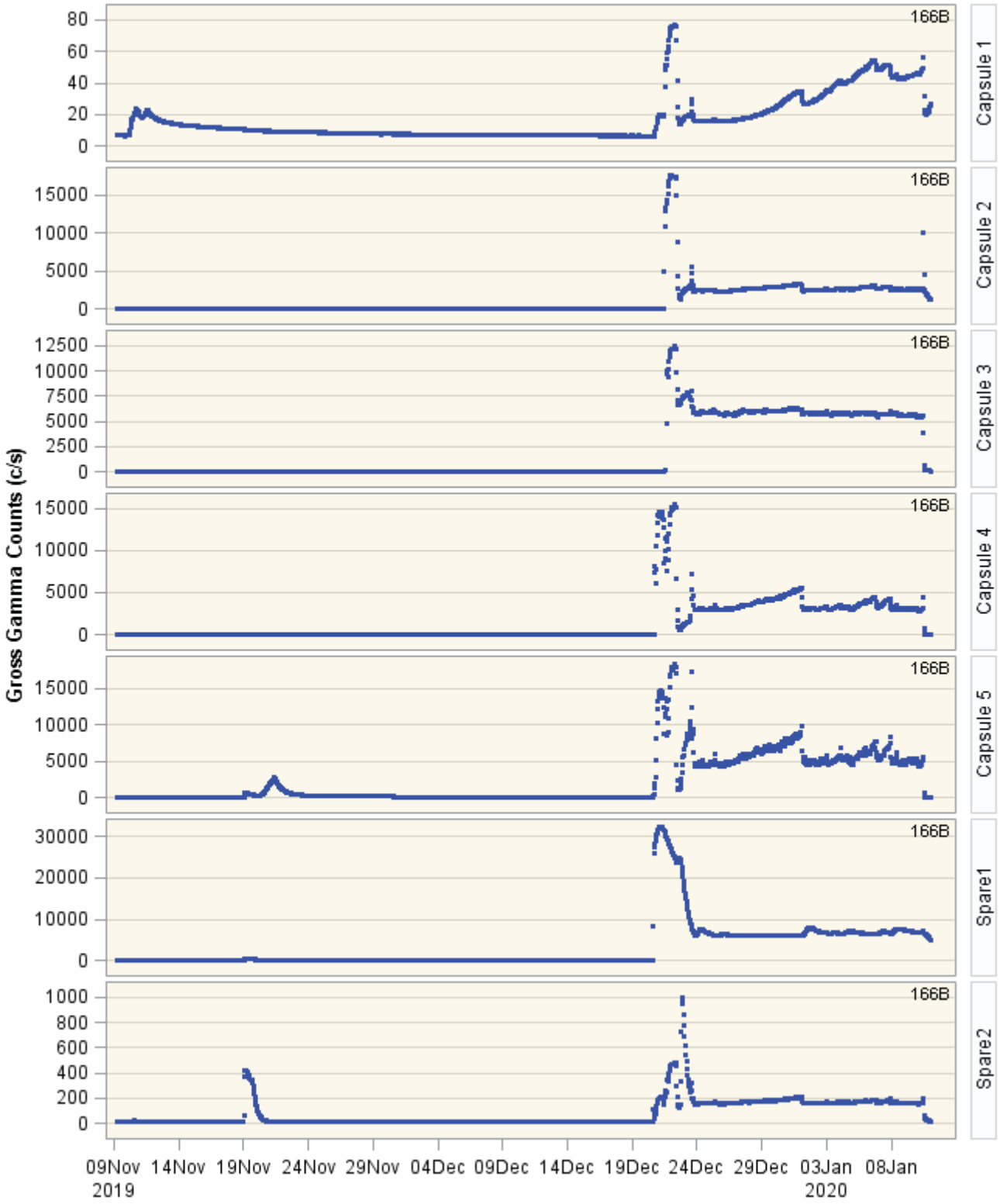

Figure 38. Cycle 166B GG release rate data AGR-5/6/7 Capsules 1–5 and Spare 1 and 2.

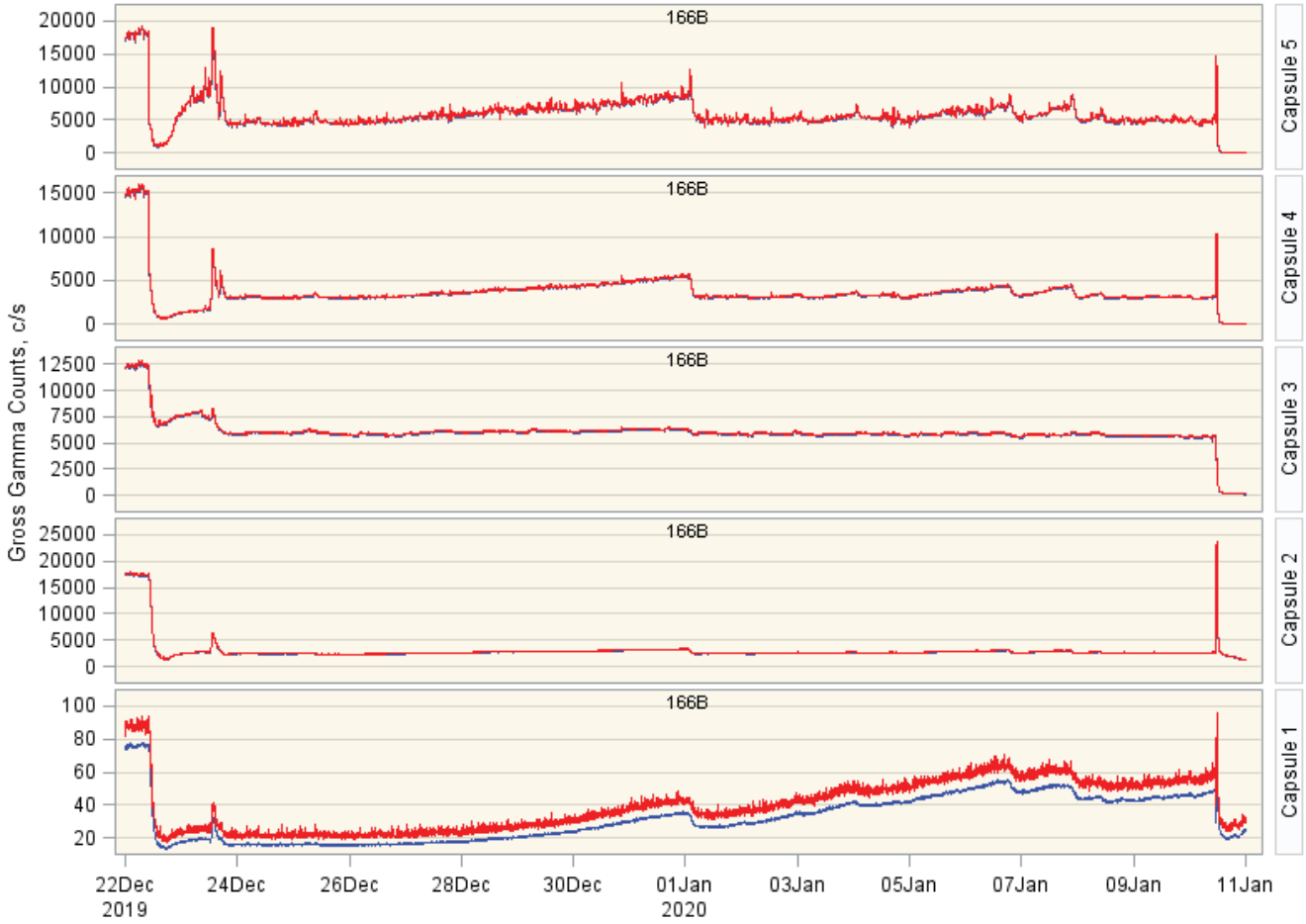

Figure 39. Cycle 166B GG data from December 22,2019 to the end of Cycle 166B. No clear indications of particle failures were present in Capsules 2–5.

7.12 Cycle 167A

Irradiation for Cycle 167A began on February 27, 2020 and ran through March 14, 2020. Cycle 167A was ran at 5 MW except for the last day of the cycle in which the power was increased to 20 MW. During this short cycle, an attempt was made to resume measurements of fission gas release from Capsule 1, and the gas relief valve was opened to allow a small flow of ~5 sccm to be delivered to Capsule 1. However, the outlet gas line was completely clogged resulting in zero Capsule 1 outlet flow. The R/B values for krypton and xenon are lower than average because of significantly lower fuel temperatures. Since the reactor was at full power for less than one day and fuel temperatures were low, there were no observable fuel failures as is illustrated in Figure 40–43.

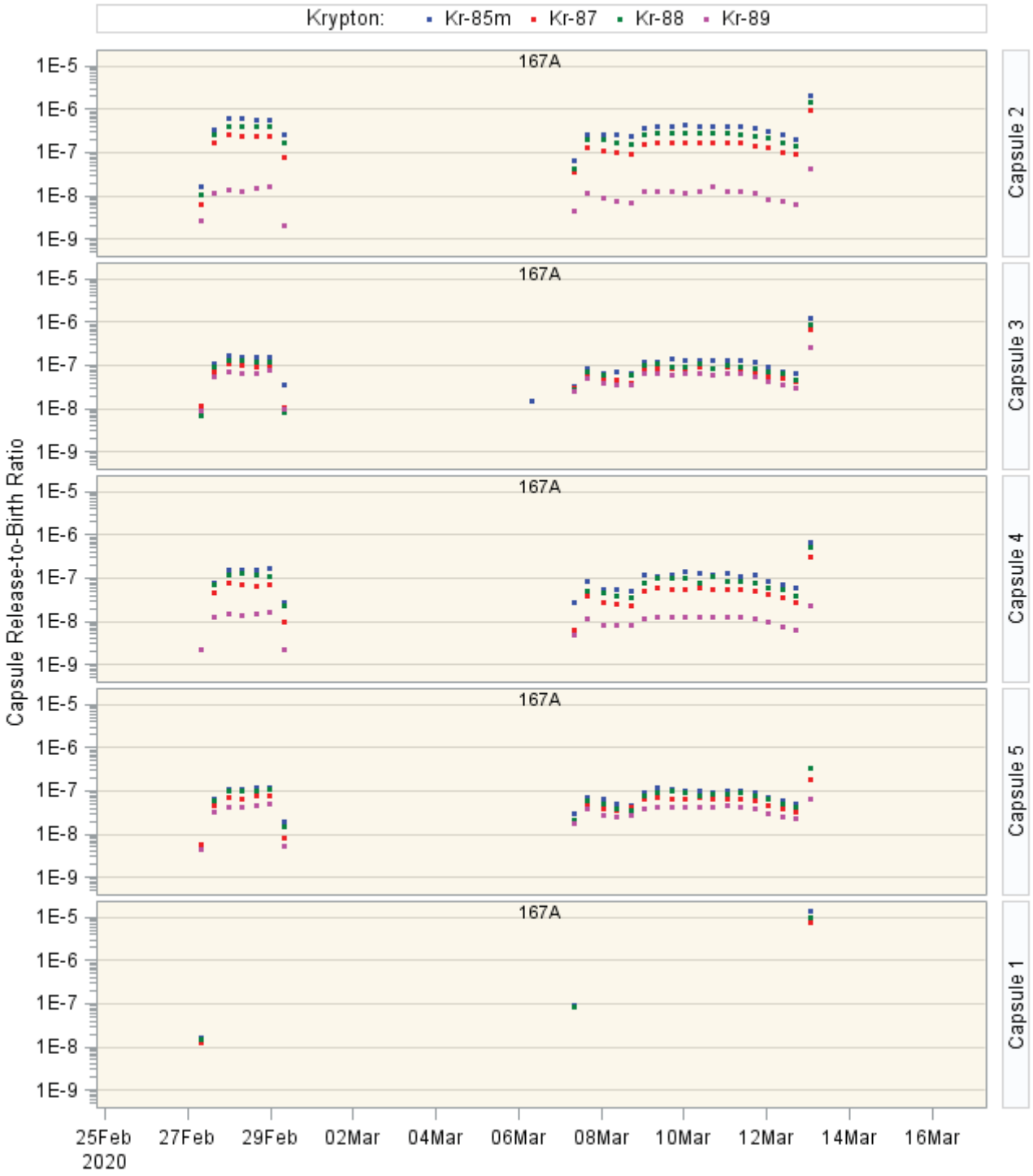

Figure 40. Cycle 167A release-to-birth ratios for selected krypton isotopes for AGR-5/6/7 Capsules 1–5.

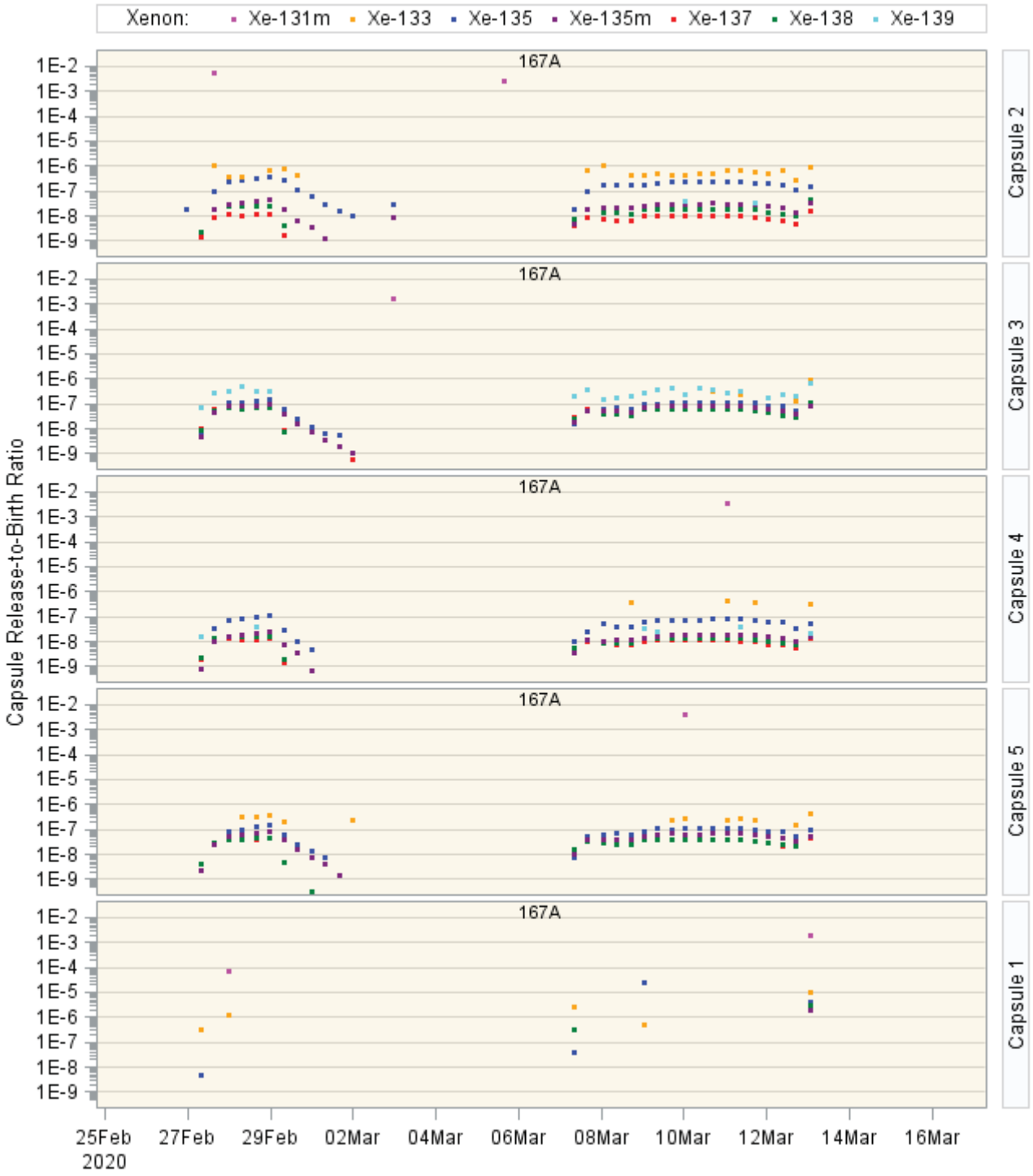

Figure 41. Cycle 167A release-to-birth ratios for selected xenon isotopes for AGR-5/6/7 Capsules 1–5.

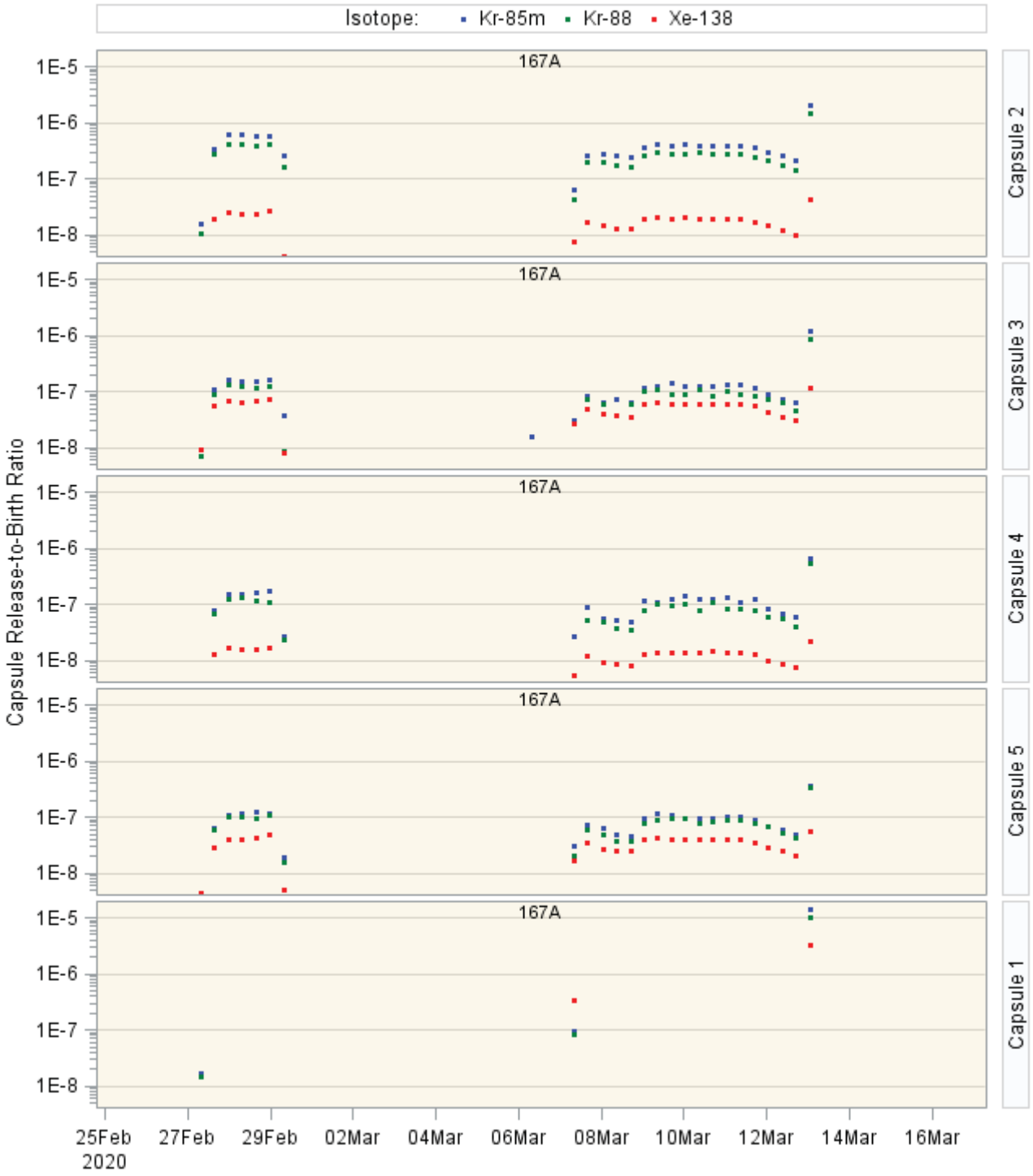

Figure 42. Cycle 167A release-to-birth ratios for selected krypton and xenon isotopes for AGR-5/6/7 Capsules 1–5 where equilibrium is believed to have been reached within the capsule based on half-life.

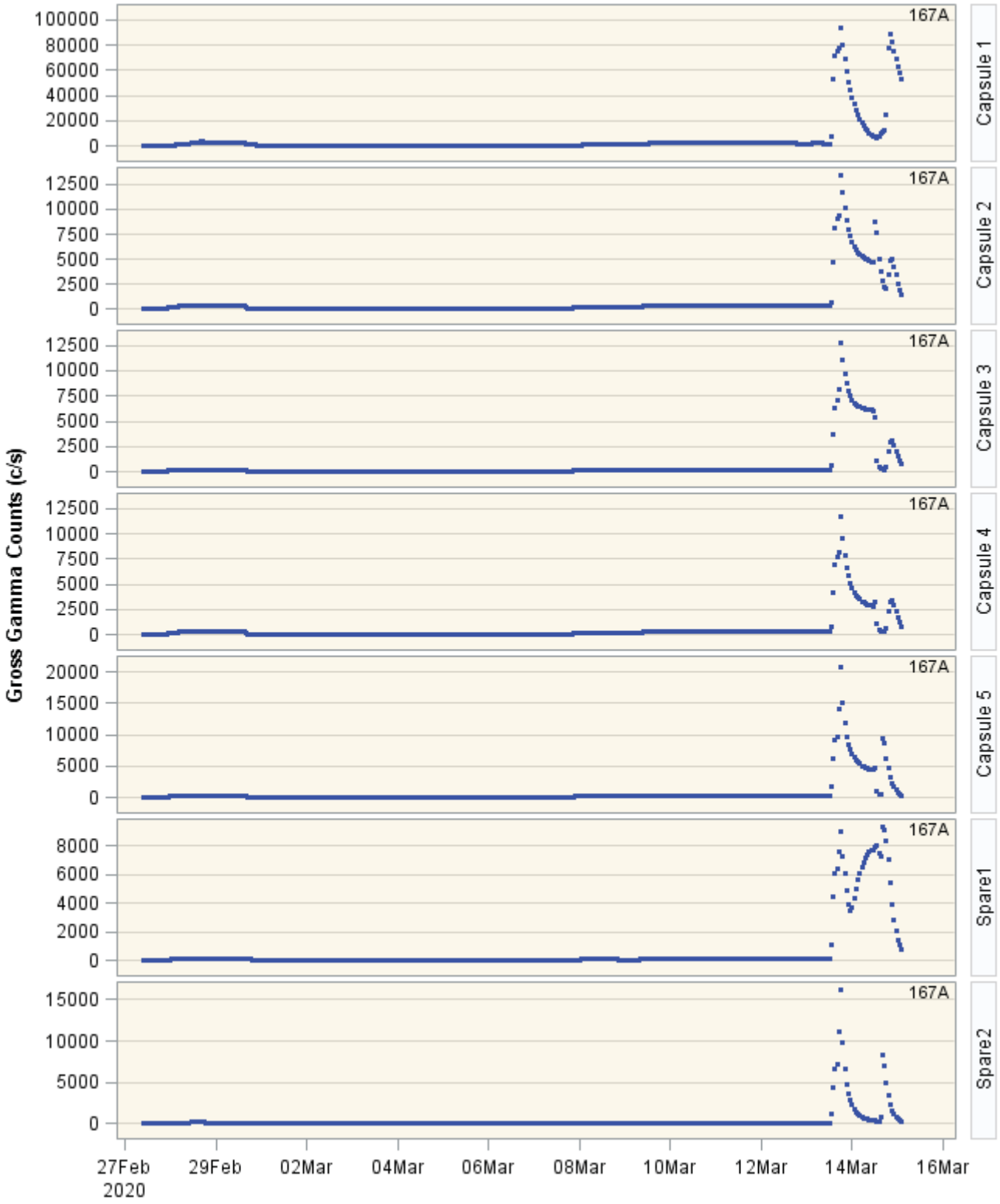

Figure 43. Cycle 167A GG release rate data AGR-5/6/7 Capsules 1–5 and Spare 1 and 2.

7.13 Cycle 168A

Irradiation for Cycle 168A began on April 13, 2020 and ran through July 22, 2020 with two SCRAMS from May 4–14, 2020 and June 2–July 2, 2020. Cycle 167A was maintained at a northeast lobe power of 20 MW. Since the failures that were observed in Capsule 1 at the end of Cycle 166A, fission gas from Capsule 1 was observed in every capsule. To try to quantify this, a test was planned for the beginning of Cycle 168A to test the diffusion effect. This test was performed by pushing neon into Capsule 1 and helium into all other capsules to search for the gamma signature of activated neon (Ne-23) in the Capsule 2–5 at the respective FPMS. A clear signature of activated neon was seen in the other capsules when this was done as shown in Figure 44.

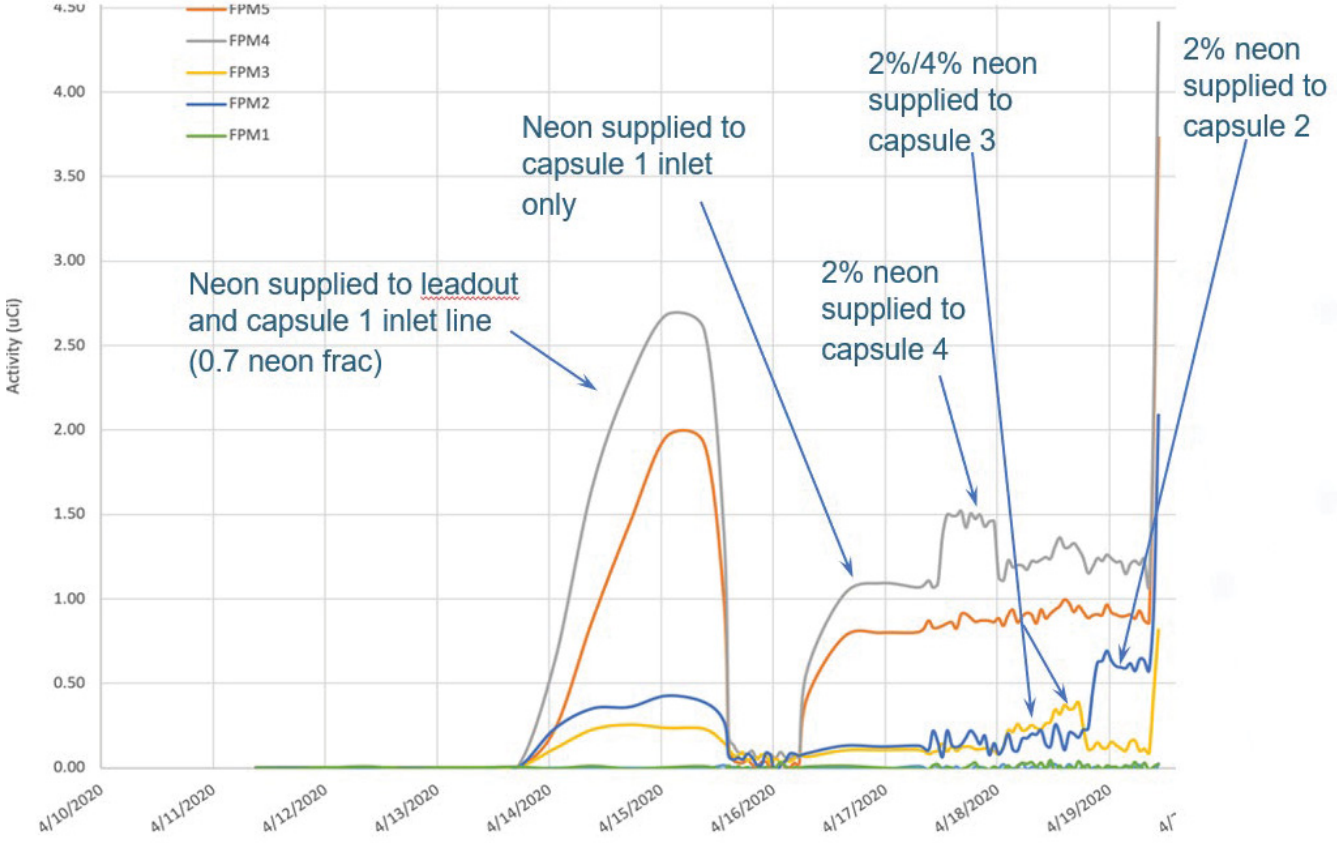

Figure 44. Activated Ne-23 activity showing contamination from Capsule 1 into Capsules 2–5 [11].

Capsule 1 FPM did not show much reliable activity because there was no flow through its outlet; however, all the other capsules showed a response in Ne-23 activity at the respective FPMS verifying that Capsule 1 was contaminating the other capsules. Once the initial test was completed, small amounts of neon were supplied to the other capsules to ensure that the FPM's were correctly reacting to activated neon. Diffusion calculations were also performed and are documented in ECAR-5114.

With Capsule 1 isolated and fission gas from leadout entering each subsequent capsule during Cycle 168A, the ability to assess fuel failures became more challenging. From a general observation of data from Figure 45through 47, it appears that new failures may have occurred in Capsule 2 and 3 but this

increase in activity could also be caused by contamination from the leadout into Capsule 2 and 3. To try to verify this, the GG data needs to be compared to the isotopic data obtained for the same time period.

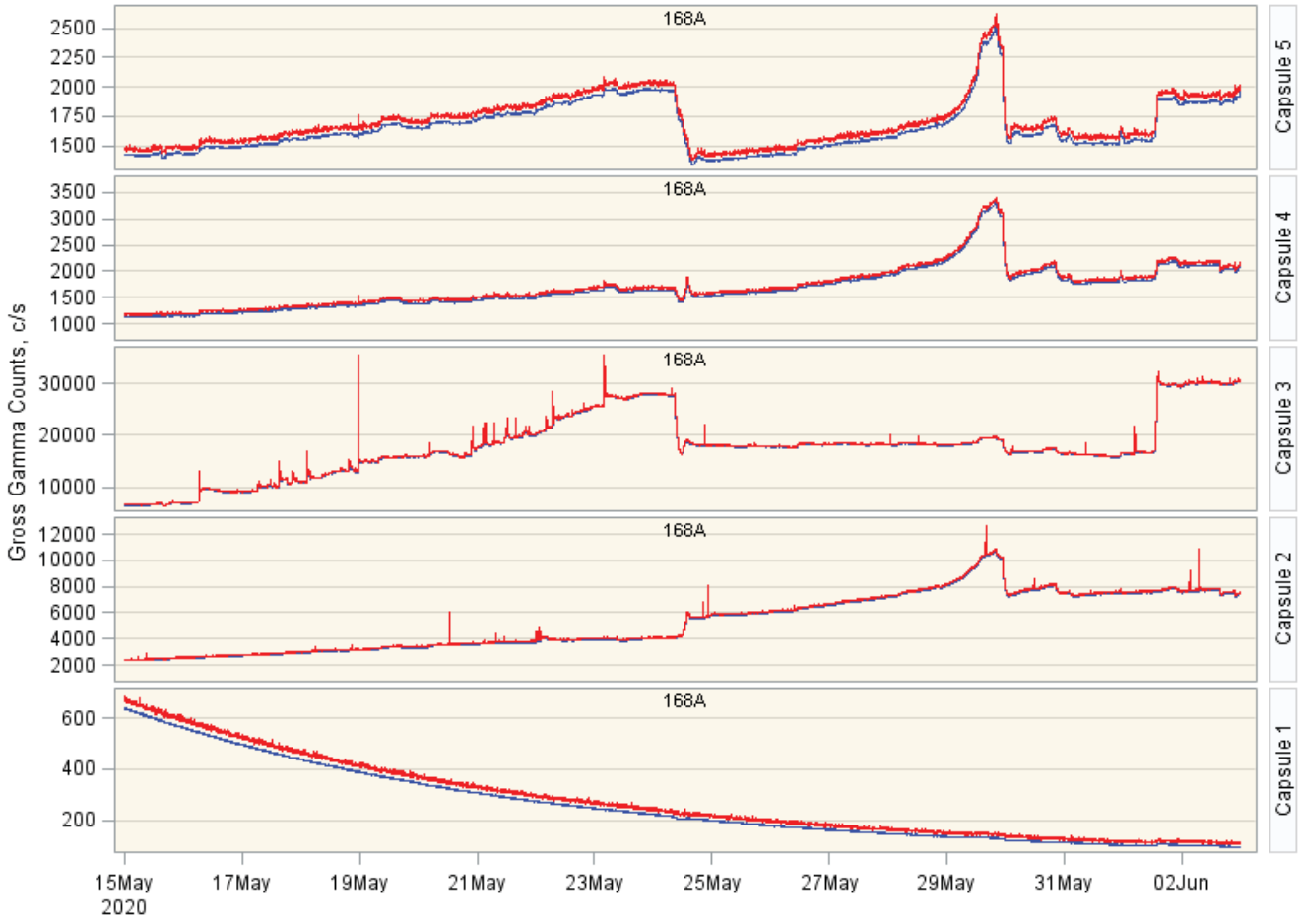

Figure 45. High-resolution GG data for the first half of Cycle 168A. Capsule 1 is isolated and the decrease in Capsule 3 activity from May 24–June 1, 2020 was the result of decreasing the temperature to Capsule 3.

For the time period of May 14–21, 2020, there appears to be approximately a handful of particle failures based on the consistent hourly activity values for each corresponding spike that was observed on the GG system using the long-lived Xe-133 isotope as the primary indicator of fuel performance (Figure 46). A look at the comparatively shorter-lived isotopes of Kr-85m, Kr-87, and Kr-88 also indicate a similar trend (see Figure 47) as these isotopes would have decayed away when traveling through the leadout into the respective capsules and passing in front of the respective FPMS. The question marks in Figure 47denote an increase in Xe-133 activity observed but may not be indicative of failed fuel. Examination of isotopic data and data from the GG for Capsule 3 for the period of July 3–22, 2020 yield no strong indication that additional particles failed during that timeframe. The GG line in Figure 48is overlayed on top of the isotopic data and is not plotted to scale for trending purposes.

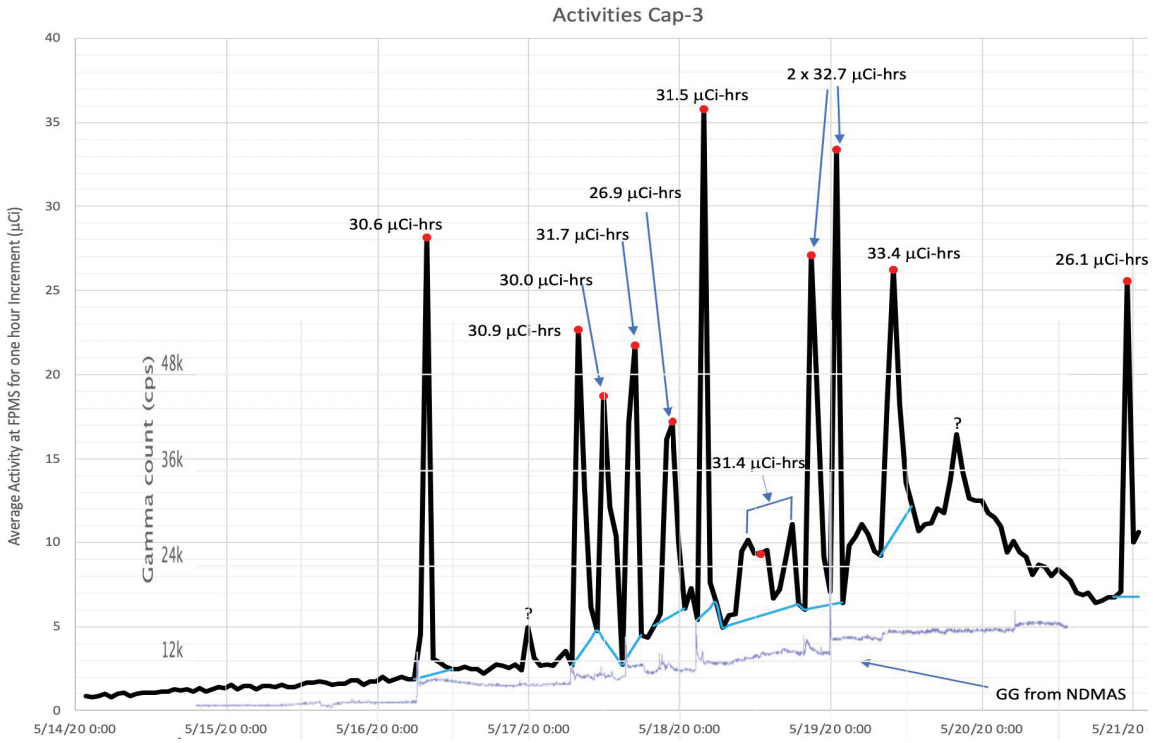

Figure 46. Cycle 168A, Capsule 3 hourly Xe-133 activity with corresponding GG data for May 14–21,2021.

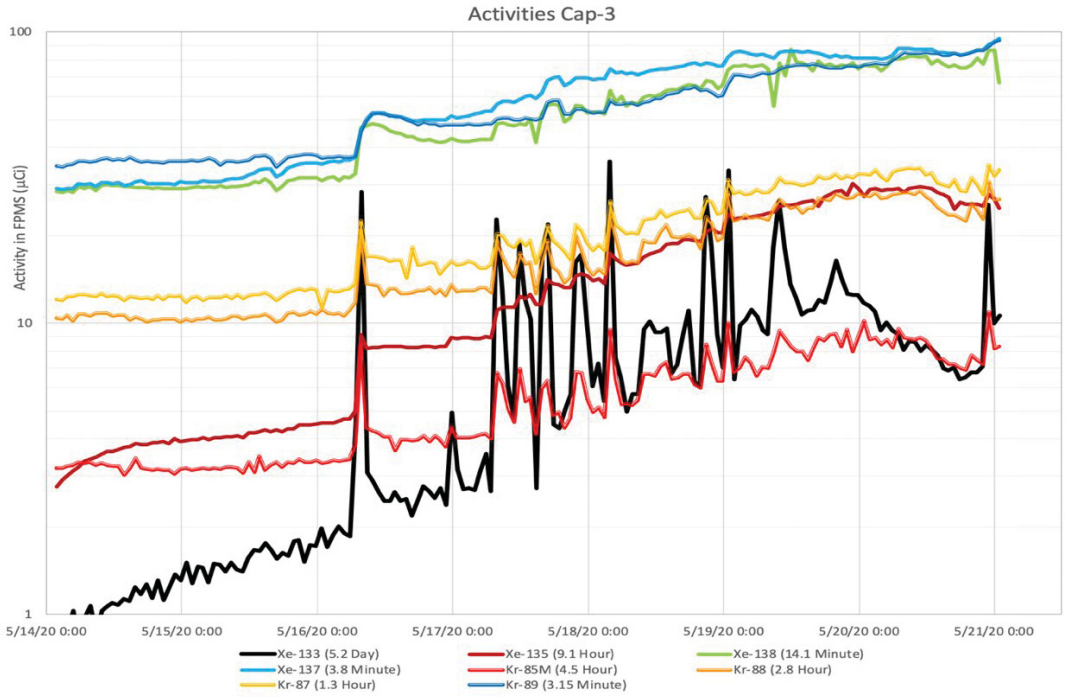

Figure 47. Cycle 168A, hourly isotopic activity for Capsule 3 from May14–21, 2020.

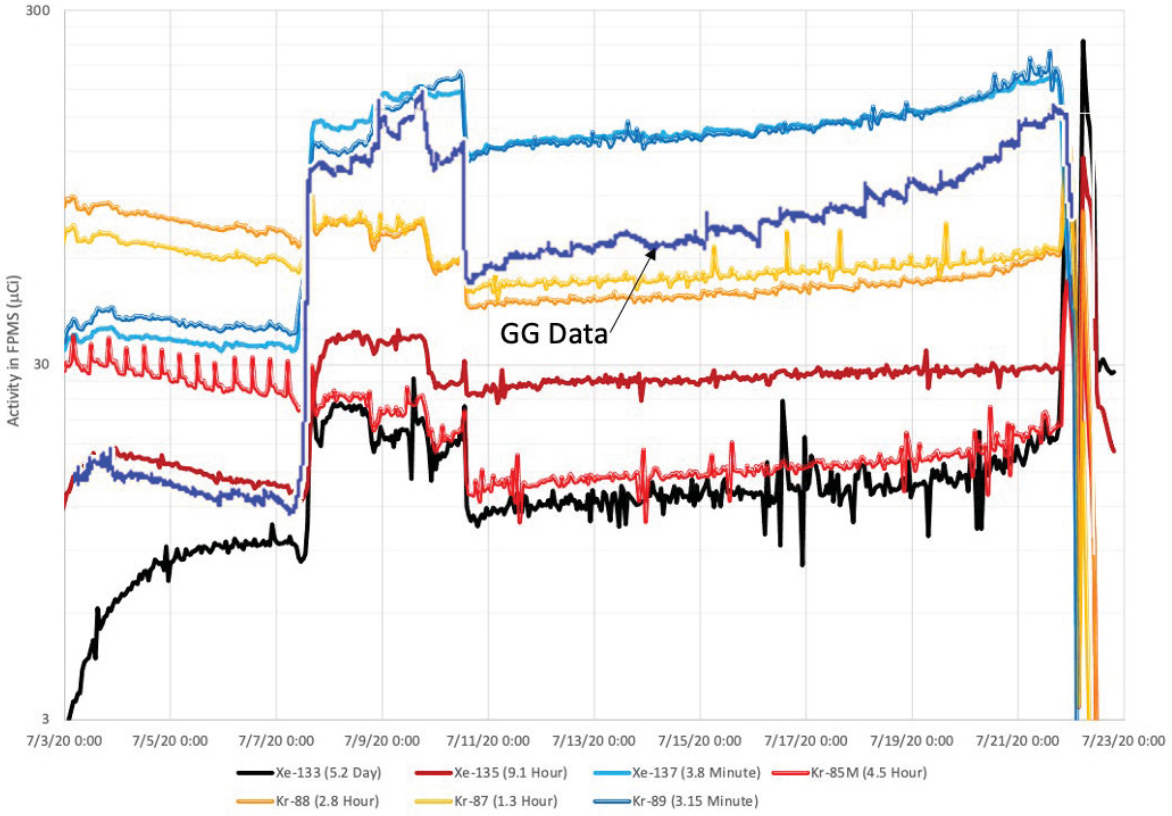

Figure 48. Cycle 168A, hourly isotopic activity with GG data overlayed for Capsule 3 from July 3–22, 2020.

What we have learned from past AGR experiments is even though the “spikes” resemble classic “particle failures,” they may not always be particle failures, and the events observed on the GG system (see Figure 49) are system indicators that need to be coupled with isotopic information. Xe-133 was selected because of its long half-life and the fact that it is primarily seen in systems where fuel has failed.

Figure 50captures the GG events (3.5 s) overlaid on 1-hour incremental isotopic data for Capsule 2 from April 20–April 23, 2020. As can be seen, some of the increases in the GG activities correlate to the increase in Xe-133. Unlike the analysis performed for Capsule 3, the Xe-133 activity is not consistently in a particular mCi-hr range. If you recall for Capsule 3, the size of the activity spikes in Xe-133 were all consistently in the 26–33 mCi-hr range. The consistency in size suggested single particle failures. The range for Capsule 2 data for this period ranges from 7–20 mCi-hr. Some of these events occurred over an hour of time while the Xe-133 activity peaks during that time are not represented by the classic “particle failure” model. We have seen this sort of behavior in past AGR experiments, and these longer events can be classified as failures that did not result in the same level of fission product release. Upon closer examination in Figure 51, notice that Xe-135 and Kr-85M also trend with the Xe-133 isotope; however, the method of fission gas release is not the same as in Capsule 3. This could because Capsule 2 is geometrically different from Capsule 3 and the method by which fission gas diffuses out of the capsule is at different rate.

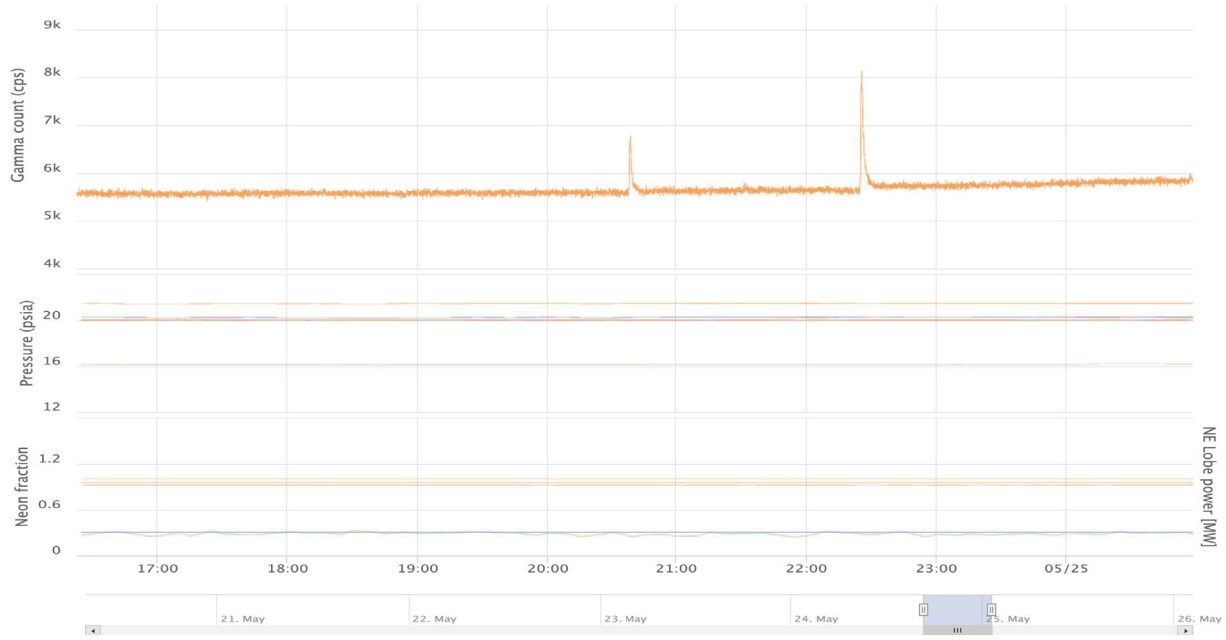

Figure 49. Cycle 168A, Capsule 2. A GG event was observed on May 24, 2020 which resembles a "classic" particle failure.

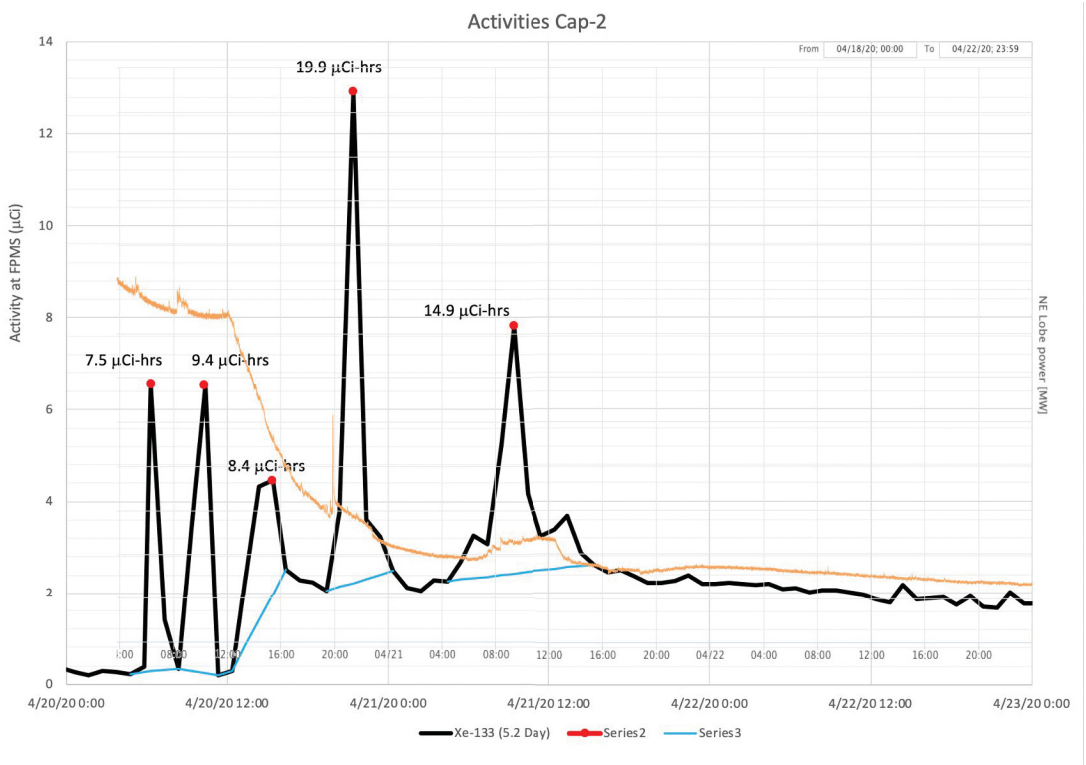

Figure 50. Cycle 168A, Capsule 2 for April 20–23, 2020. A comparison of Xe-133 to the overlaid GG data.

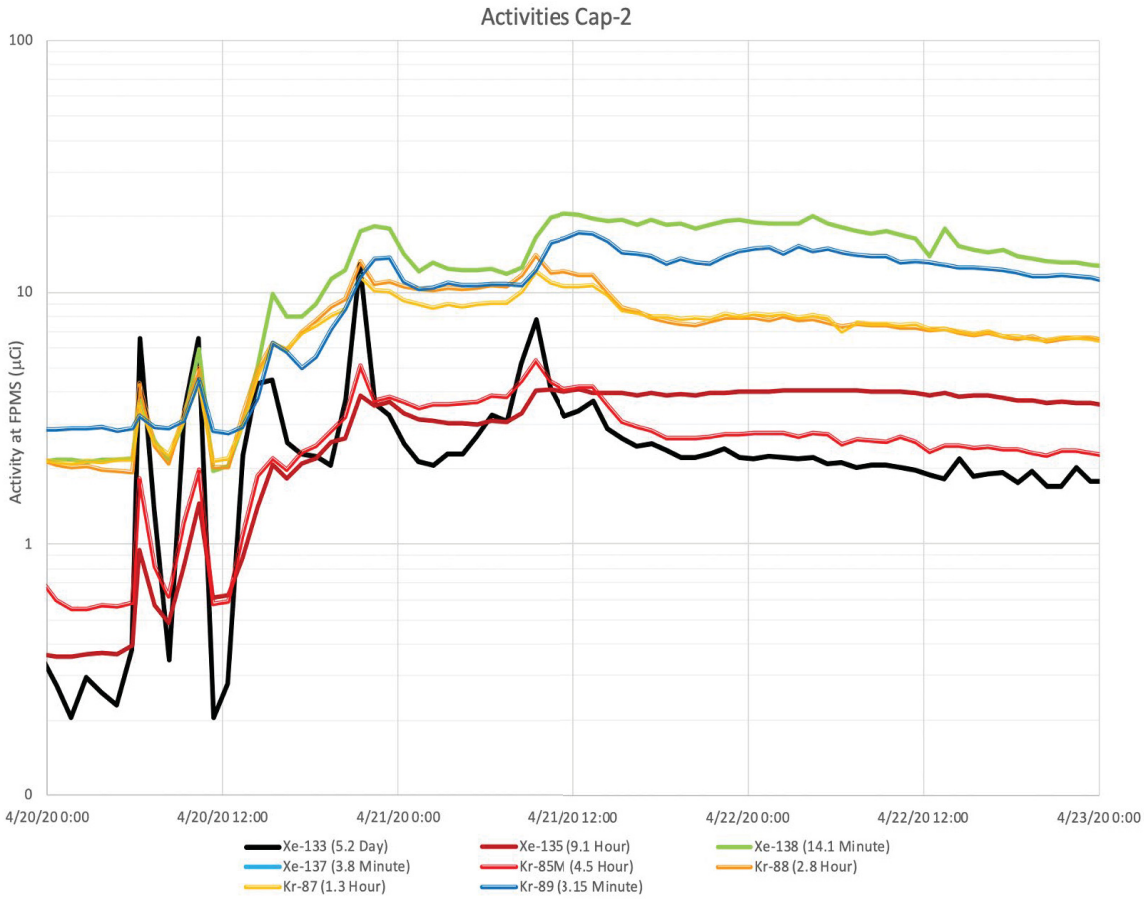

Figure 51. Cycle 168A, Capsule 2 for April 20–23, 2020.

The method of reviewing Xe-133 was also applied to the timeframe from May 18–26, 2020 (see Figure 52). The GG during this period captured many spikes in activity during this timeframe. Some of these events span longer periods of time and are smeared in the 1-hour incremental measurements as the events in the GG system happened within minutes. The increases in Xe-133 with question marks over the peaks can be failures, but the activity of that region is considerably less than areas where the Xe-133 has a drastic uptick. In the the question mark data, the GG shows multiple increases in activity in a relatively short amount of time. Examination of isotopic data and data from the GG for Capsule 2 for July 3–22, 2020 yield no strong indication that additional particles failed during that timeframe. The GG line in Figure 53is overlayed on top if the isotopic data and is not plotted to scale for tending purposes.

Figure 54–57 are summarized plots for the entire Cycle 168A. Flow to Capsule 1 was mostly isolated with several unsuccessful attempts to flow small amount of gas for fission gas release measurement at the respective FPMS. To obtain the measurements, the leadout outlet line was opened with lower pressure than pressure in Capsules 2–5. In-leakage from the leadout into all of the capsules is apparent in Figure 54-57. From a review of the data, a few particle failures may have occurred in Capsule 2 due to the close proximity and fission gas leakage from Capsule 1. If the leak in Capsule 1 is near the capsule head, then it is in close proximity to the base of Capsule 2 where the leadout gas can enter through the gaps and the thru- tubes and penetrate the capsule base. Capsule 3 had on the order of a dozen GG spikes typical of a particle failure. These spikes and subsequent increase in GG

background indicate that particle failures occurred in this capsule. Capsules 4 and 5 had no apparent spikes, and their variations in GG counts could be attributed to a small leakage of fission gas from Capsule 1.

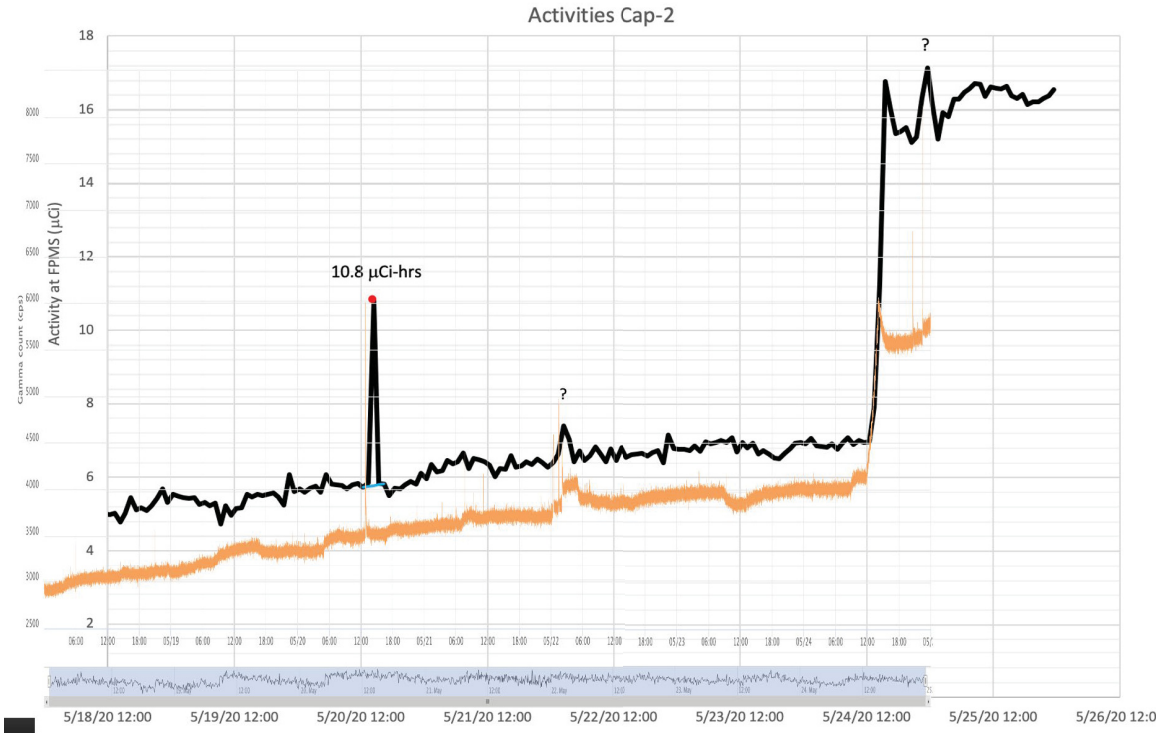

Figure 52. Cycle 168A, Capsule 2 for May 18–26, 2020.

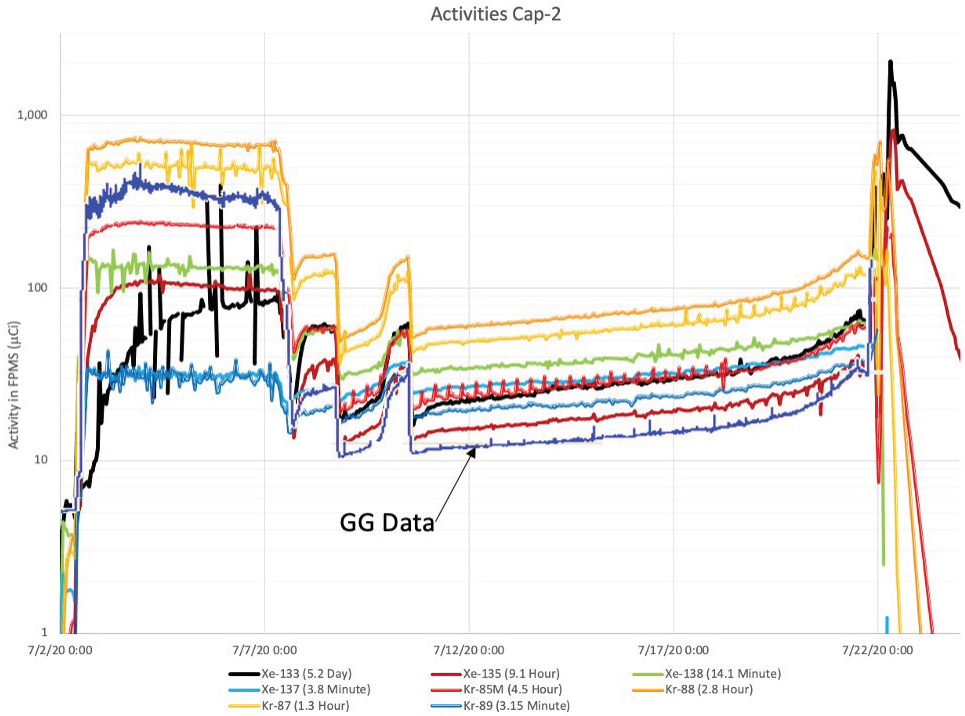

Figure 53. Cycle 168A, hourly isotopic activity with GG data overlayed for Capsule 2 from July 3–22, 2020.

Figure 54. Cycle 168A release-to-birth ratios for selected krypton isotopes for AGR-5/6/7 Capsules 1–5.

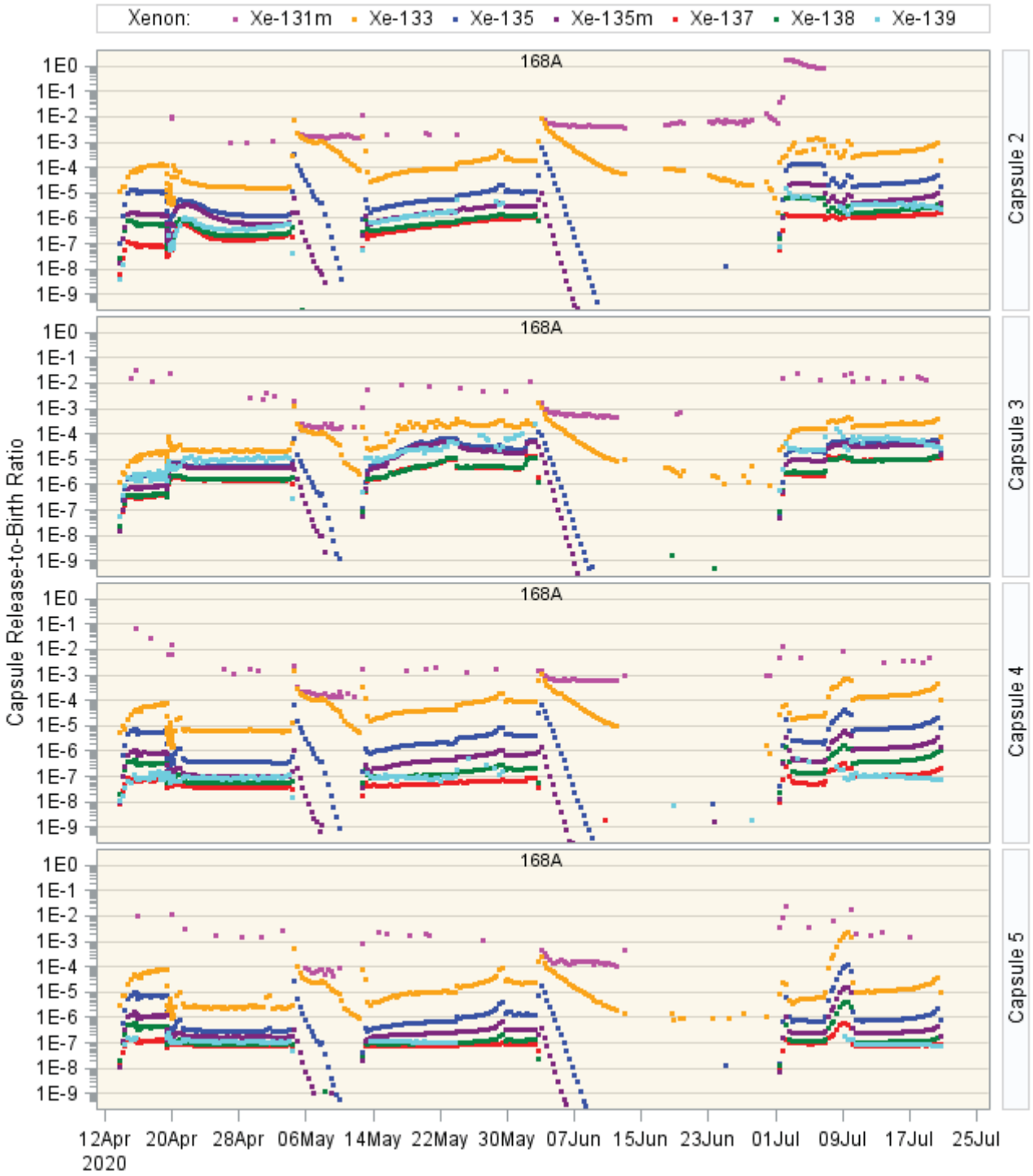

Figure 55: Cycle 168A release-to-birth ratios for selected xenon isotopes for AGR-5/6/7 Capsules 1–5. The decay of Xe-133 and presence and decay of Xe-131m is apparent during the reactor shutdown periods which is indicative of the presence of Capsule 1 fission gas in all capsules.

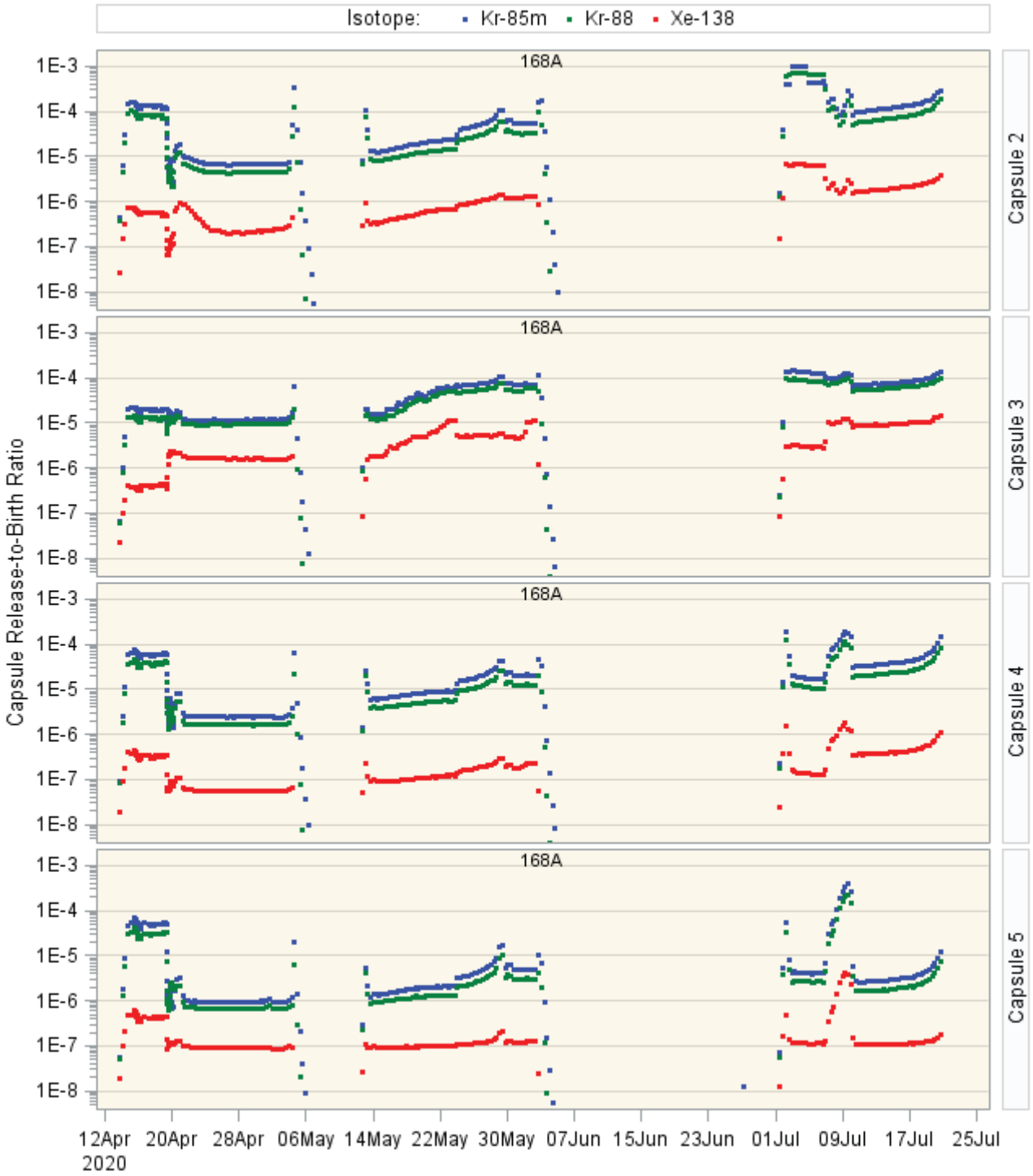

Figure 56. Cycle 168A release-to-birth ratios for selected krypton and xenon isotopes for AGR-5/6/7 Capsules 1–5 where equilibrium is believed to have been reached within the capsule based on half-life.

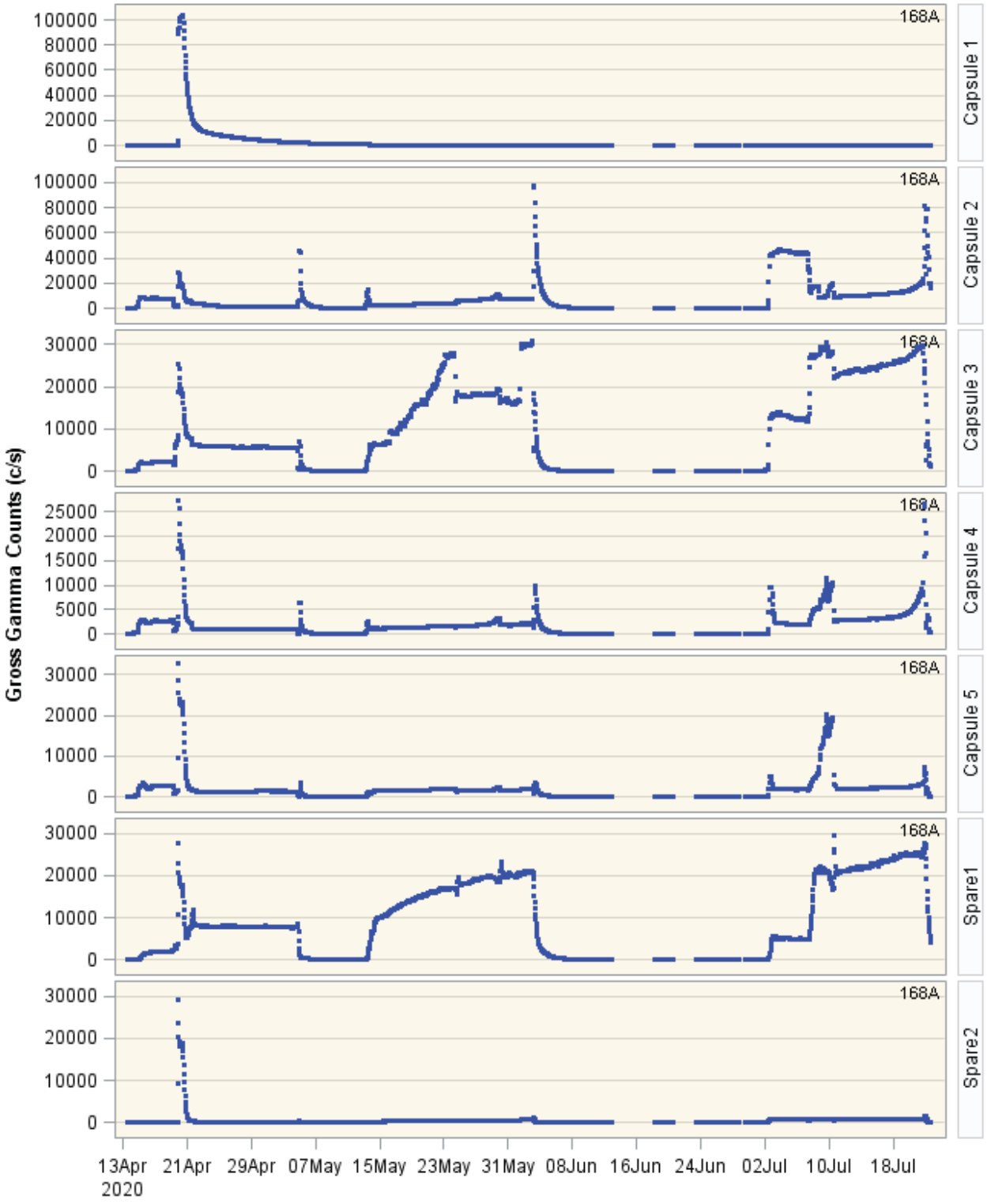

Figure 57. Cycle 168A GG release rate data AGR-5/6/7 Capsules 1–5 and Spare 1 and 2. Spare 1 is monitoring the leadout flow which is contaminated from Capsule 1.

7.14 Conclusion

The AGR-5/6/7 experiment was irradiated from February 16, 2018 to July 22,2020 in the north east flux trap. All AGR-5/6/7 operating cycle R/Bs and GG data were reviewed for accuracy and completeness. Figure 58–61 summarize the R/Bs and GG data for the entire AGR-5/6/7 experiment.

For all cycles evaluated in this report, there are no indications that the FPMS failed to capture data reliably with the exception being at the end of Cycle 166A where experimental conditions involving Capsule 1 led to the total detector saturation for FPMS Station 1. During irradiation and at the end of each cycle, each FPM was put through an “On the Fly” energy calibration [7] and a standard energy calibration test. All data were reliably verified per test plans mentioned earlier in this document.

The performance of nuclear fuel is typically evaluated using the R/B ratio, which is the ratio of the released activity of an isotope from the fuel to the predicted birth rate of the isotope during irradiation. Daily fission product birthrates for the following 12 isotopes were provided by as-run neutronics calculations: Kr-85m, Kr-87, Kr-88, Kr-89, Kr-90, Xe-131m, Xe-133, Xe-135, Xe-135m, Xe-137, Xe-138, and Xe-139. These birthrates were coupled to the calculated release rates obtained from isotopic activities measured at the FPMS.

This ECAR detailed the calculational method used to determine the R/B for the 12 measured isotopes, Kr-85m, Kr-87, Kr-88, Kr-89, Kr-90, Xe-131m, Xe-133, Xe-135, Xe-135m, Xe-137, Xe-138, and Xe-139. Release activities were reported as an average for the 8-hour counting interval during normal irradiation conditions to reduce measurement uncertainty. However, during the initial test of the leadout flow system, release rates were recorded at a much higher frequency, which led to a slightly higher uncertainty.

During the first five cycles (i.e., 162B–165A), fission-gas isotope R/B ratios were stable in the 10^{-8}–10^{-6} range and no in-pile particle failures were observed based on the GG counts. During this time, the higher exposed kernel fraction and high-fuel particle temperatures in Capsule 1 led to the maximum R/B value of around 2×10^{-6} for Kr-85m. Table 4 provides a summary of the measured R/B and their uncertainty statistics for the krypton and xenon isotopes of interest for the first AGR-5/6/7 cycles. A comprehensive summary table can be found in Appendix H.

The gas line issues in Capsule 1 occurred from the fourth cycle (i.e., 164B) and were mitigated to minimize crosstalk between capsule gas lines. Since Capsule 1 was isolated, its fission product release measurements were not possible during the last three cycles (i.e., 166B, 167A, and 168A). Capsule 1 gas line issues caused fission gas leakage into Capsules 2–5 to various degrees over time starting from Cycle 166A. By the end of Cycle 166A, a significant number of in-pile failures occurred in Capsule 1, causing a substantial increase in fission gas activities and saturated the FPMS HPGe detector, increasing activity in the 1A primary that was picked up by the GG NaI(Tl) detectors.

Capsule 1 gas line issues caused fission gas leakage into Capsules 2–5 to various degrees over time starting from Cycle 166A. Particularly, increased and unstable R/Bs for most isotopes in Capsules 4 and 5 can be attributed to fission gas leakage from Capsule 1. As a result, R/Bs for all capsules from mid-cycle of Cycle 166A are considered uncertain because of undefined contamination from Capsule 1. However, they can be used when the leaking amount from Capsule 1 can be roughly estimated or

negligible (i.e., FG activity leakage from Capsule 1 for short-lived isotopes can be considered negligible due to decay before reaching Capsules 4 and 5).

Table 4. AGR-5/6/7 measured R/B and uncertainty statistics for krypton and xenon isotopes for the first five cycles (162B-165A).

Isotope	Half-life (min)	Measured R/B			Uncertainty [a] (%)		
		Average	Minimum	Maximum	Average	Minimum	Maximum
Kr-85m	268.7	3.53E-07	2.15E-10	1.95E-06	6.8	5.8	49.5
Kr-88	170.4	2.35E-07	1.16E-09	8.26E-07	6.4	5.8	24.5
Kr-87	76.0	2.88E-07	7.35E-11	1.11E-06	6.9	5.8	42.3
Kr-89	3.2	6.36E-08	5.74E-10	5.11E-07	9.7	5.8	36.2
Kr-90	0.5	1.40E-06	3.02E-09	3.44E-05	33.6	13.9	49.6
Xe-131m	17162.0	2.60E-03	3.74E-05	3.03E-02	42.0	27.5	50.0
Xe-133	7558.9	6.10E-07	4.28E-09	7.87E-05	17.8	6.0	50.0
Xe-135	545.8	1.47E-07	1.12E-09	9.09E-07	6.8	5.8	48.5
Xe-135m	15.3	9.89E-08	6.10E-10	6.07E-07	6.5	5.8	27.6
Xe-138	14.1	3.24E-08	5.34E-10	3.16E-07	8.8	5.8	33.8
Xe-137	3.8	5.31E-08	6.51E-11	2.71E-07	6.2	5.8	37.0
Xe-139	0.7	1.89E-08	3.72E-10	1.18E-06	33.0	9.5	50.0

[a] Only R/B values with uncertainty less than 50% and a standard 8-hour interval are used.

Green rows are for shortest isotopes with uncertainty less than 10% on average.

Red rows are for either too short or too long isotopes high uncertainty (more than 30% on average).

In addition, numerous particle failures were also observed in Capsule 3 and perhaps a few in Capsule 2 during Cycle 168A. No in-pile failures were observed in Capsules 4 and 5 and is supported by the lack of distinct increases in activity as captured by the GG system. Increased and unstable R/Bs in Capsules 4 and 5 can be contributed to fission gas leakage from Capsule 1. R/B's for all capsule from mid-cycle of Cycle 166A are considered suspect because of contamination from Capsule 1. While the data are considered inadequate for quantitative determination of the number of particle failures that may have occurred in Capsules 2 – 5, they can be used to establish approximate, conservative upper bounds on particle performance. The bounding conditions will be addressed in the final AGR-5/6/7 as-run report.

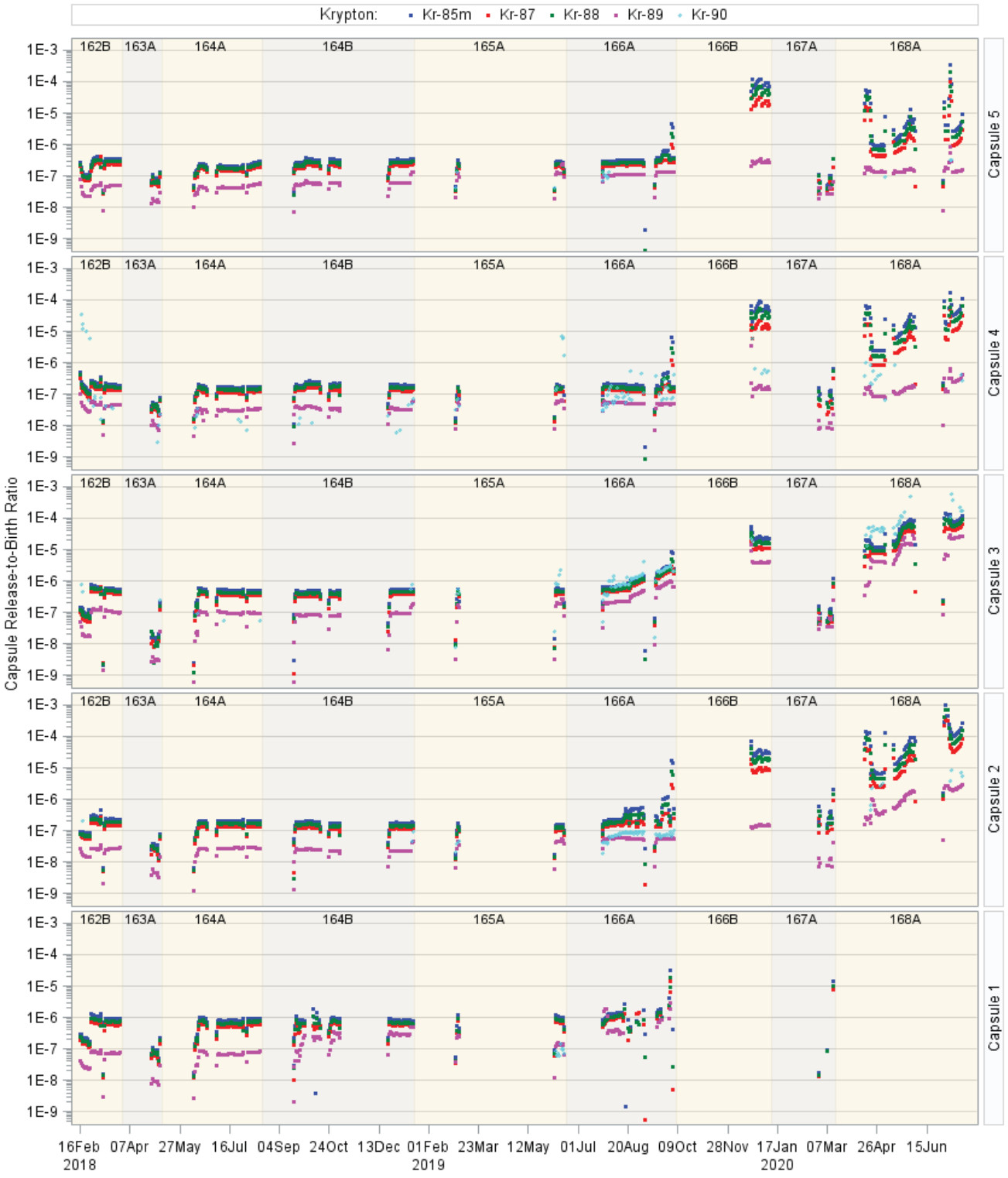

Figure 58. Summary of AGR-5/6/7 release-to-birth ratios for selected krypton isotopes for Capsules 1–5.

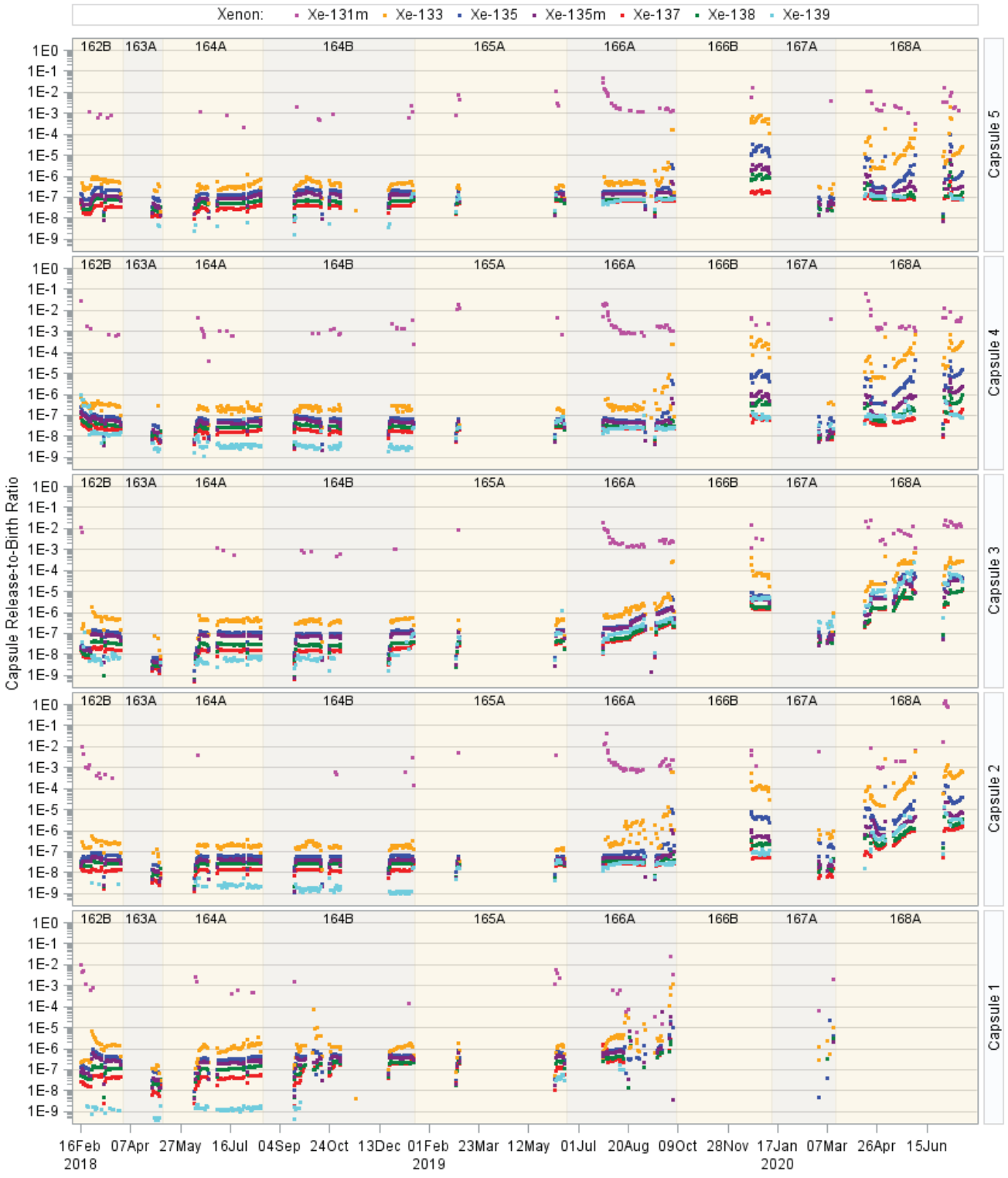

Figure 59. Summary of AGR-5/6/7 release-to-birth ratios for selected xenon isotopes for Capsules 1–5.

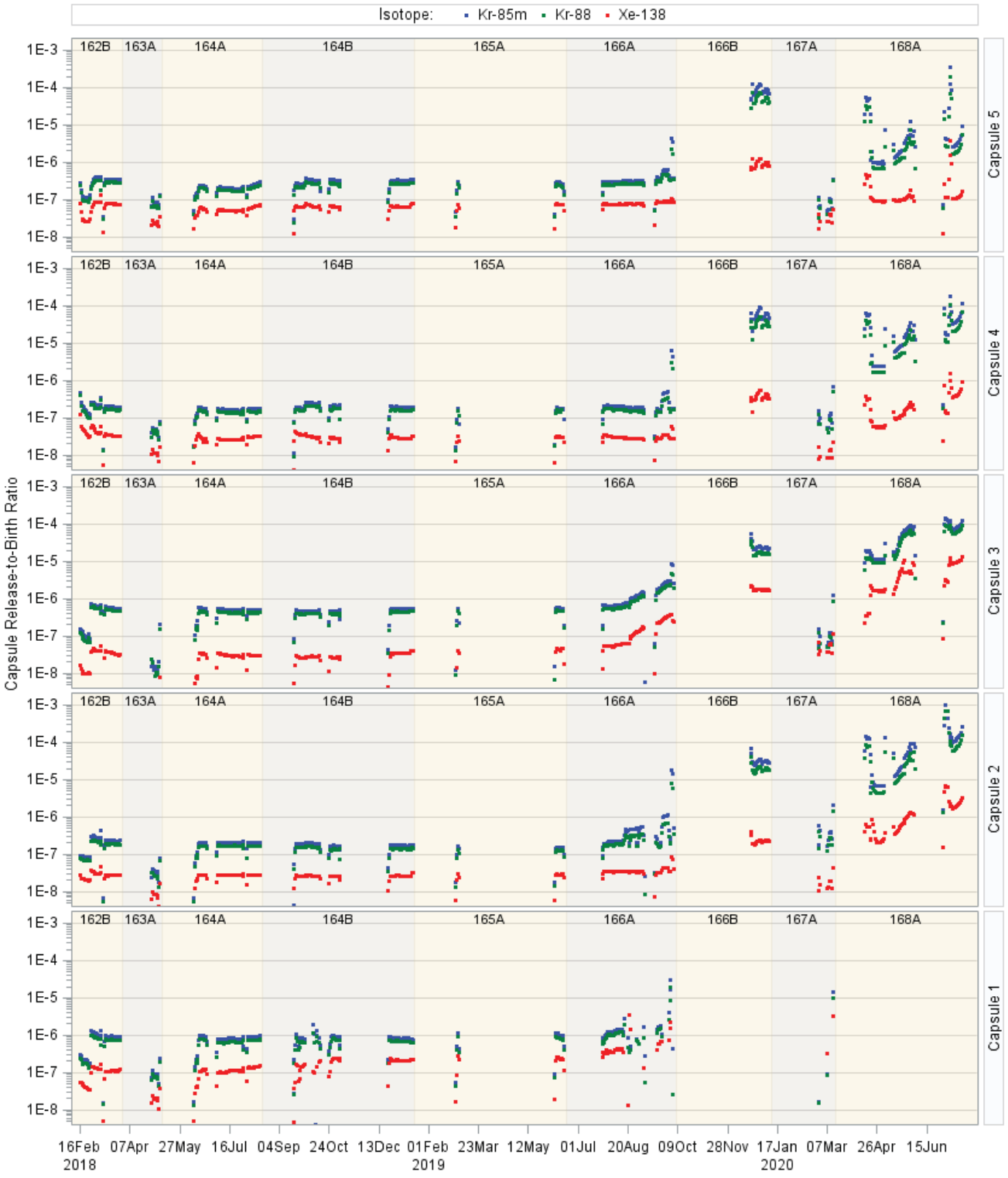

Figure 60. Summary of AGR-5/6/7 release-to-birth ratios for selected krypton and xenon isotopes for Capsules 1–-5 where equilibrium is believed to have been reached within the capsule based on half-life.

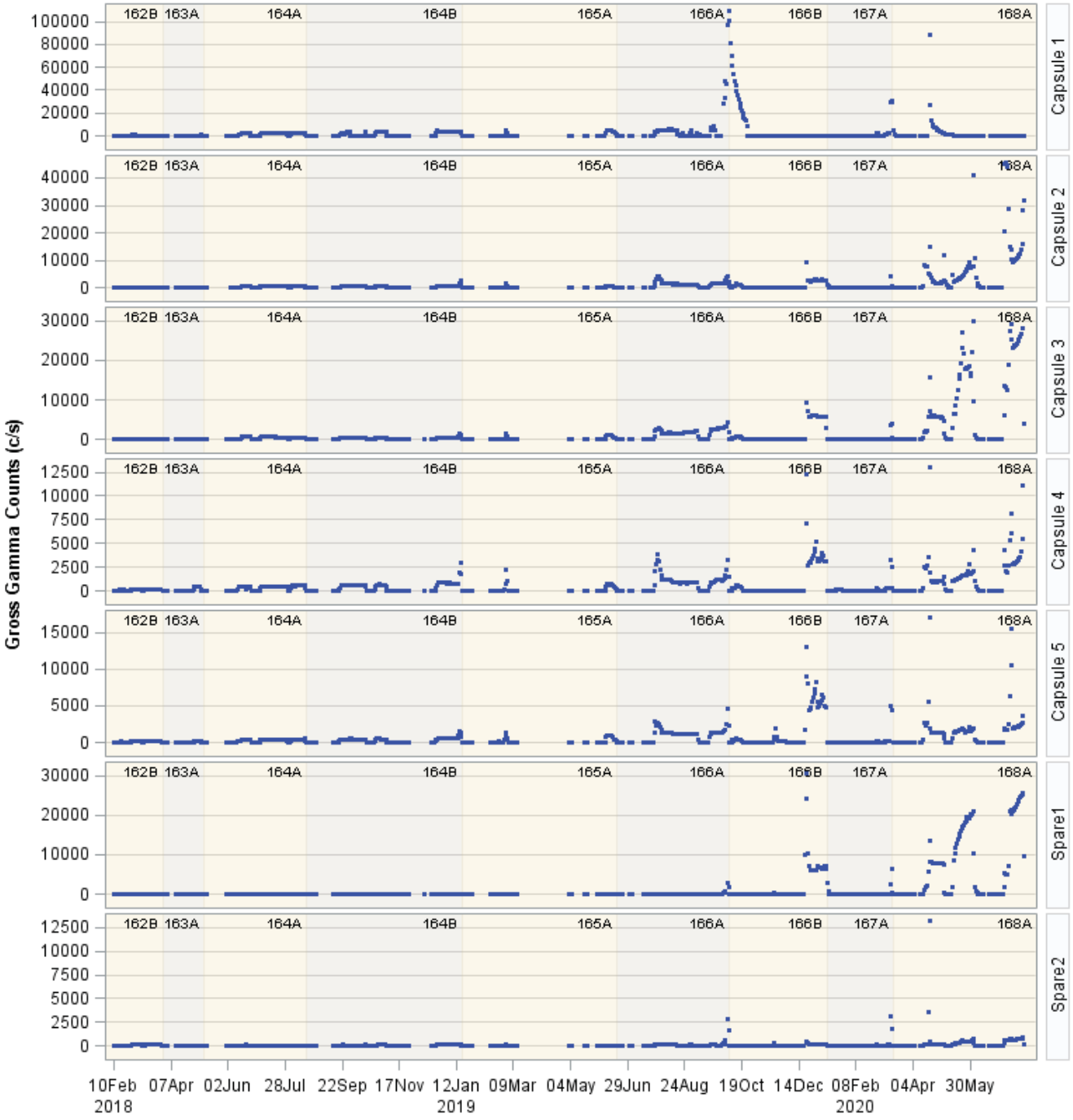

Figure 61. Summary of AGR-5/6/7 GG release rate data.

8.0 REFERENCES

1. Scates, D .M, E. L. Reber, and D. Miller. 2020. “Fission Gas Monitoring for the AGR-5/6/7 Experiment.” Nuclear Engineering and Design 358 (March): 110417. http://doi.org/10.1016/j.nucengdes.2019.110417.
2. Mclaac, C.V. 1992. “Concentrations of Fission Product Noble Gases Released during the NPRMHTGR Fuel Compact Experiment-1A.” ST-PHY-92-032, Vol. 1 & 2.
3. Scates, D. M. 2014. “The Effect of Birthrate Granularity on the Release- to-Birth Ratio for the AGR-1 In-Core Experiment.” Nuclear Engineering Design 271 (May): 231–237. https://doi.org/10.1016/j.nucengdes.2013.11.037.
4. Sterbentz,J. 2020. “JMOCUP Physics Depletion Calculations for the As-Run AGR-5/6/7 TRISO Particle Experiment in ATR Northeast Flux Trap.” ECAR-5321, Rev. 0, Idaho National Laboratory.
5. Killian, E. W. and J. K. Hartwell. 2000. “PCGAP: Users guide and algorithm description.” INEEL/EXT 2000 00908, Idaho National Laboratory. https:/doi.org/10.2172/800710.
6. Killian, E. W. and L. V. East. 1998. “PCGAP: Application to analyze gamma-ray pulse-height spectra on a personal computer under Window NT®.” Journal of Radioanalytical and Nuclear Chemistry 233 (1–2): 109–114. https:/doi.org/10.1007/BF02389656.
7. Reber, E. L. and D. M. Scates. n.d. “Automatic Internal Energy Calibration by OnTheFly for AGR-5/6/7.” INL/EXT-21-62709, Idaho National Laboratory.
8. MCP-2875, “Proper Use and Maintenance of Laboratory Notebooks,” March 2012.
9. Pham, B. T. and D. M. Scates. 2019. “AGR-5/6/7 Release-to-Birth Ratio Data Analysis for Cycles 162B, 163A, 164A, and 164B.” INL/EXT-19-54457, Rev. 0, Idaho National Laboratory.
10. Pham, B, et al. 2020. “AGR-5/6/7 Experiment Monitoring and Simulation Progress.” INL/EXT 19-55429, Rev. 1, Idaho National Laboratory.
11. Palmer, J. 2020. “AGR-5/6/7 Gas System – Analysis of Various Anomalies Encountered During Irradiation.” ECAR-5114, Rev.0, Idaho National Laboratory.

Appendix A

Transport Volume Technique and Method, Plug flow Assumption

The methodology captured in this Appendix was developed to correct for the increased activation saturation factor and calculate downstream transport volumes for the AGR-5/6/7 Capsules.

The transport volumes for AGR-5/6/7 were determined using the measured activities in the sample volume (V_s) of Ne-23, Kr-89, Xe-135m, Xe-137, and Xe-138. This method of determining transport volumes is different from past AGR experiments because of the difficulty of detecting neon at low flow rates (30 sccm) for this AGR experiment. To compensate, the transport volume testing was performed at higher flow rates than in past AGR leadout flow and transport volume-testing experiments. AGR-1 and AGR-2 transport volumes were determined exclusively with Neon-23 activity data. Flow conditions during the AGR-5/6/7 leadout and transport volume-testing experiment were held constant for multiple hours while spectrometer counting periods were set to 60-minute intervals, therefore test conditions were considered steady-state.

Each isotope has unique proportionality constant (K_x), which is dependent on many things such as neutron flux, isotope birthrate, capsule temperature, capsule diffusion, half-life, etcetera. However, K_x is independent of the transport volume. Assuming the proportionality constant K_x, is stable during the acquisition period, equations correlating the activity at the FPM trap, the proportionality constant and the transport volume can be formulated.

For Neon-23, the corresponding equation for activated neon at the FPM sample chamber ($M_{Ne\text{-}23}$), the transport volume ($V_{transport}$) and the Ne-23 proportionality constant ($K_{Ne\text{-}23}$) can be written as:

$$M_{Ne-23} = K_{Ne-23} * f1 * f2 * f3 \quad \text{(eq.1)}$$

Where:

$f1$ is the correction associated with the decay within the capsule volume ($V_{capsule}$) and where *f is* the capsule outlet flow.

$$f1 = \left(1 - e^{\frac{-V_{capsule} * \lambda_{Ne-23}}{f}}\right) \quad \text{(eq.2)}$$

$f2$is the correction associated with the decay within the transport volume ($V_{transport}$) *for neon-23.*

$Vi_{n\text{-}core}$, is the region where neon-23 is continuously activated within the reactor until it leaves the activation region.

$$f2 = e^{\frac{-(V_{transport} - V_{in-core}) * \lambda_{Ne-23}}{f}} \quad \text{(eq.3)}$$

and *f*3 is the correction associated with the decay within the sample volume (V_{sample}).

$$f3 = \left(1 - e^{\frac{-V_{sample} * \lambda_{Ne-23}}{f}}\right) \quad \text{(eq.4)}$$

For the krypton and xenon isotopes, the equations associating the activities in the FPM sample chamber activity (M_x), the transport volume ($V_{transport}$) and the proportionality constant (K_x) is slightly simpler:

$$M_x = K_x * f4 * f5 \quad \text{(eq.5)}$$

Where:

$f4$ is the correction associated with the decay within the transport volume (*V_{tran}).*

$$f4 = e^{\frac{-V_{transport} * \lambda_x}{f}} \quad \text{(eq.6)}$$

and $f5$ is the correction associated with the decay within the sample volume (*Vs).*

$$f5 = \left(1 - e^{\frac{-V_{sample} * \lambda_x}{f}}\right) \quad \text{(eq.7)}$$

The resultant set of equations each have a unique variable K_x and a shared variable $V_{transport}$. The remainder of the values including $V_{in-core}$,V_{sample}, $V_{capsule}$, λ_X, and ***f (capsule outlet flow*** rate) are known for each measurement, captured in Table A-1 and were provided in an e-mail dated 04/23/2018 from Joe Palmer. For each capsule, the flow rate was independently set at 60 sccm (58 sccm helium, 2 sccm neon), 50 sccm (48 sccm helium, 2 sccm neon) and 40 sccm (38 sccm helium, 2 sccm neon). By offsetting the capsule flow, multiple unique conditions for each isotope were formed. This variation in capsule flow distinguished the relationship between flow and the amount of noble fission gas measured at the FPMS thus allowing for the use of standard statistical methods to determine individual isotope proportionality constants and transport volumes.

The small uncertainties in the measured outlet flow rates are negligible. Therefore, the uncertainties in the averaged $V_{transport}$ were computed by normal error propagation techniques using the uncertainties of the measure data (σMx).

Table A-1. AGR-5/6/7 capsule specific volumes.

Capsule	V_{cap} (cc)	$V_{in\text{-}core}$ (cc)	V_{sample} (cc)
1	480.14	1.13	58
2	281.86	0.84	58
3	96.68	0.58	58
4	214.67	0.34	58
5	214.67	0.12	58

Appendix B

Transport Volume Fit

In the AGR-1 and AGR-2 experiments the transport volume from the outlet of the capsule to the respective FPMS were determined using standard leadout flow/transport testing Ne-23 protocols. For AGR-3/4 the leadout flow/transport testing Ne-23 protocols were augmented with the remaining fission gas isotopes to determine the transport volumes. It is believed the increased capsule volumes in AGR-3/4 were the primary reason the remaining fission gas isotopes were necessary in the transport volume calculations. For AGR-5/6/7 the capsule volumes became even larger. The increase capsule volumes cloud the transport volume calculations in multiple ways, including unknown gas flow patterns through the capsule voids and diffusion through the large graphite samples. AGR-5/6/7 also experienced leaking relief valves, line blockages and cross talk between the capsules which all compound the problem of using our current transport model (Described in Appendix A).

The transport model described in Appendix A was used in conjunction with activity data collected at the FPM, capsule specific flow rates and lobe power to determine appropriate transport volumes. The transport volumes and the K-values were determined by minimizing the chi squared between the transport model and the data. The chi squared was summed over select time frames between July 5, 2018 through January 13, 2019, when the reactor was at power and the system was reasonably stable. The following information in this appendix (Figures 62-10) is a summary that captures the isotopic activity at the respective FPMS for each isotope and calculated activities using the best fit model. This method was applied to capsules 2-5. The method did not work for Capsule 1, so the transport volume from the initial transport/leadout flow test was used. The fits are captured in Figure 102.

It is understood at this point that the current transport model would need modifications to describe the complicated systems found in AGR-5/6/7. Determining the appropriate modifications would be non-trivial and well beyond the current scope. That said, the current transport model using the best fit transport volumes are sufficient for the task of monitoring relative release rates from the capsules.

Transport Volume Fit, Capsule 2:

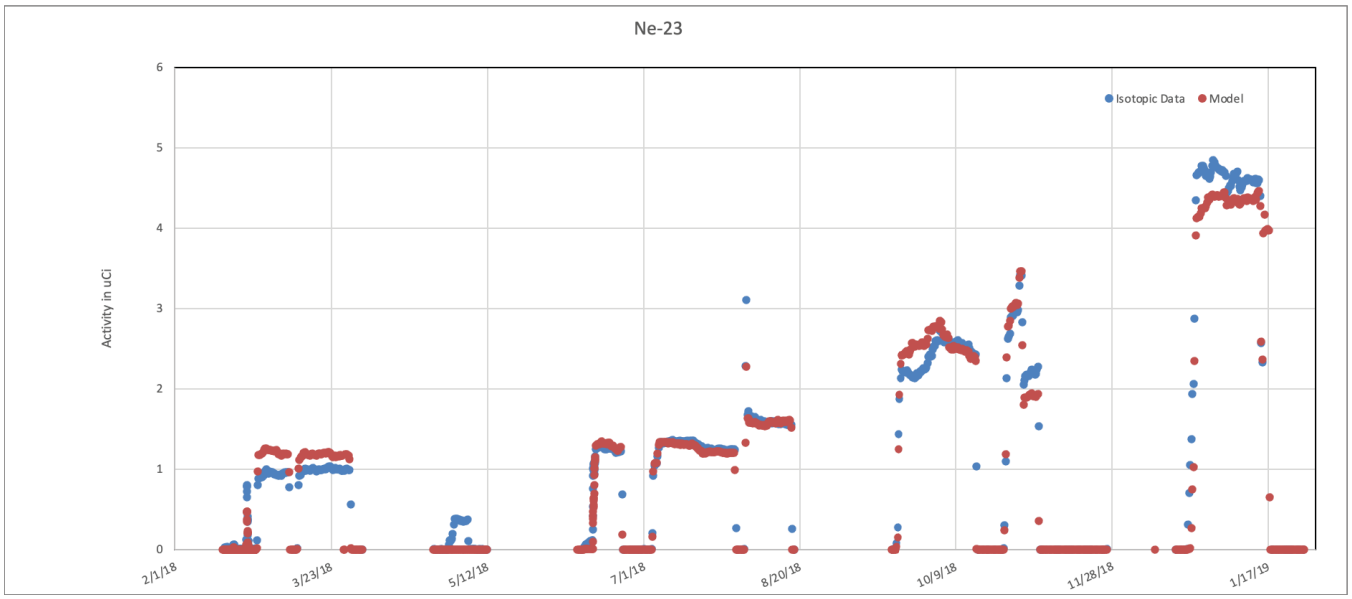

Figure B-62. Capsule 2, Neon-23 Isotopic data and the best fit model.

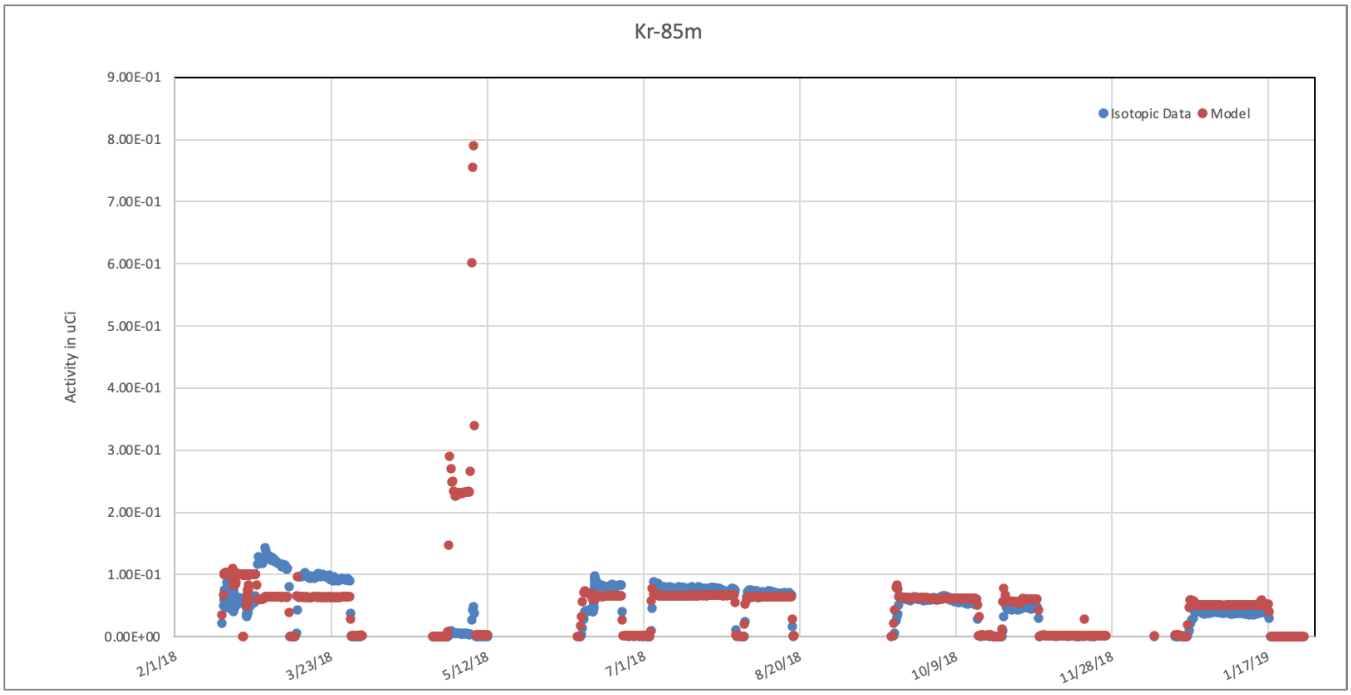

Figure B-63. Capsule 2, Neon-Kr-85m Isotopic data and the best fit model.

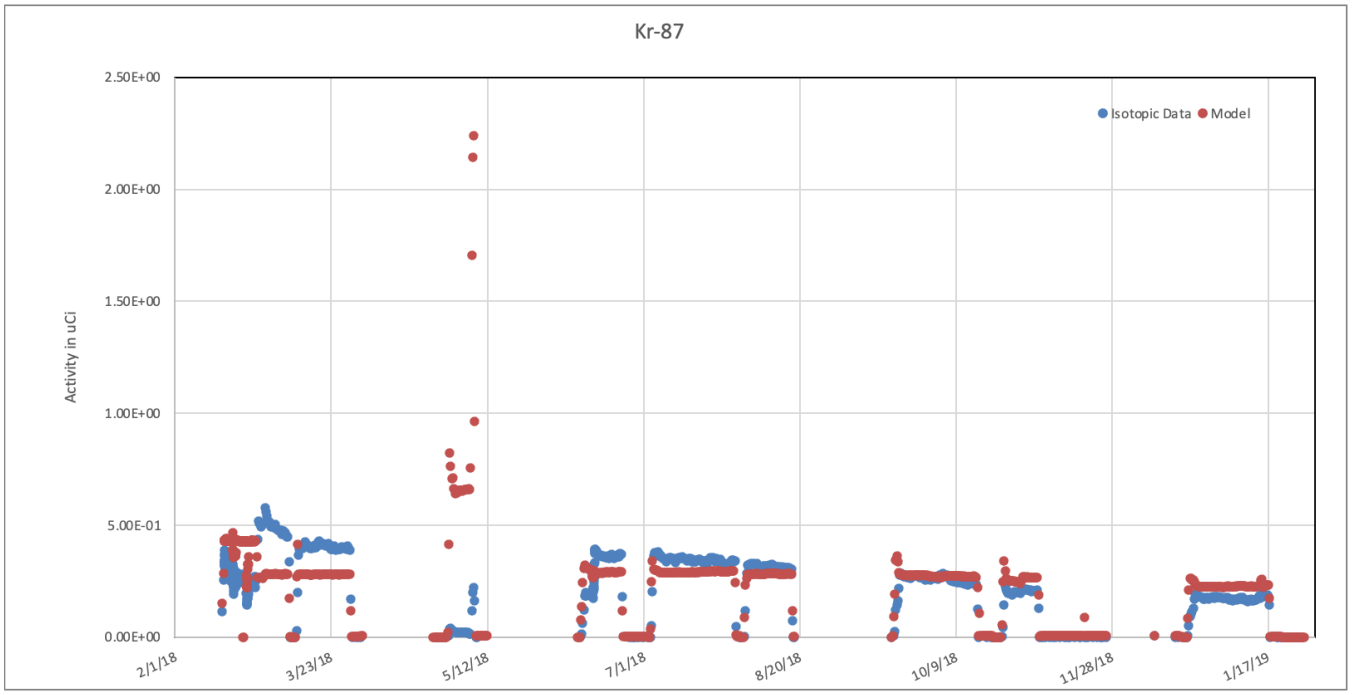

Figure B-64. Capsule 2, Krypton-87 Isotopic data and the best fit model.

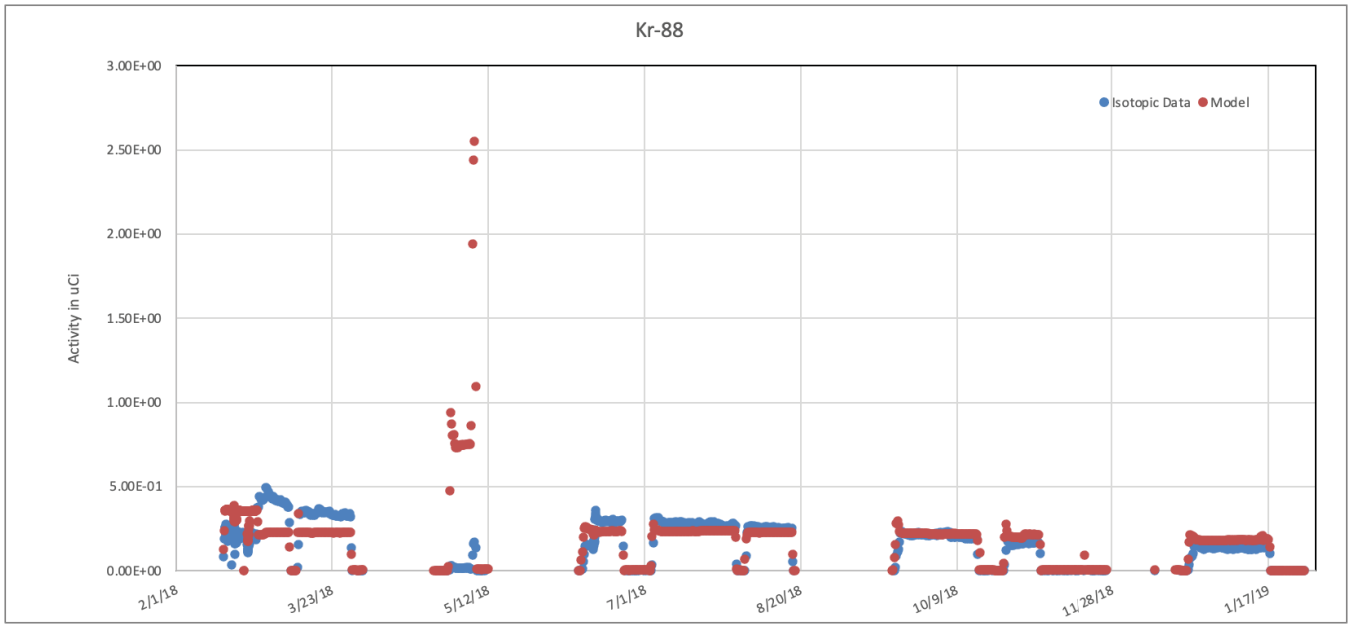

Figure B-65. Capsule 2, Krypton-88 Isotopic data and the best fit model.

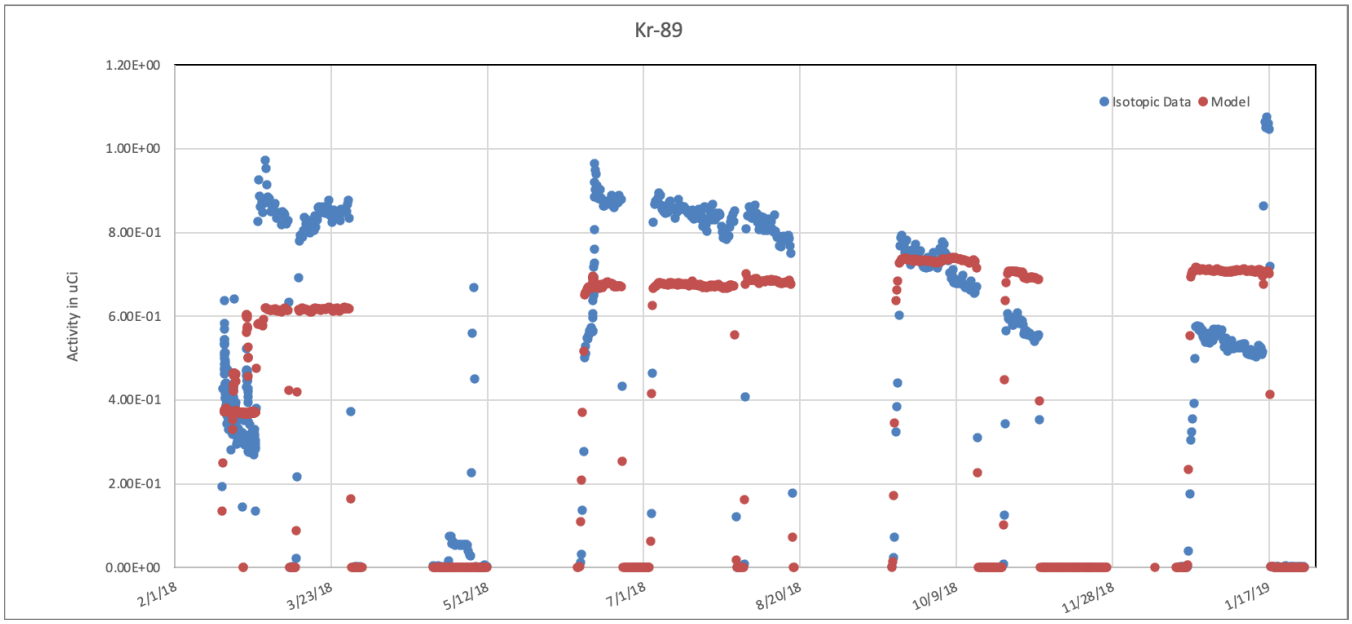

Figure B-66. Capsule 2, Krypton-89 Isotopic data and the best fit model.

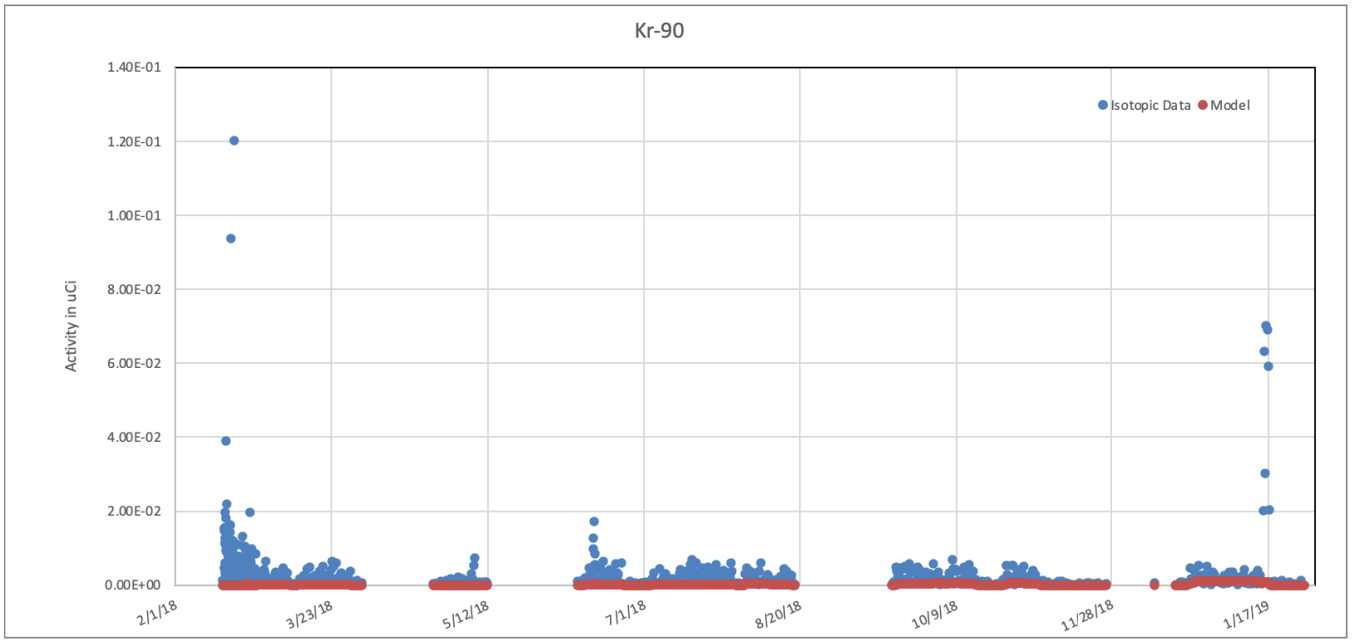

Figure B-67. Capsule 2, Krypton-90 Isotopic data and the best fit model.

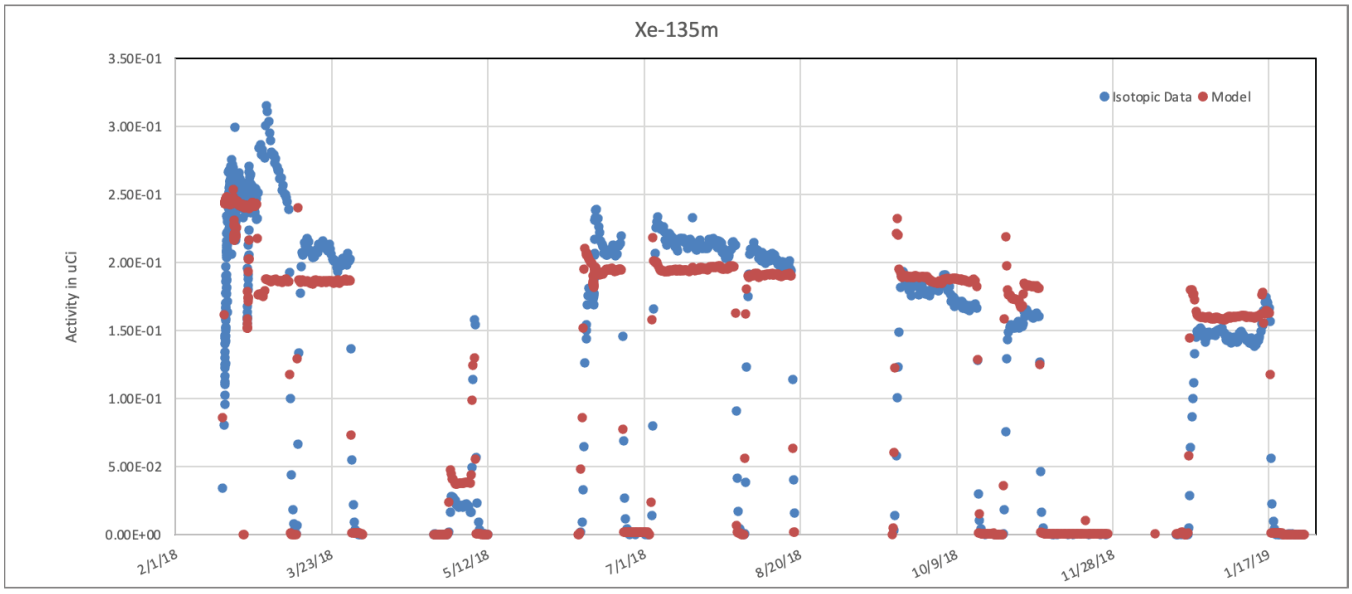

Figure B-68. Capsule 2, Xe-135m Isotopic data and the best fit model.

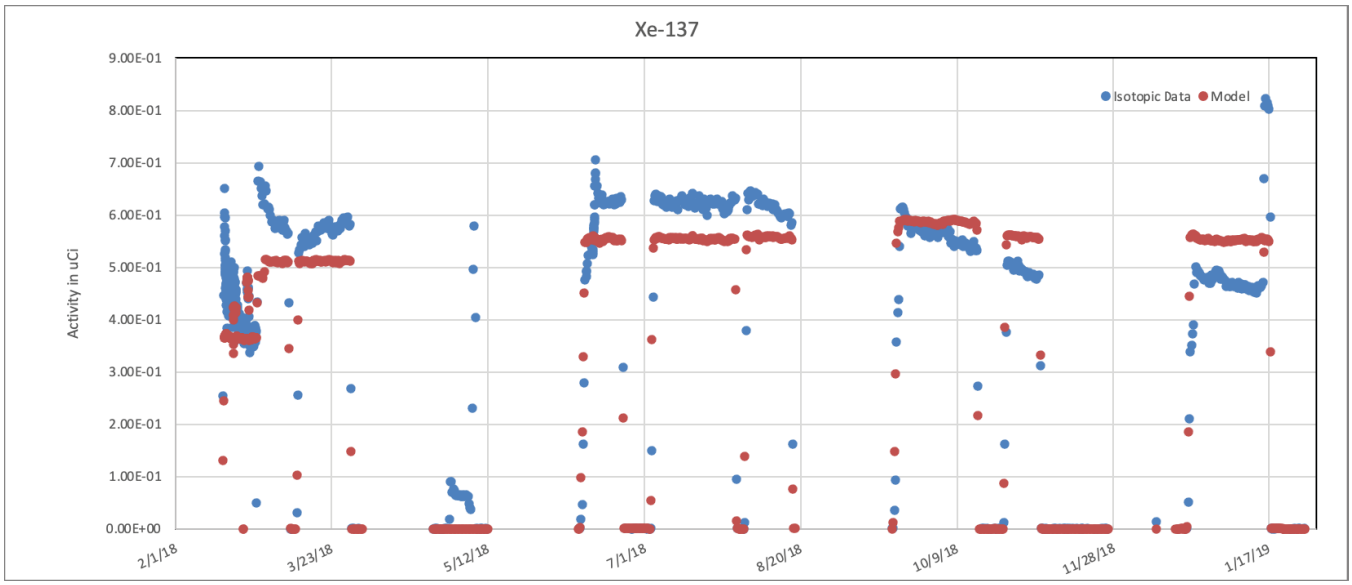

Figure B-69. Capsule 2, Xe-137 Isotopic data and the best fit model.

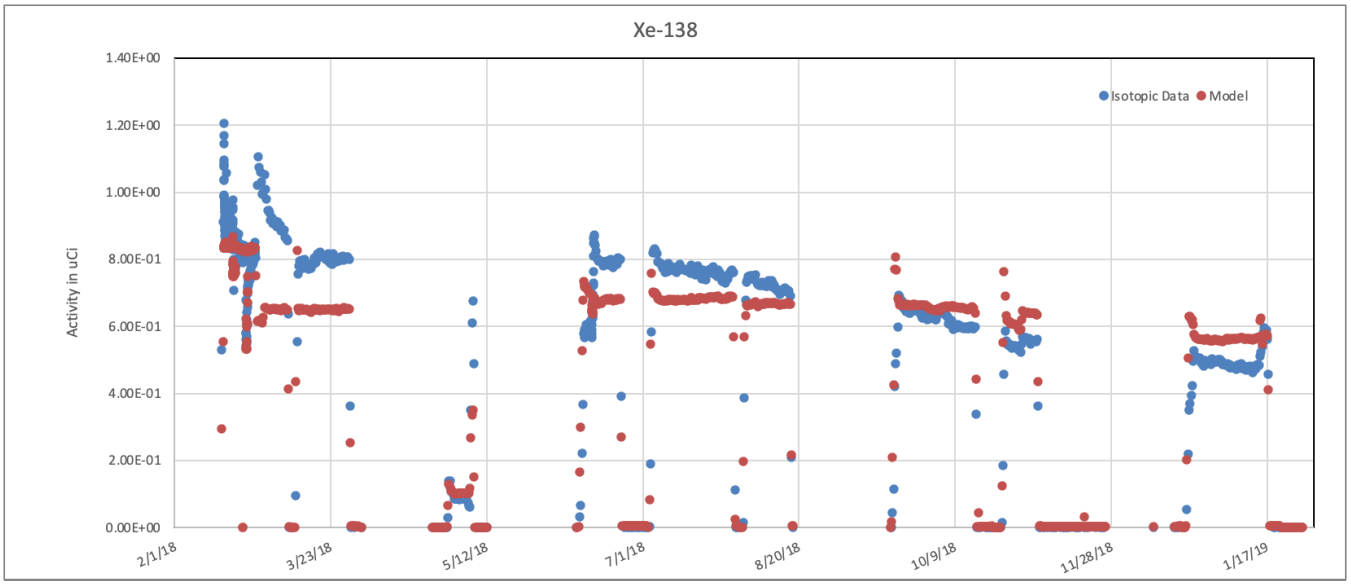

Figure B-70. Capsule 2, Xe-138 Isotopic data and the best fit model.

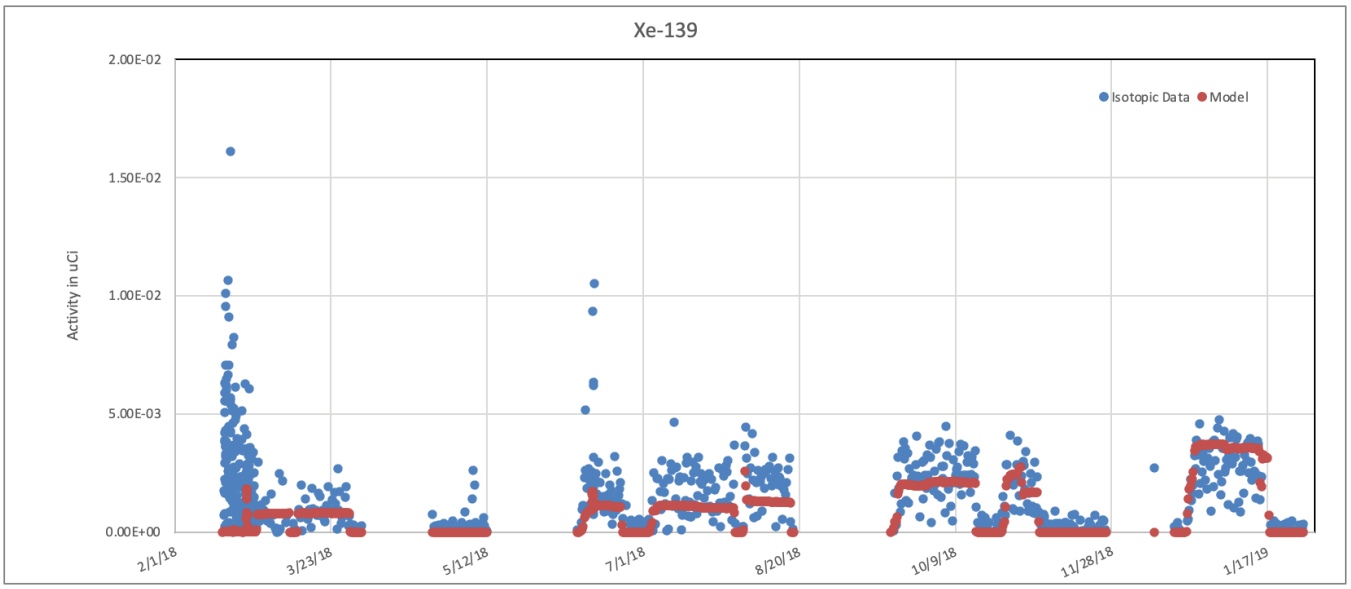

Figure B-71. Capsule 2, Xe-139 Isotopic data and the best fit model.

Transport Volume Fit, Capsule 3:

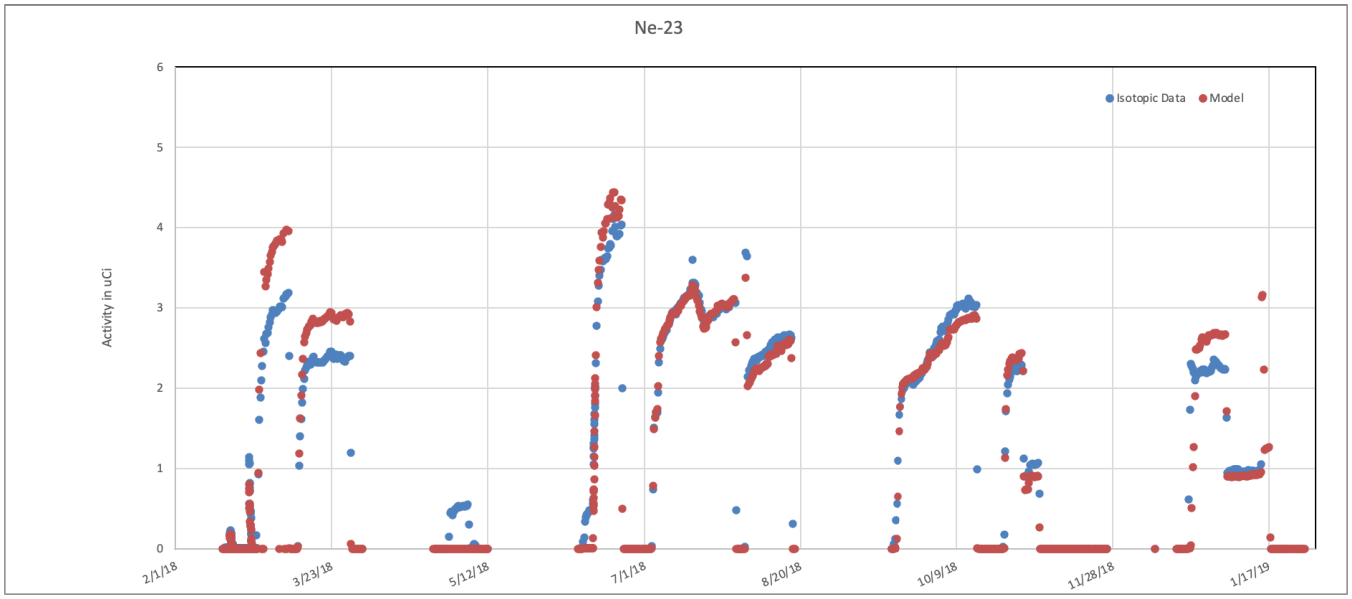

Figure B-72. Capsule 3, Neon-23 Isotopic data and the best fit model.

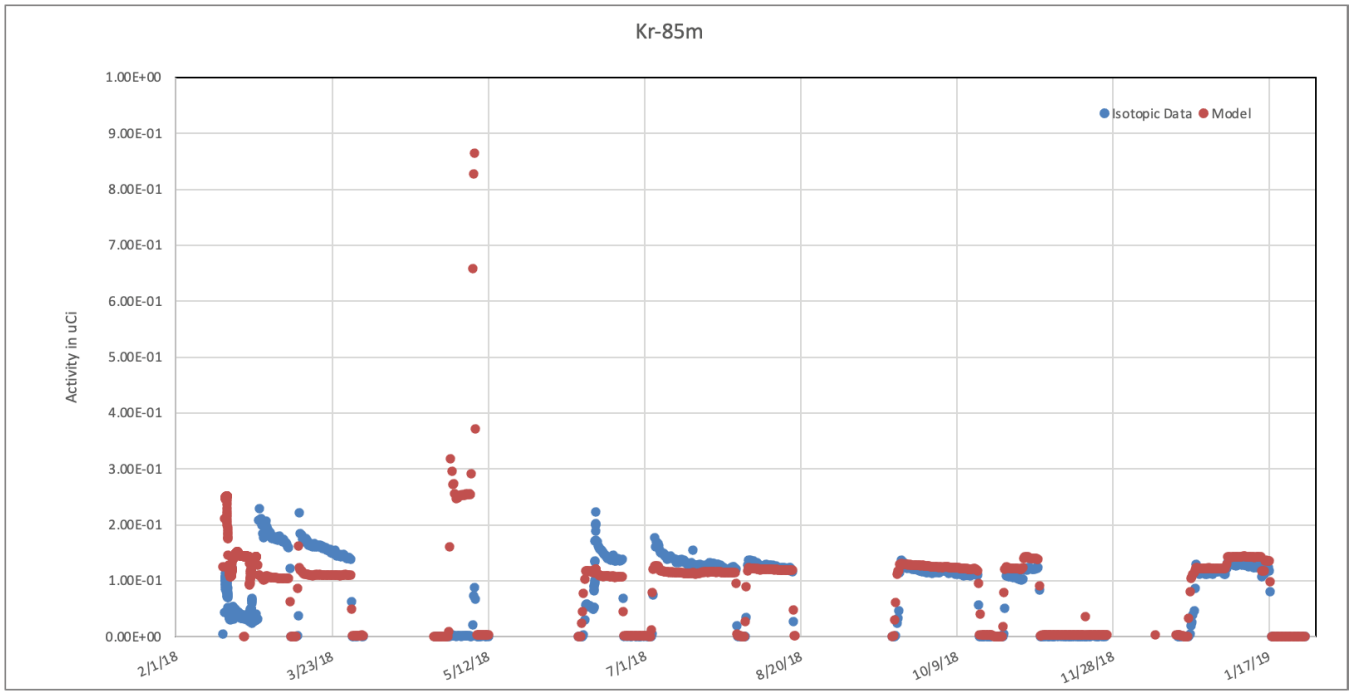

Figure B-73. Capsule 3, Krypton-85m Isotopic data and the best fit model.

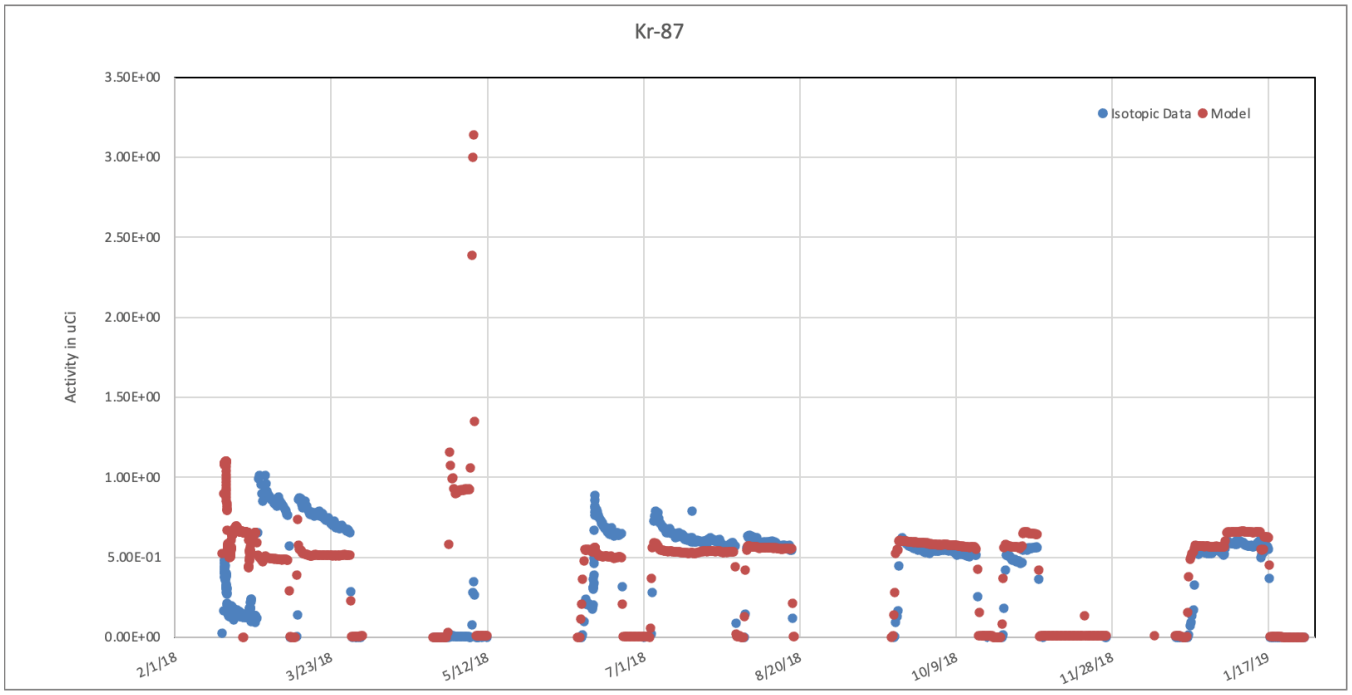

Figure B-74. Capsule 3, Krypton-87 Isotopic data and the best fit model.

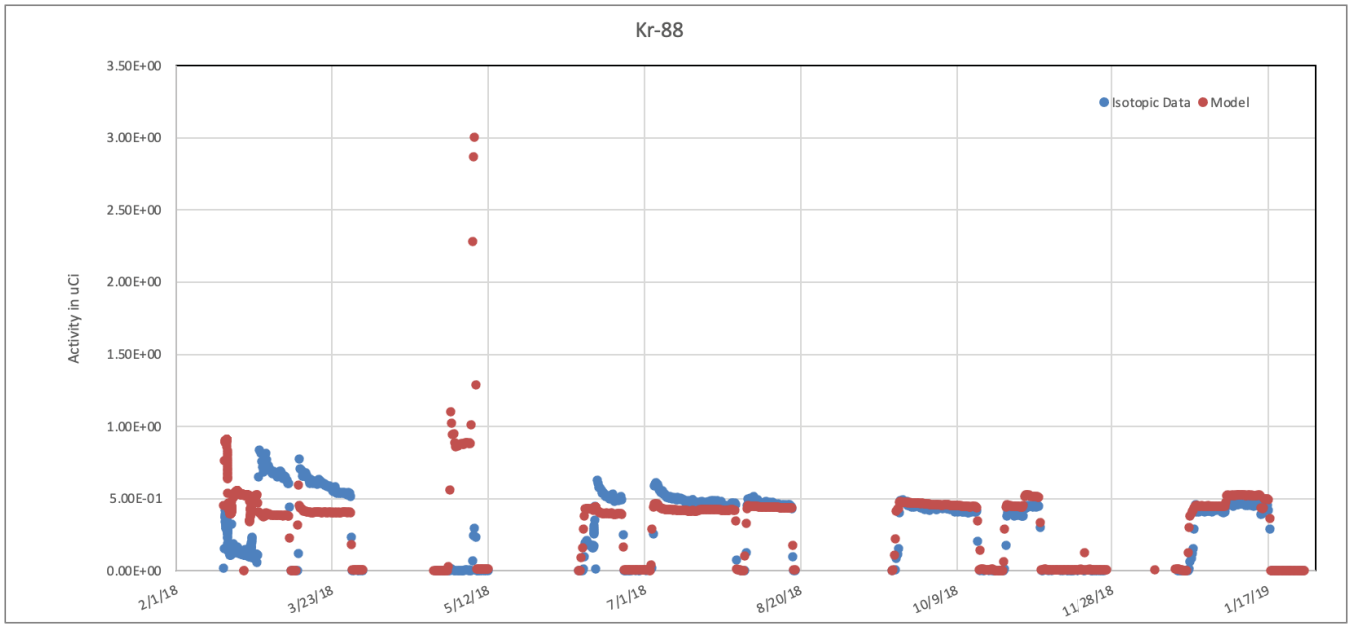

Figure B-75. Capsule 3, Krypton-88 Isotopic data and the best fit model.

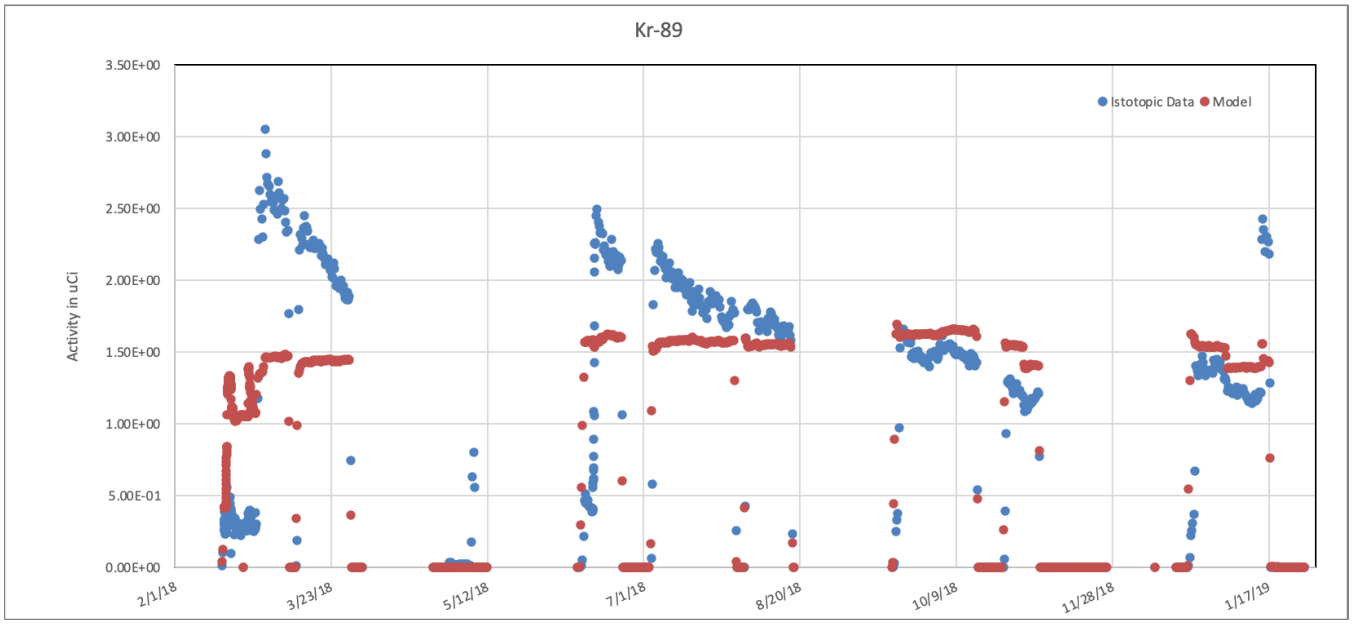

Figure B-76. Capsule 3, Krypton-89 Isotopic data and the best fit model.

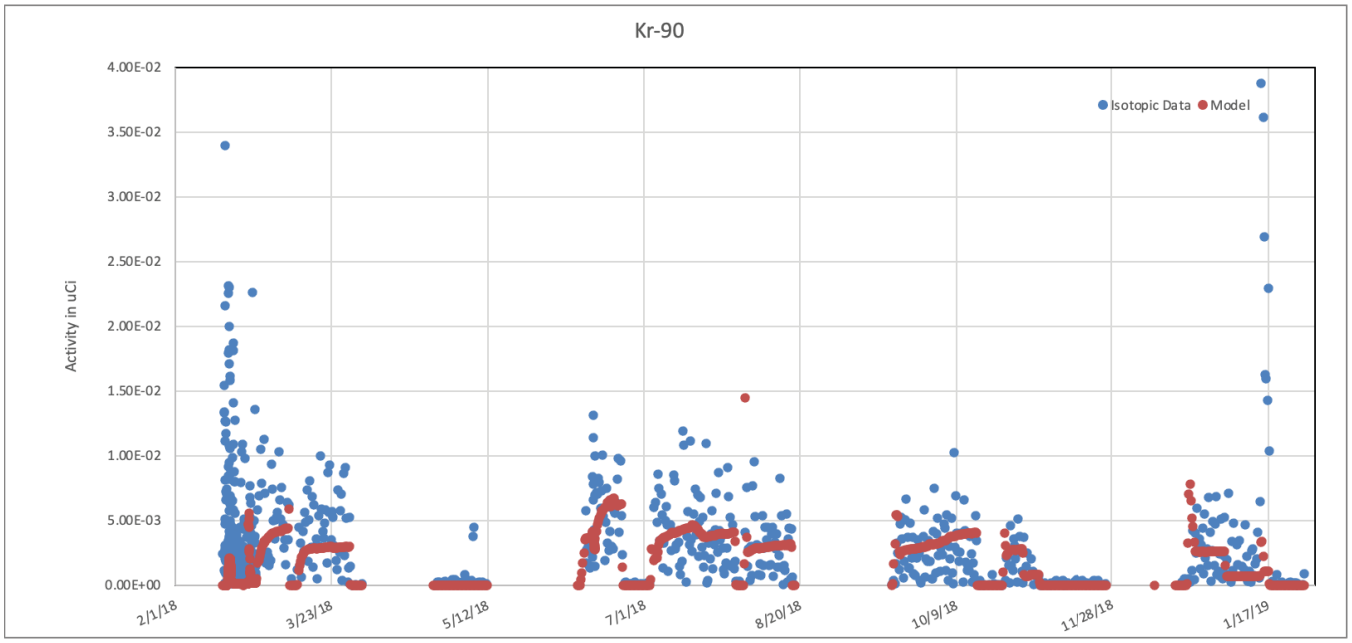

Figure B-77. Capsule 3, Krypton-90 Isotopic data and the best fit model.

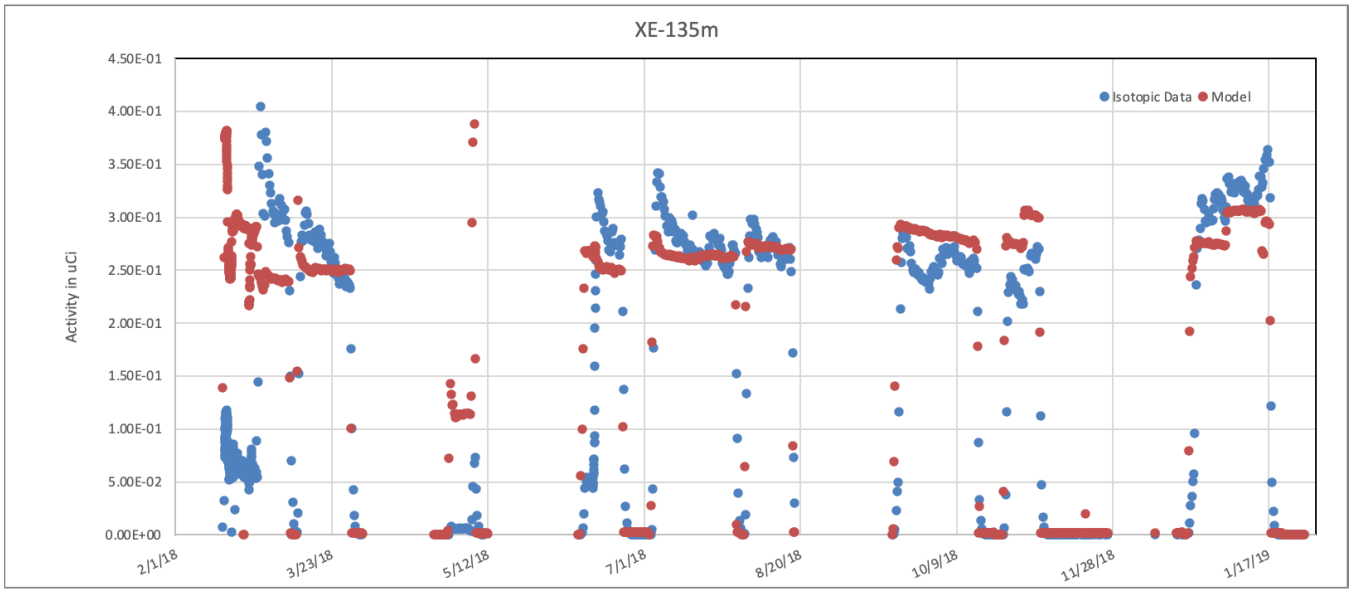

Figure B-78. Capsule 3, Xenon-135m Isotopic data and the best fit model.

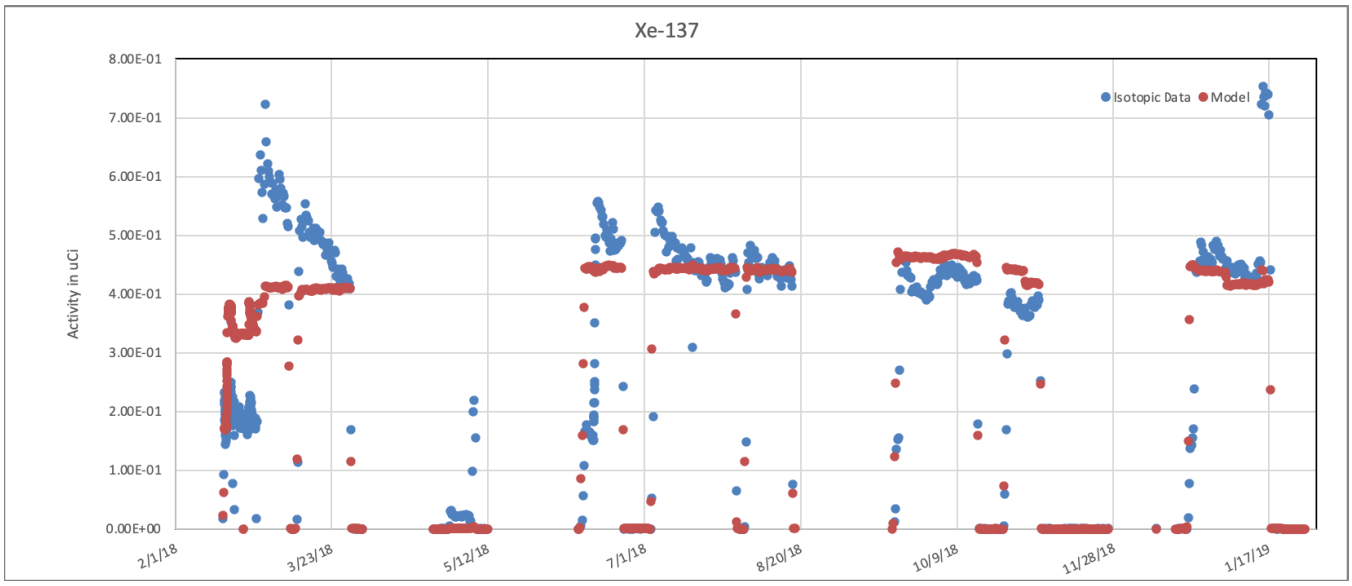

Figure B-79. Capsule 3, Xenon-137 Isotopic data and the best fit model.

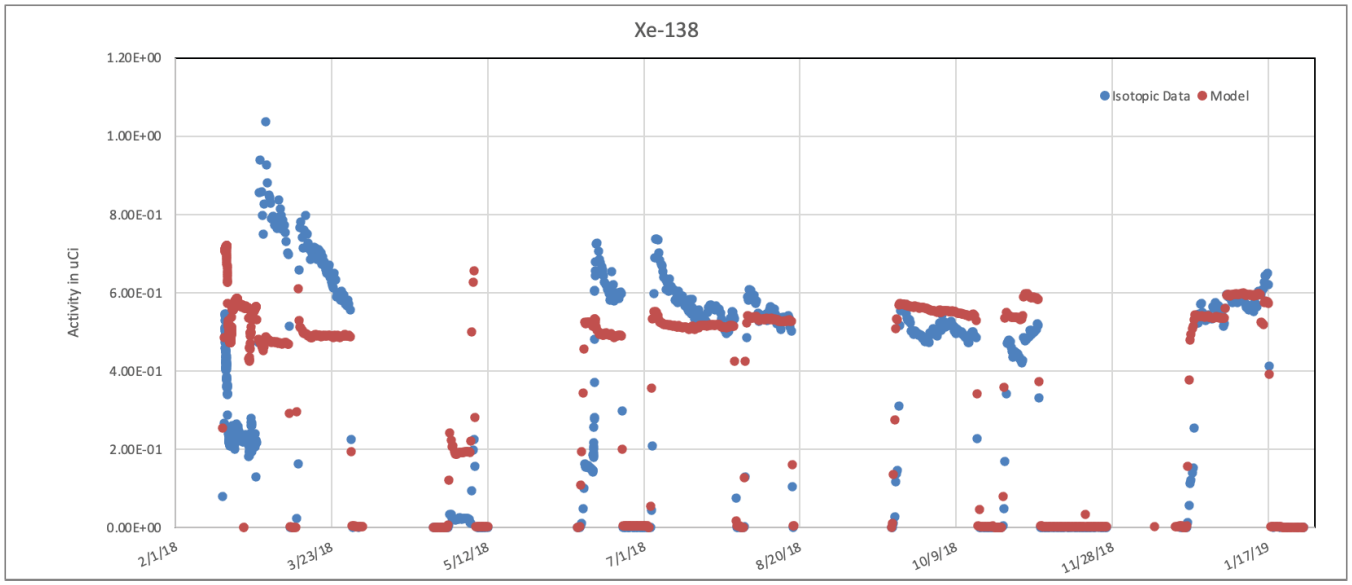

Figure B-80. Capsule 3, Xenon-138 Isotopic data and the best fit model.

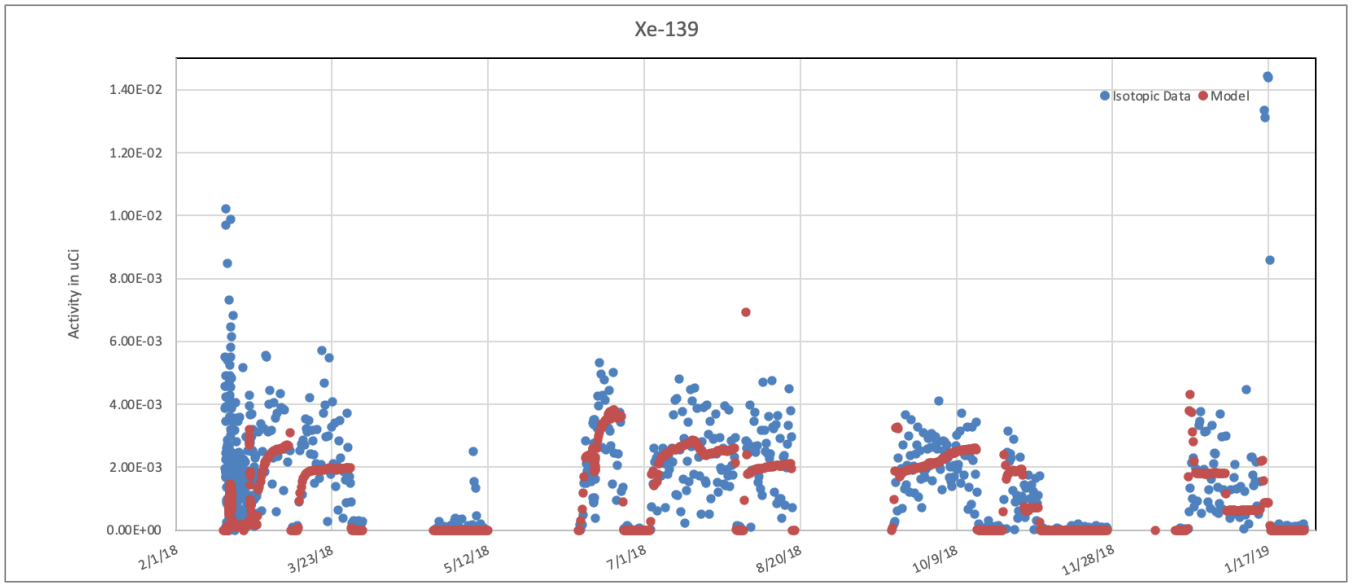

Figure B-81. Capsule 3, Xenon-139 Isotopic data and the best fit model.

Transport Volume Fit, Capsule 4:

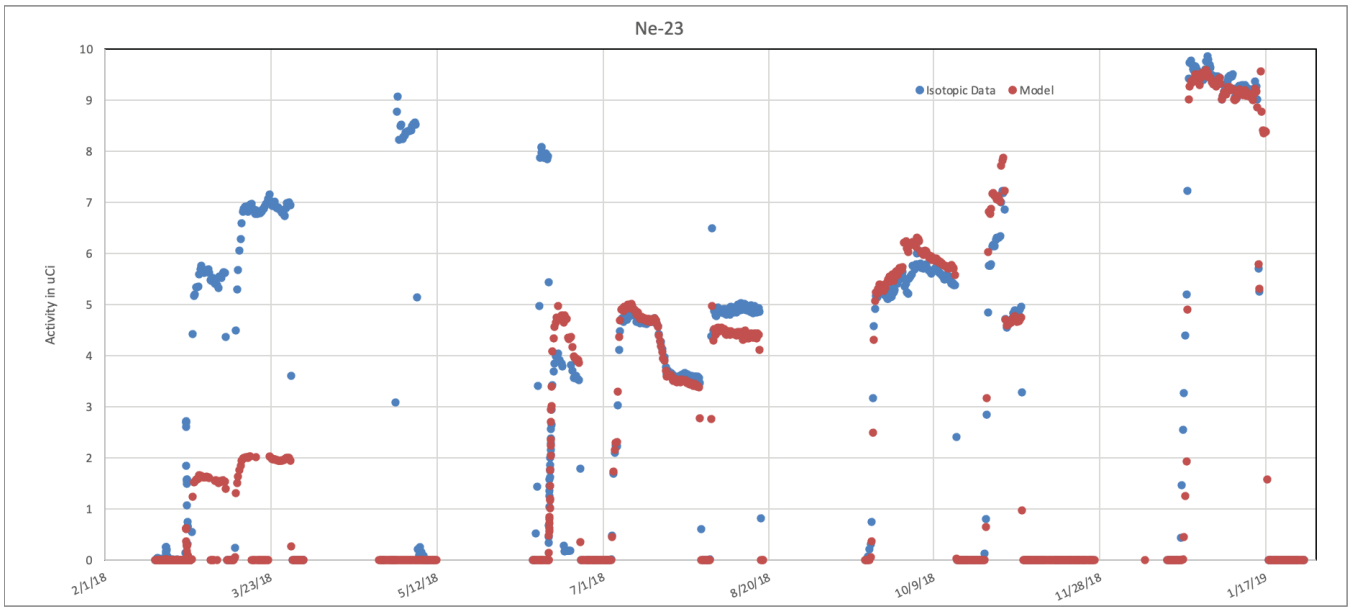

Figure B-82. Capsule 4, Neon-23 Isotopic data and the best fit model.

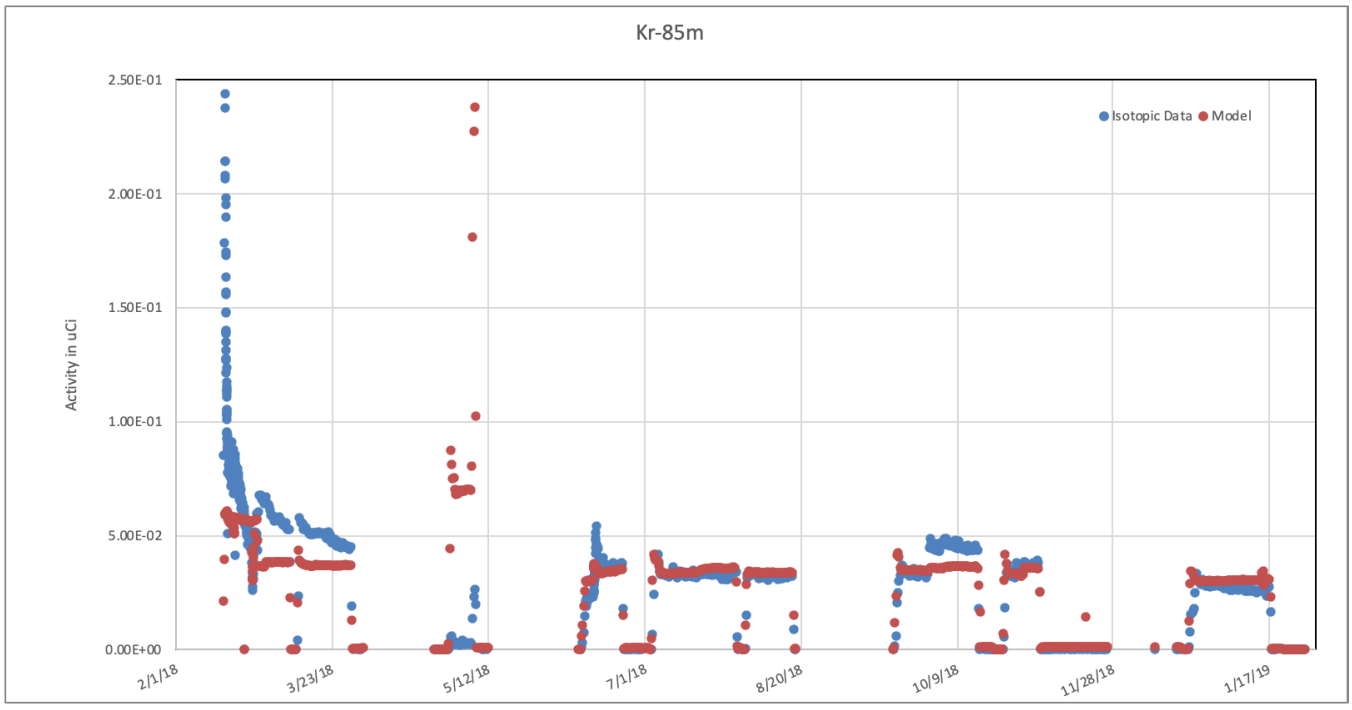

Figure B-83. Capsule 4, Krypton-85m Isotopic data and the best fit model.

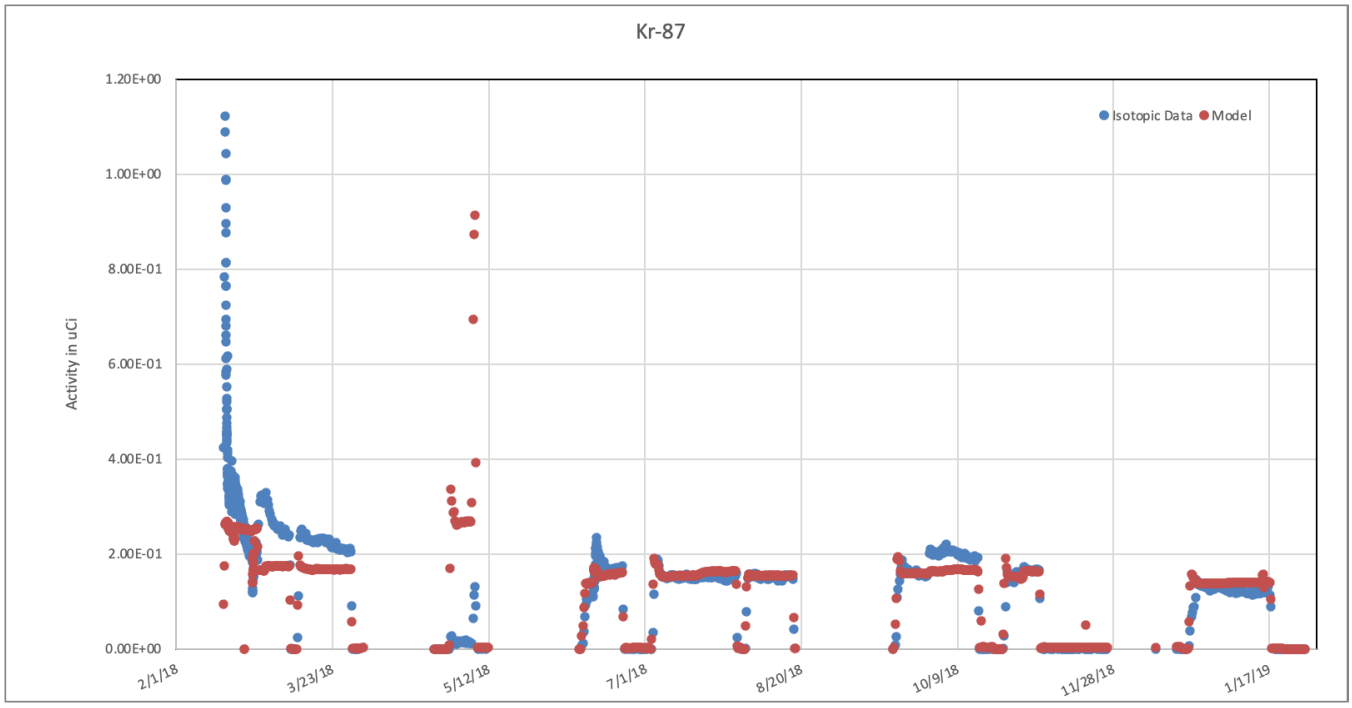

Figure B-84. Capsule 4, Krypton-87 Isotopic data and the best fit model.

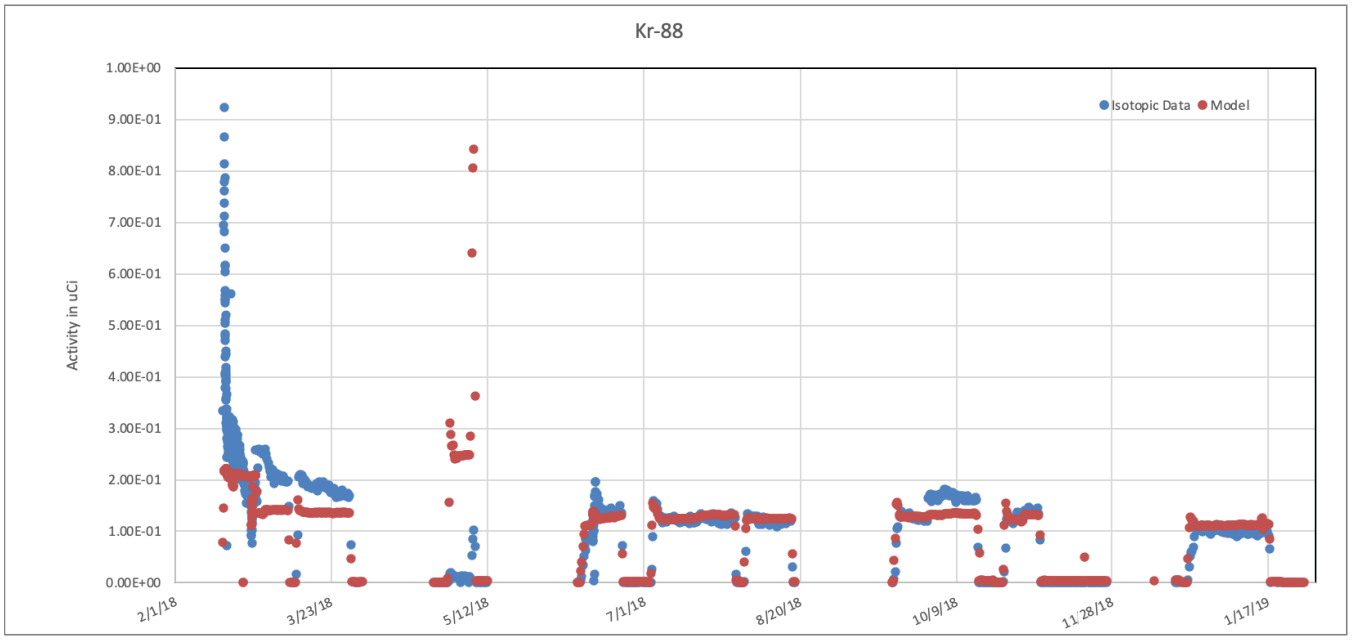

Figure B-85. Capsule 4, Krypton-88 Isotopic data and the best fit model.

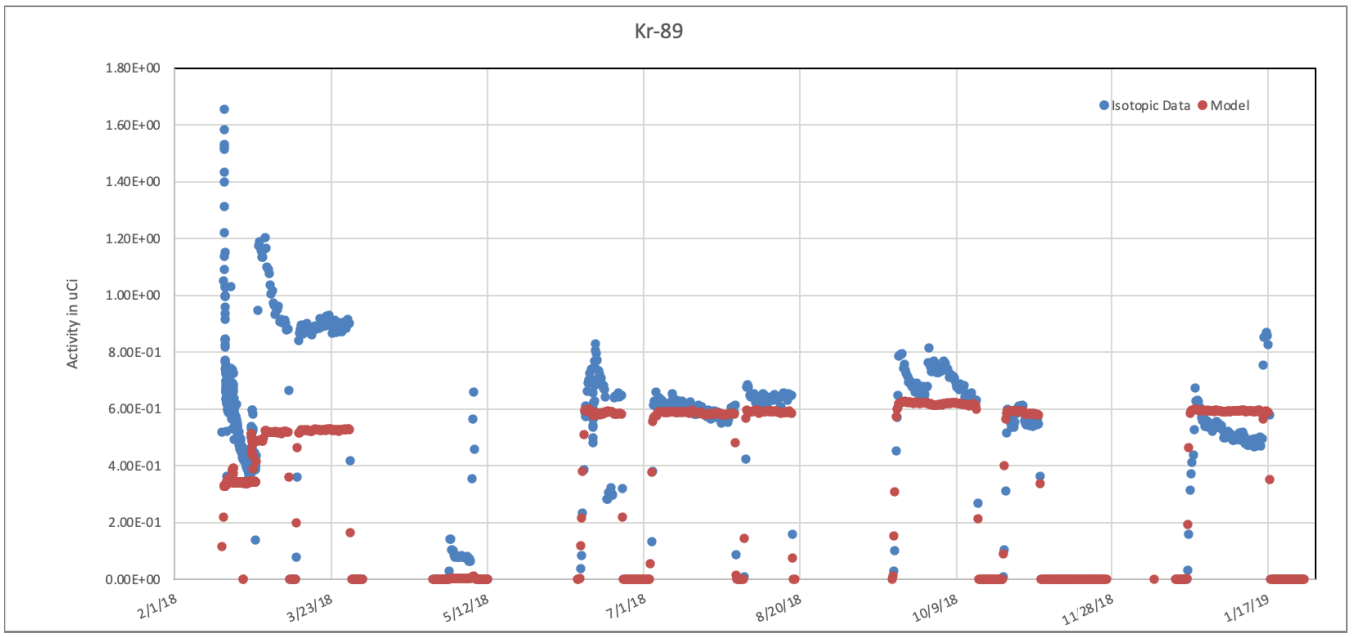

Figure B-86. Capsule 4, Krypton-89 Isotopic data and the best fit model.

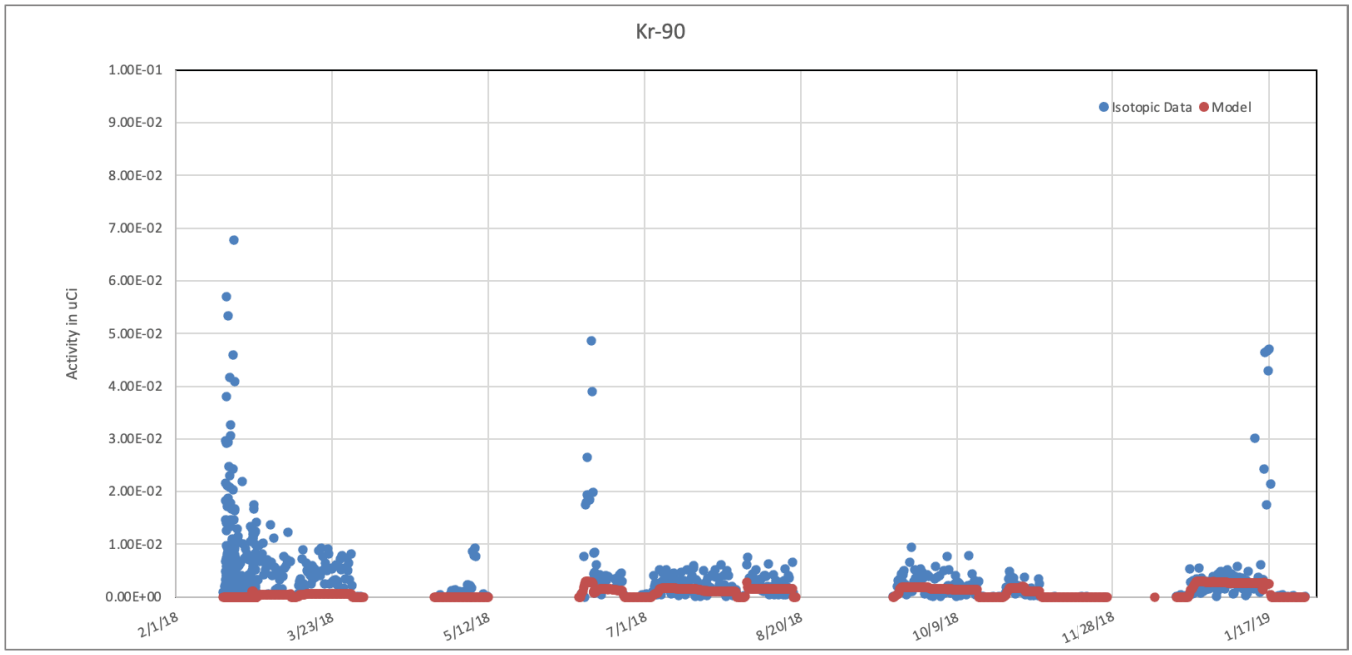

Figure B-87. Capsule 4, Krypton-90 Isotopic data and the best fit model.

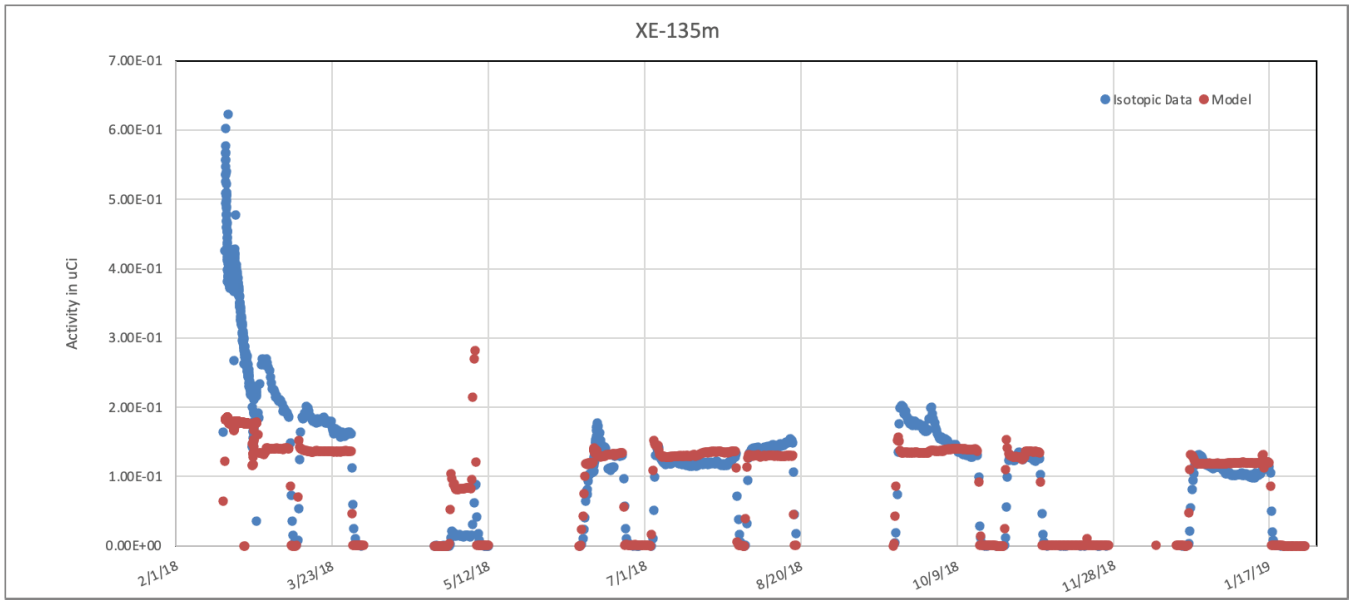

Figure B-88. Capsule 4, Xe-135m Isotopic data and the best fit model.

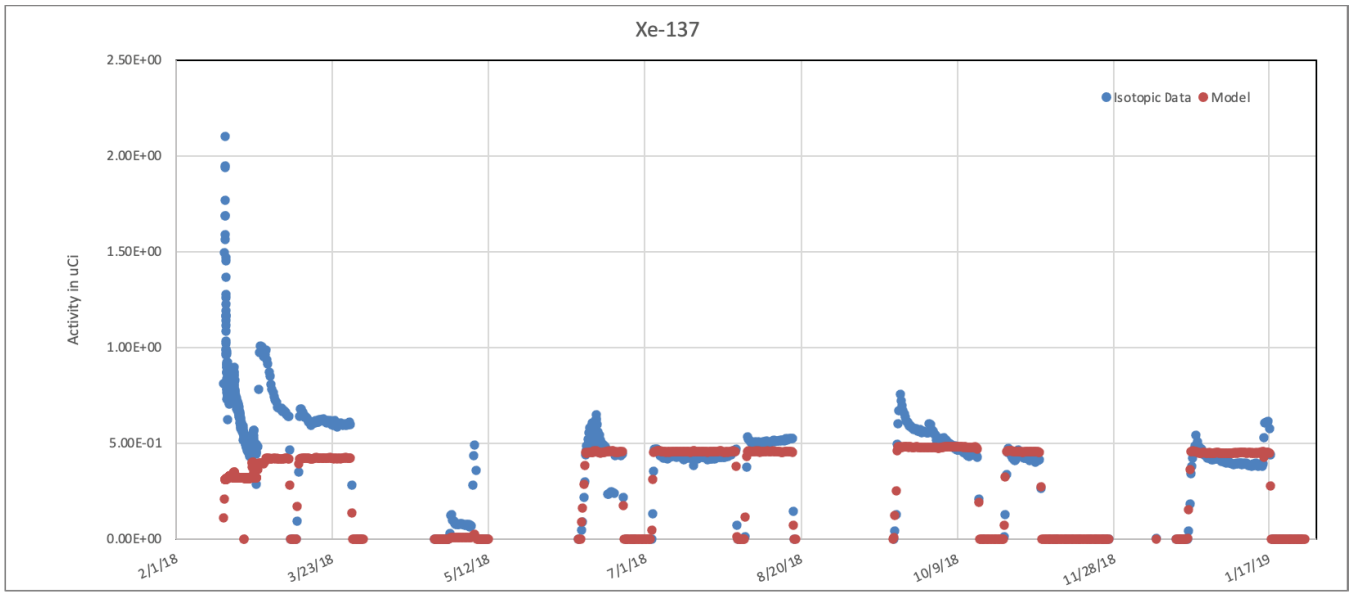

Figure B-89. Capsule 4, Xe-137 Isotopic data and the best fit model.

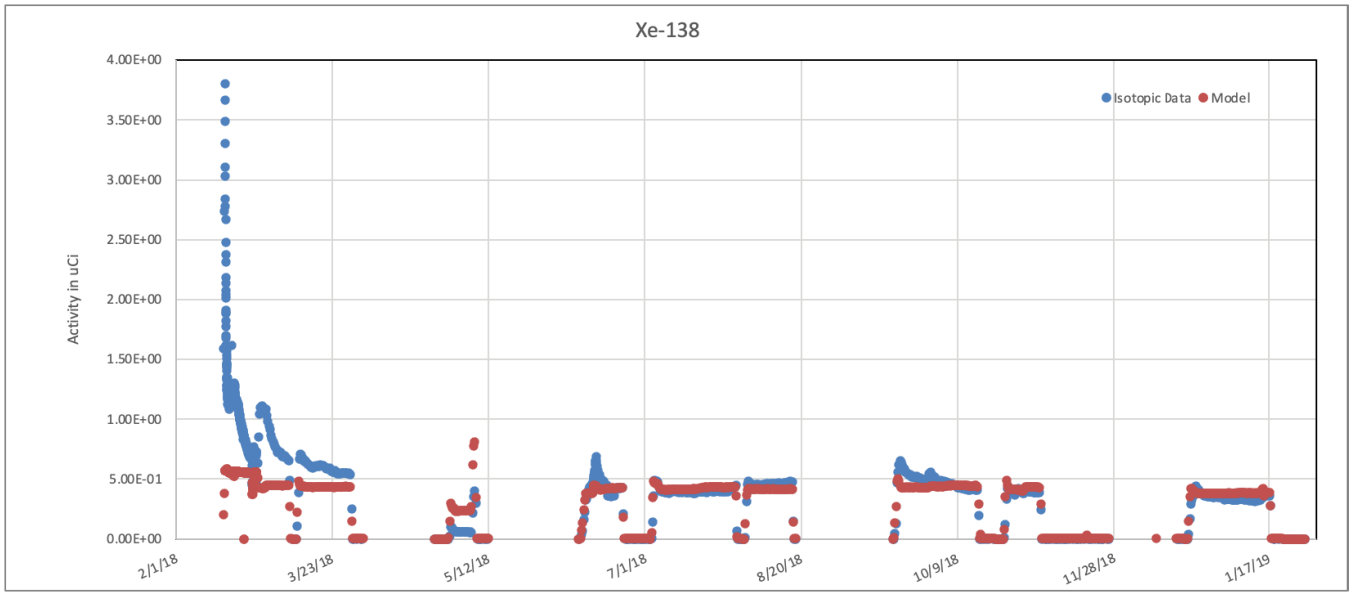

Figure B-90. Capsule 4, Xe-138 Isotopic data and the best fit model.

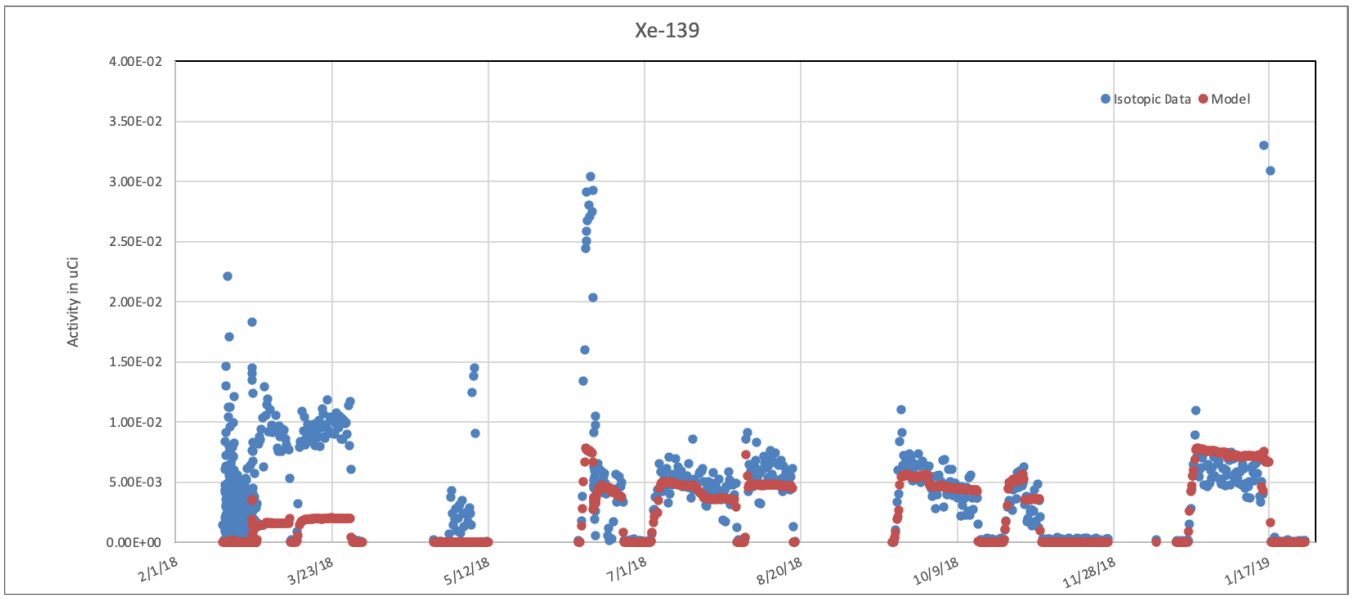

Figure B-91. Capsule 4, Xe-139 Isotopic data and the best fit model.

Transport Volume Fit, Capsule 5:

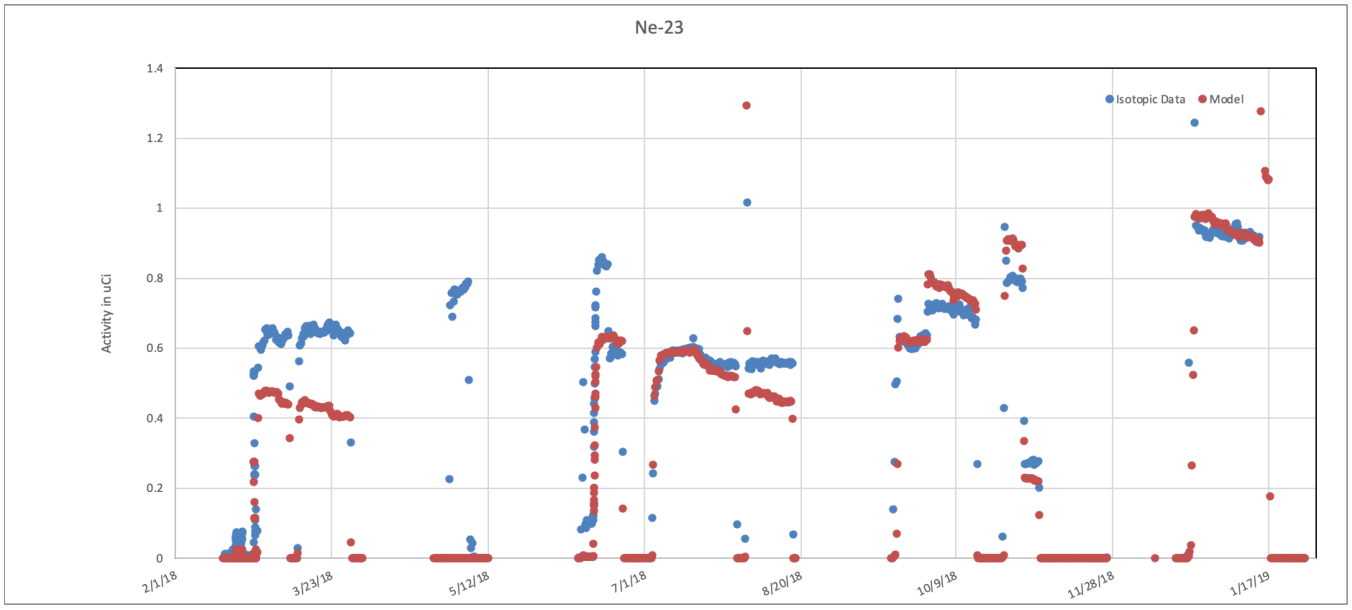

Figure B-92. Capsule 5, Neon-23 Isotopic data and the best fit model.

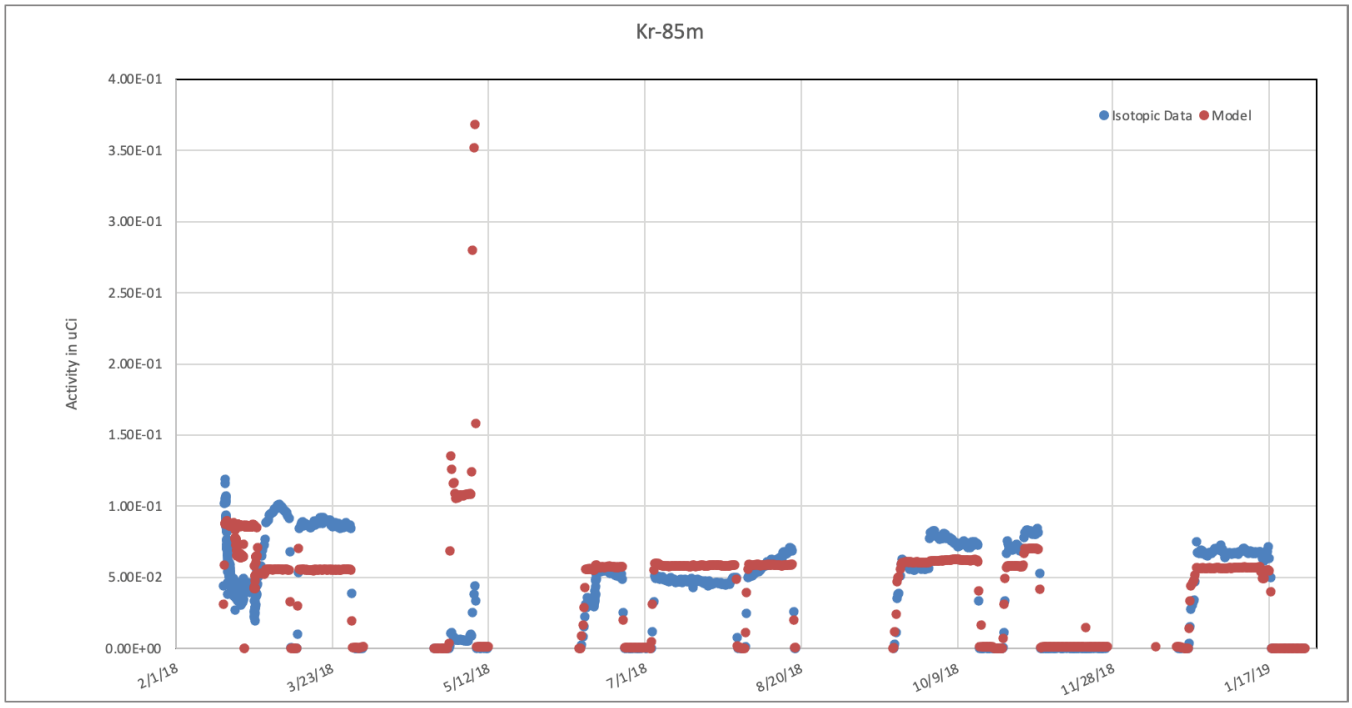

Figure B-93. Capsule 5, Krypton=85m Isotopic data and the best fit model.

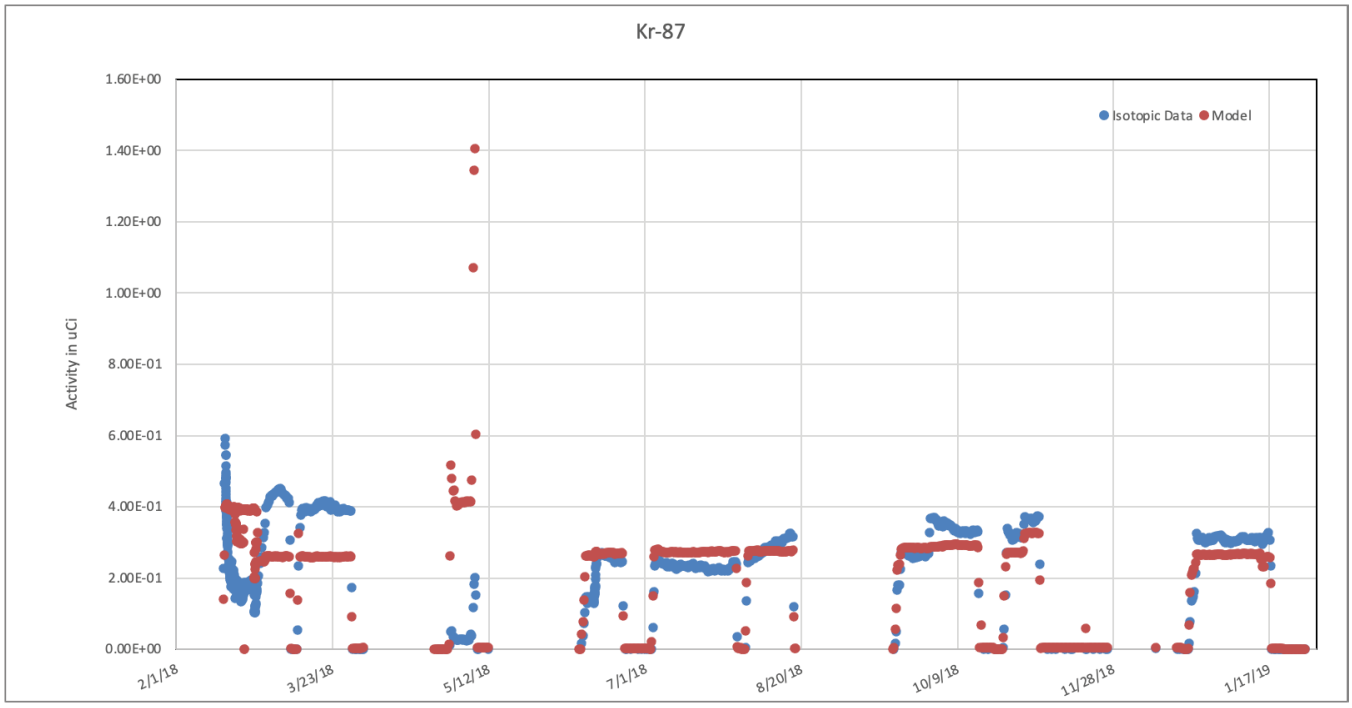

Figure B-94. Capsule 5, Krypton-87 Isotopic data and the best fit model.

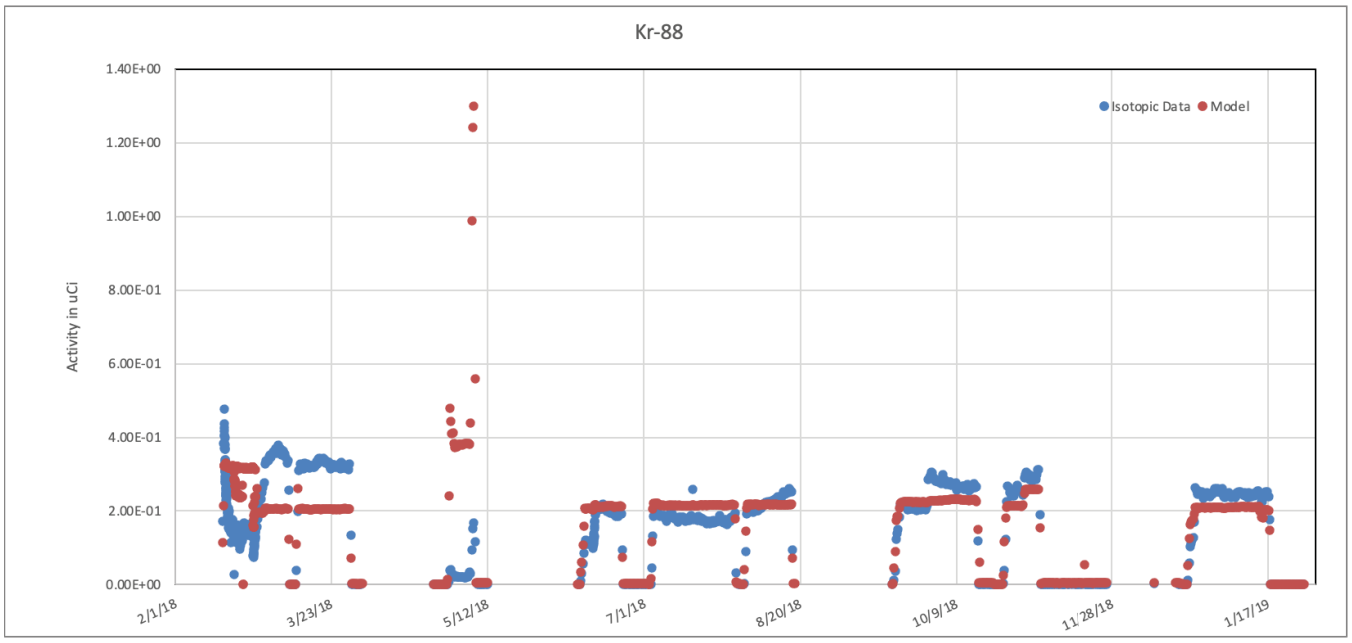

Figure B-95. Capsule 5, Krypton-88 Isotopic data and the best fit model.

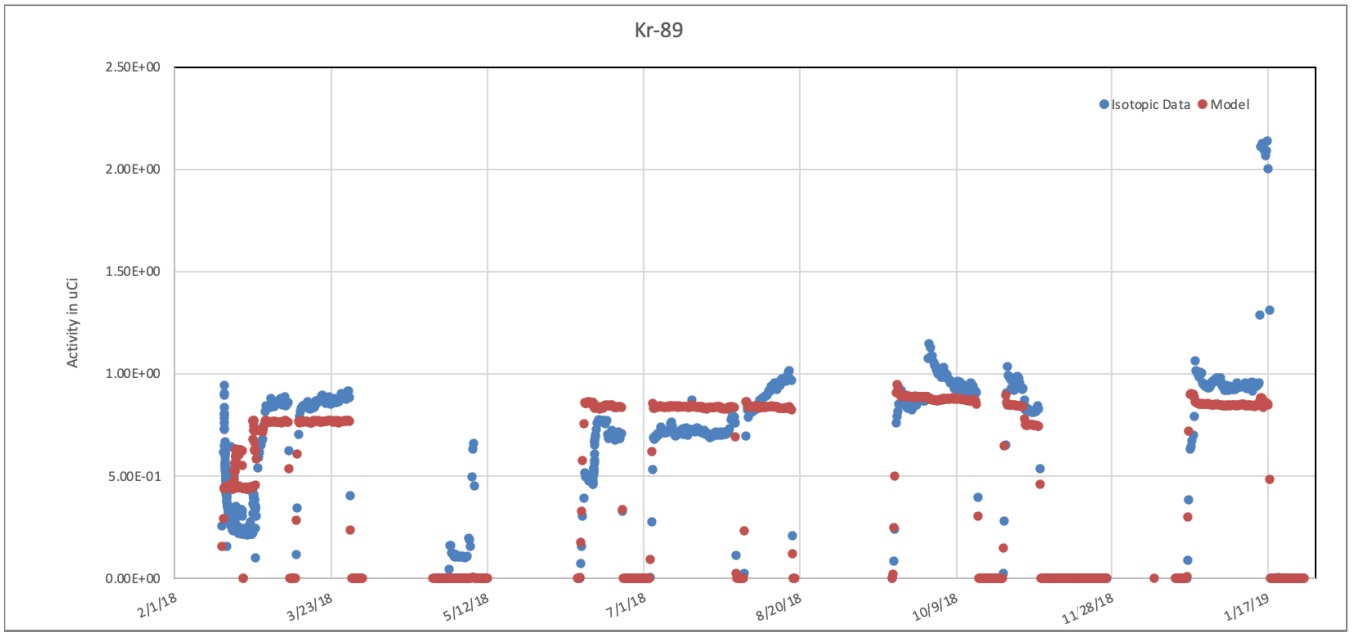

Figure B-96. Capsule 5, Krypton-89 Isotopic data and the best fit model.

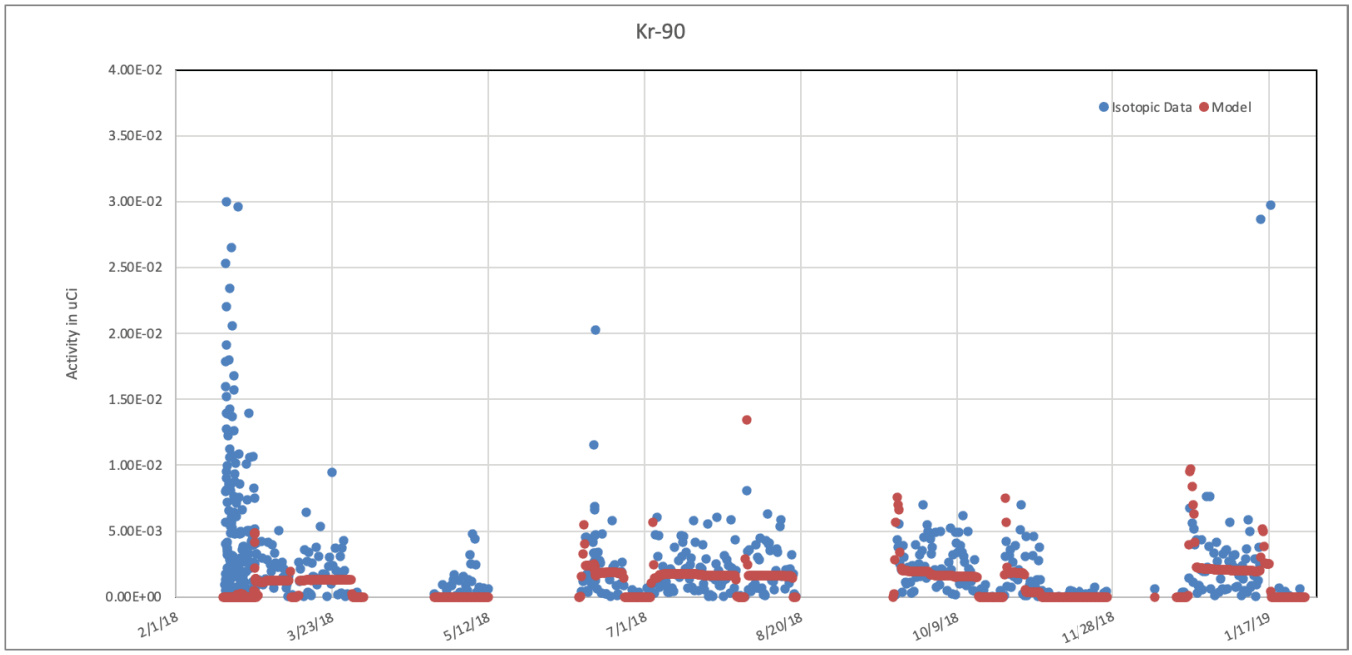

Figure B-97. Capsule 5, Krypton-90 Isotopic data and the best fit model.

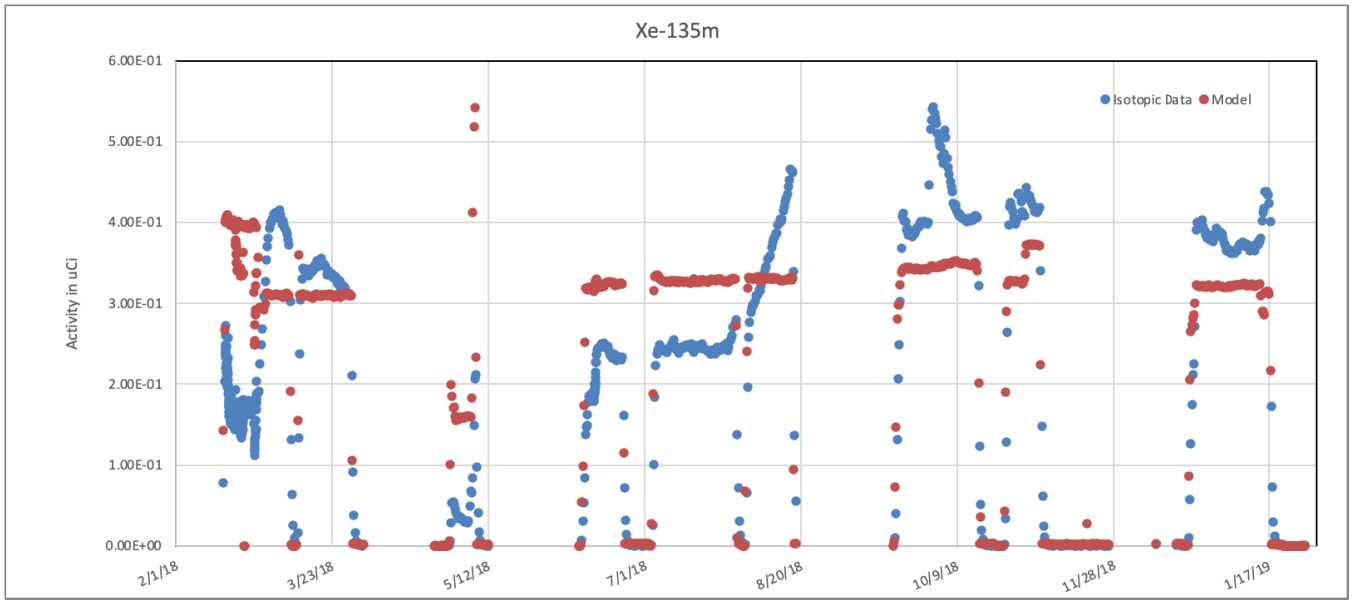

Figure B-98. Capsule 5, Xenon-135m Isotopic data and the best fit model.

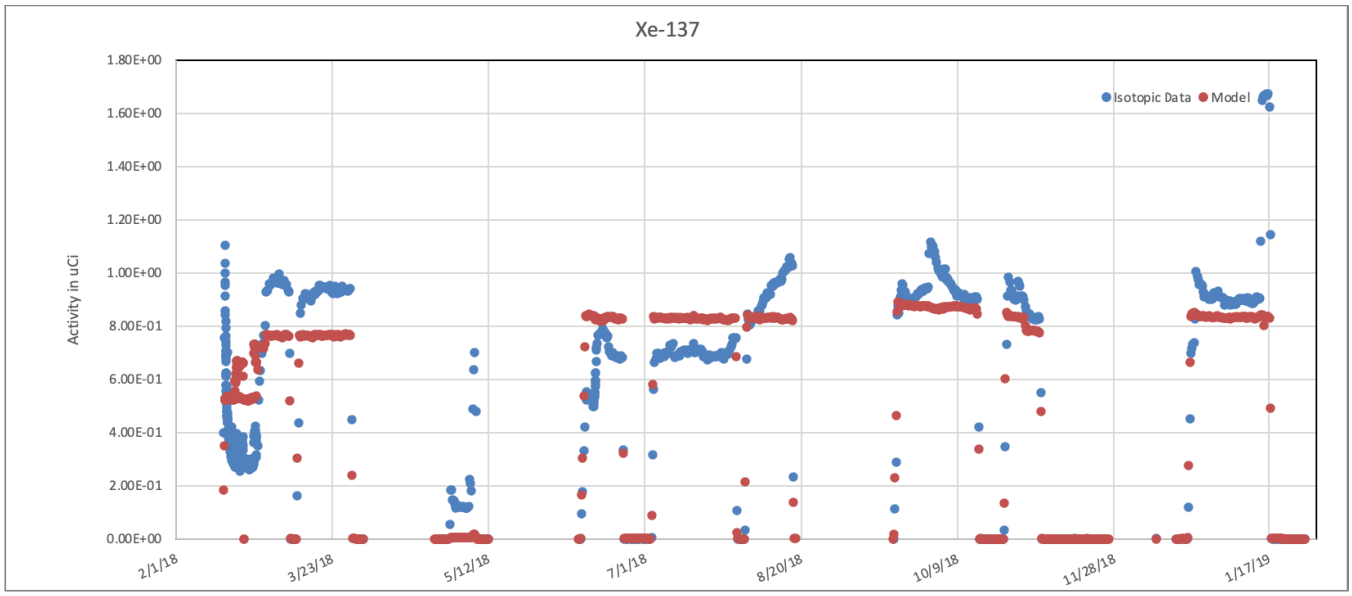

Figure B-99. Capsule 5, Xenon-137 Isotopic data and the best fit model.

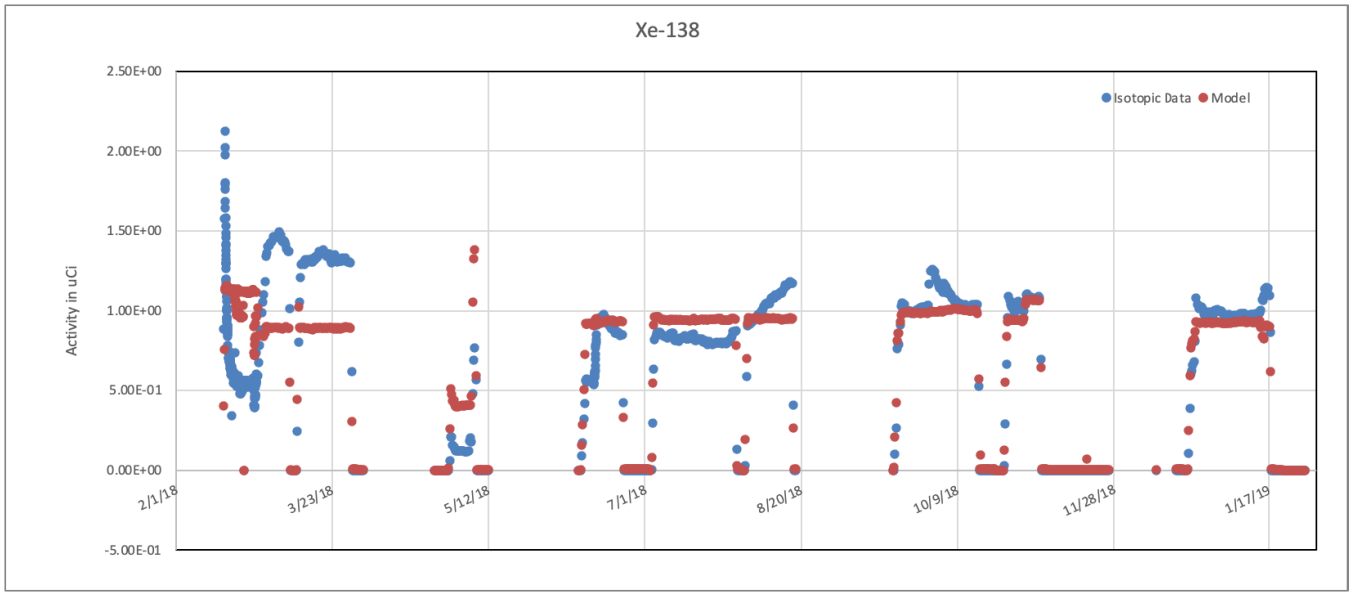

Figure B-100. Capsule 5, Xenon-138 Isotopic data and the best fit model.

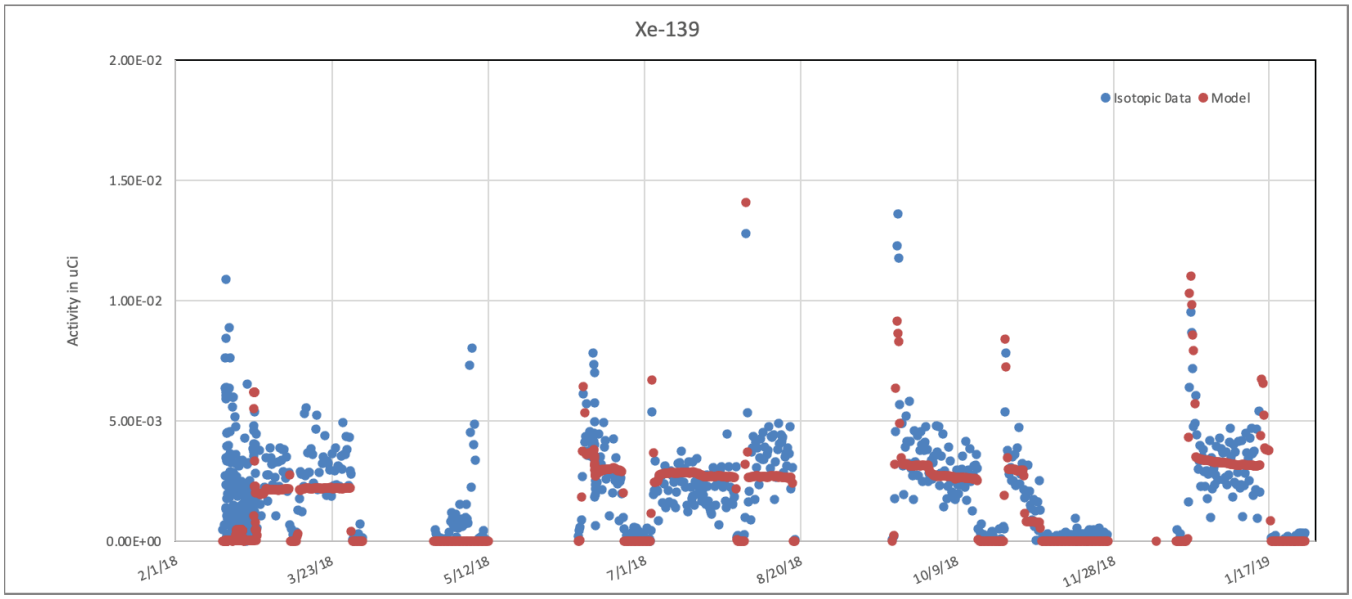

Figure B-101. Capsule 5, Xenon-139 Isotopic data and the best fit model.

Transport Volume Fit, Capsule 1:

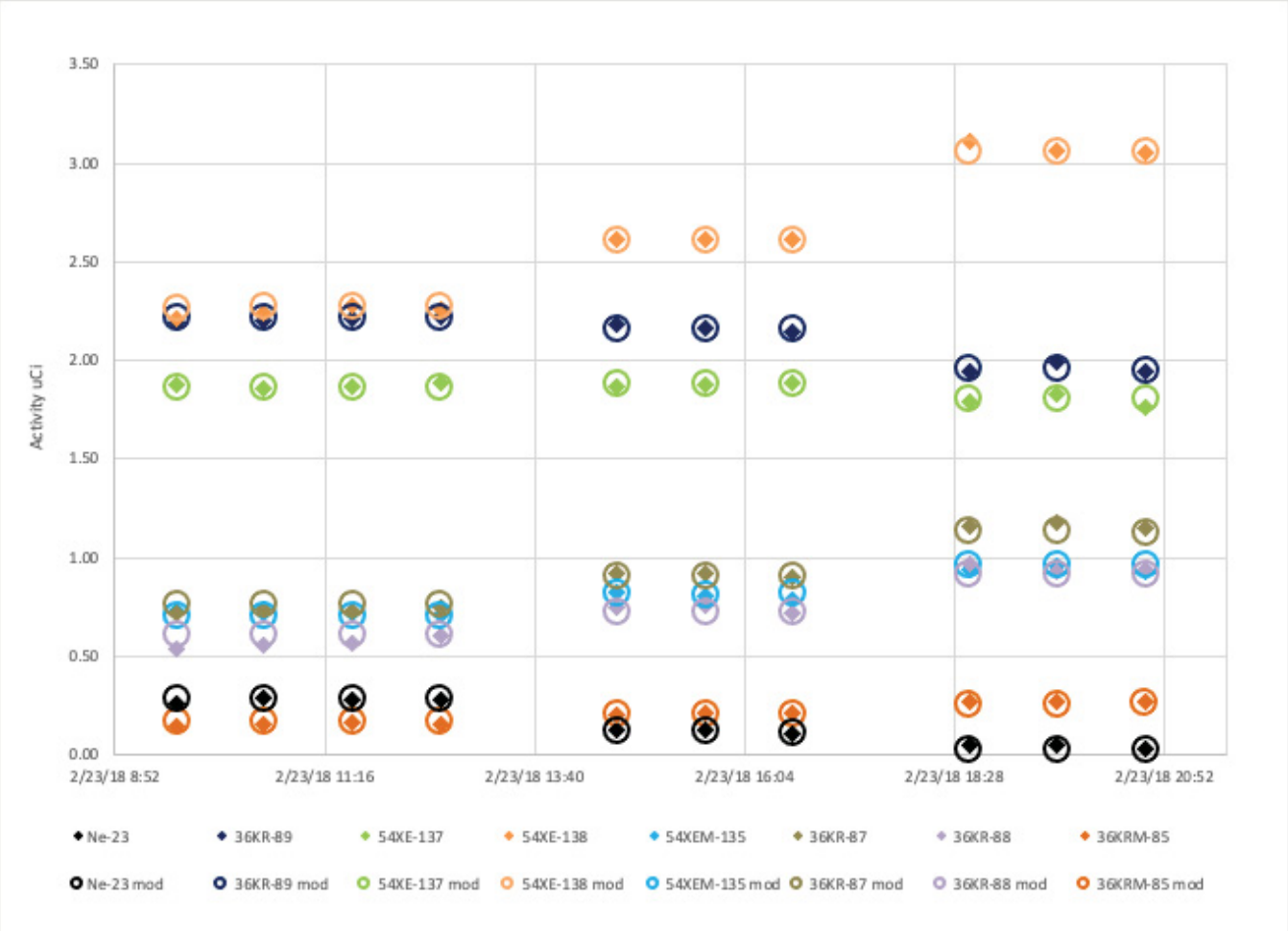

Figure B-102. Capsule 1, Isotopic data and model for 3 flow rates obtained during the initial lead out flow testing during cycle 162B.

For the legend in Figures 103-112, Parameter A means the data used to determine the transport volumes was collected during cycle 162B and consisted of a series of 20-minute measurements with flow step changes. Parameter B means the data used to determine the transport volumes was collected during cycle 164A and 164B with nominal flow and 8-hour standard run times. Parameters A and B were then used to calculate release rates for a time period during cycle 168A. For isotopes that have half-lives' that are near or greater than that of 14.1 minutes, Parameters A and B exhibit minimal differences in calculated release rate activity even though the transport volumes are different (Table A-1).

B1. Comparison of AGR-5/6/7 Transport Volumes

	AGR-5/6/7 Transport Volumes (CC)	
Transport Volumes Determined During:	Cycle 162B (Parameter A)	Cycle 164A and 164B (Parameter B)
Capsule 1	240 ± 13	240 ± 13*
Capsule 2	279 ± 18	282 ± 13
Capsule 3	169 ± 30	317 ± 07
Capsule 4	183 ± 26	293 ± 04
Capsule 5	240 ± 13	282 ± 23

*Capsule 1 Transport Volume was not determined using cycle 164A and 164B data therefore cycle 162B transport volume value is repeated and is used in the release rate calculated for the AGR-5/6/7 experiment.

For Kr-89, parameter B over predicted the release rate relative to parameter A for capsules 3,4 and 5 however; parameter B was consistent with parameter A in capsule 2. The same trend is observed for Kr-90, Xe-137 and Xe-139 all of which have half-lives less than 14.1 minutes. The test was not applied to capsule one during cycle 168A as the capsule was primarily isolated. This minimalistic check seems to imply that for the larger volume capsules the transport volume determination may have minimalistic impact on longer lived isotopes of interest. Transport volume determination and diffusion will play a drastic role in determination of release rates for shorter lived isotopes. For larger capsules the transport volume experiment detailed in Section 7.3 may not need to be performed as accurate transport volume data may be generated from normal run collection times.

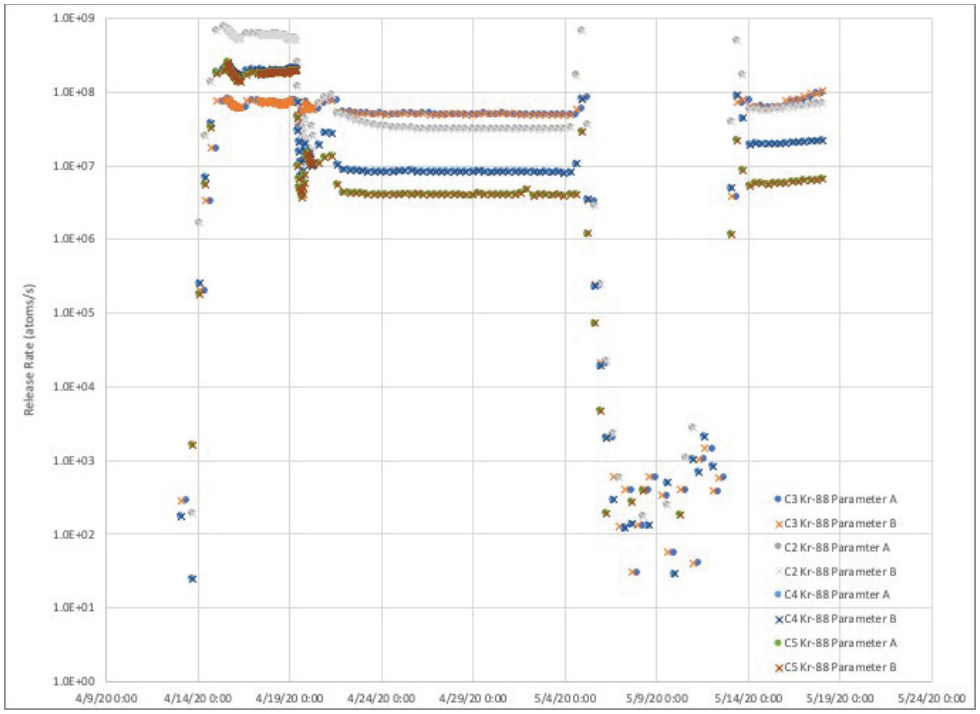

Figure B-103. A comparison of Kr-88 release data of the two test parameter time frames with the same model from Appendix A applied and compared to a data set that was not part of the model generation process.

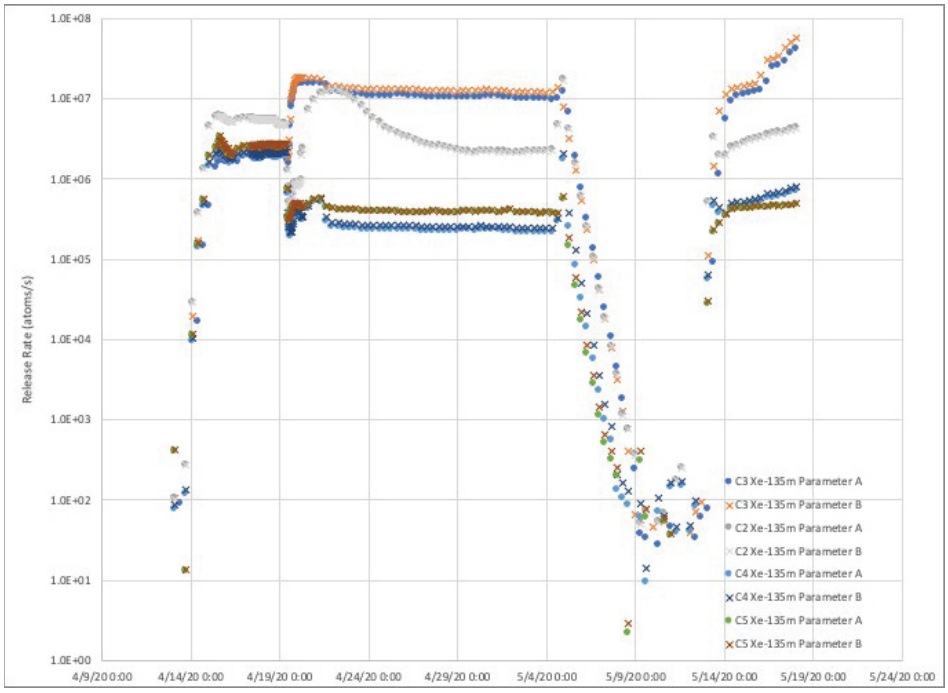

Figure B-104. A comparison of Xe-135m release data of the two test parameter time frames with the same model from Appendix A applied and compared to a data set that was not part of the model generation process.

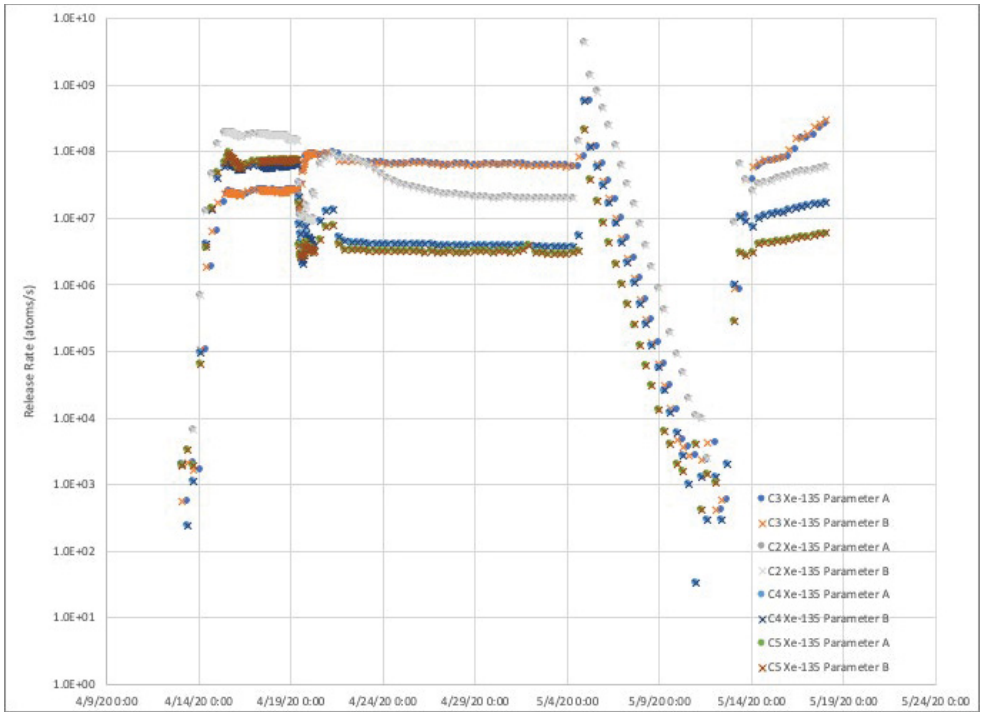

Figure B-105. A comparison of Xe-135 release data of the two test parameter time frames with the same model from Appendix A applied and compared to a data set that was not part of the model generation process.

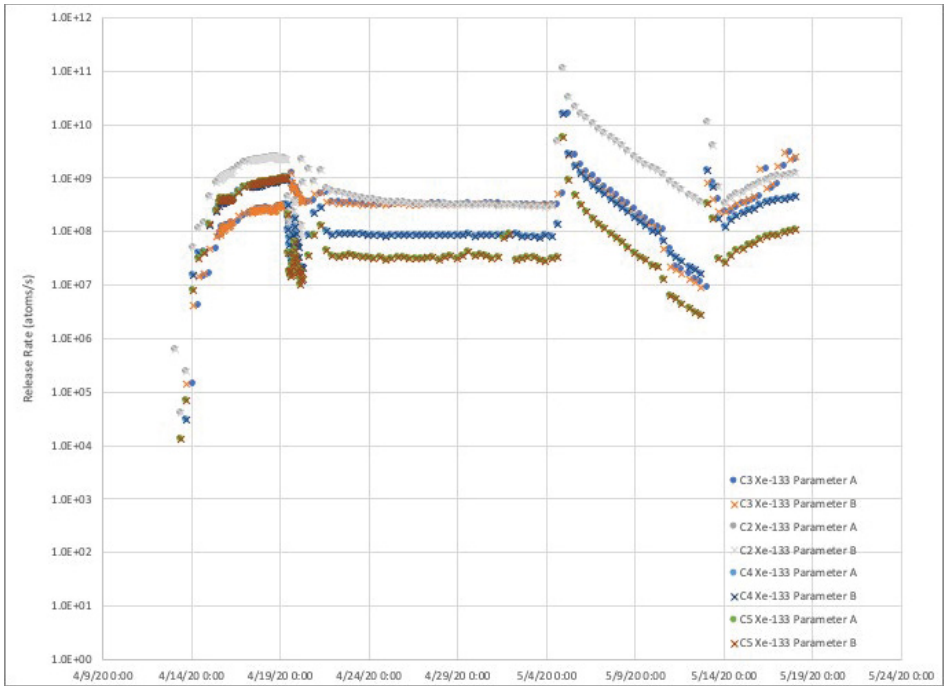

Figure B-106. A comparison of Xe-133 release data of the two test parameter time frames with the same model from Appendix A applied and compared to a data set that was not part of the model generation process.

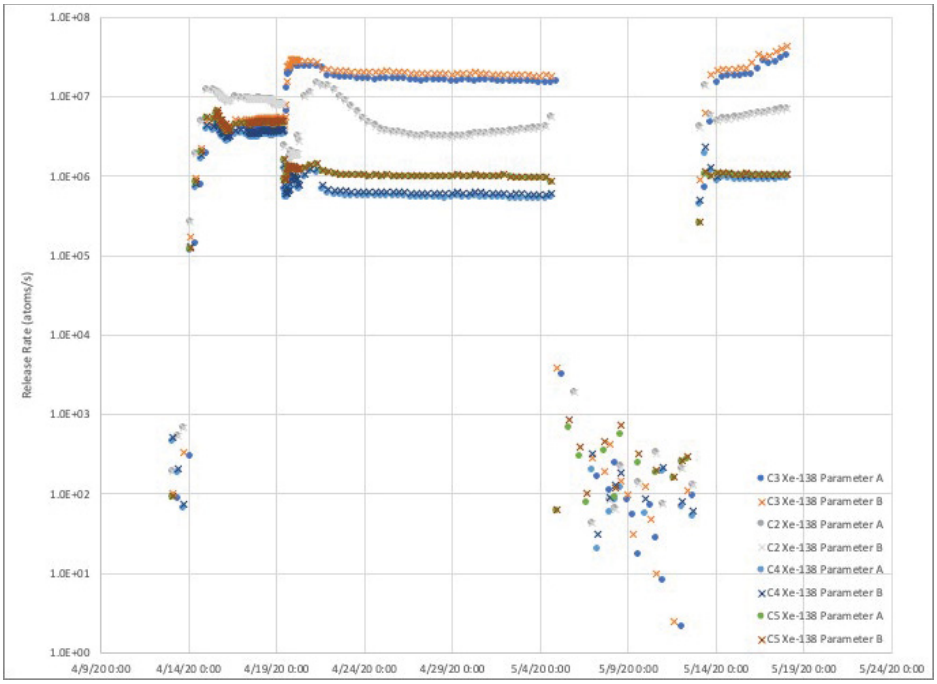

Figure B-107. A comparison of Xe-138 release data of the two test parameter time frames with the same model from Appendix A applied and compared to a data set that was not part of the model generation process.

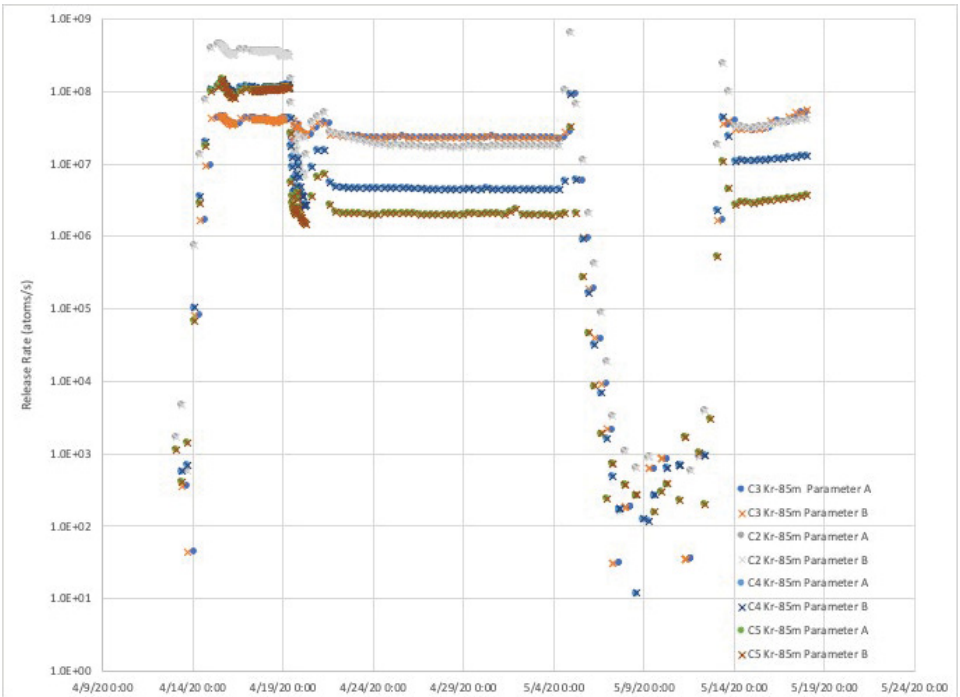

Figure B-108. A comparison of Kr-85m release data of the two test parameter time frames with the same model from Appendix A applied and compared to a data set that was not part of the model generation process.

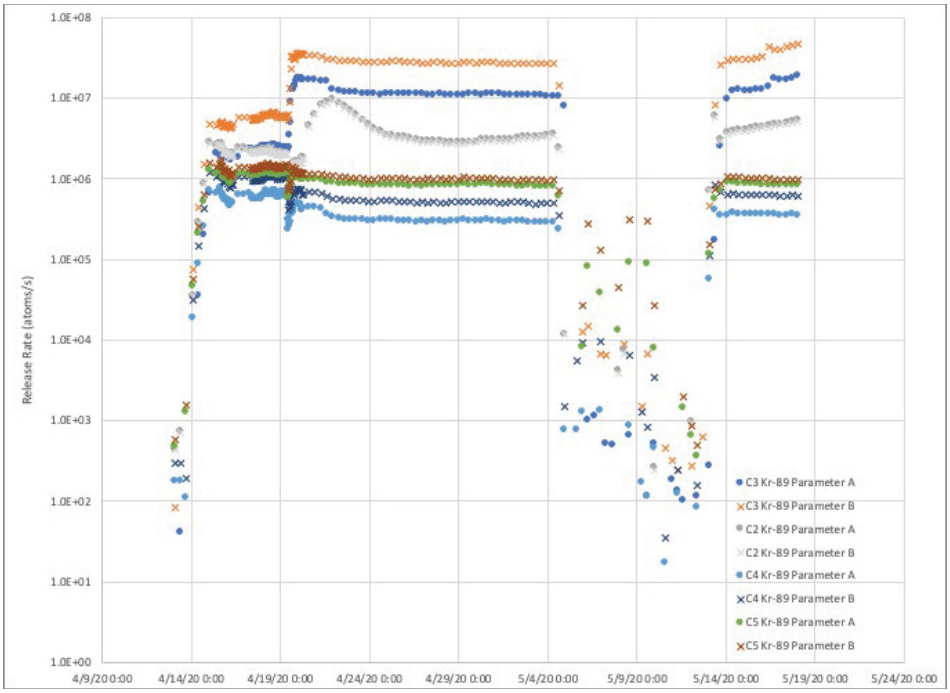

Figure B-109. A comparison of Kr-89 release data of the two test parameter time frames with the same model from Appendix A applied and compared to a data set that was not part of the model generation process.

Figure B-110. A comparison of Kr-90 release data of the two test parameter time frames with the same model from Appendix A applied and compared to a data set that was not part of the model generation process.

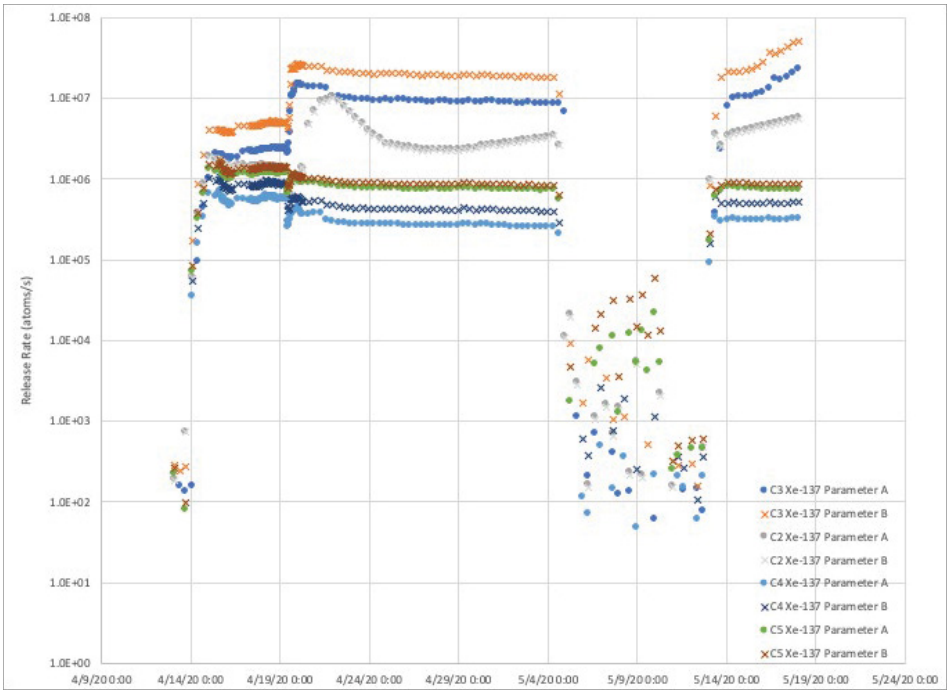

Figure B-111. A comparison of Xe-137 release data of the two test parameter time frames with the same model from Appendix A applied and compared to a data set that was not part of the model generation process.

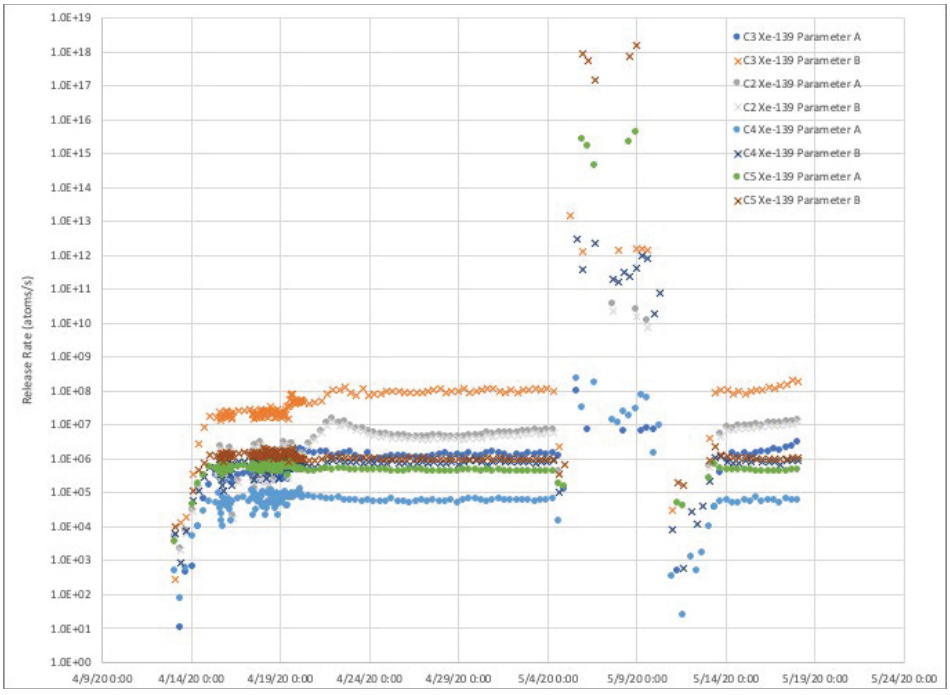

Figure B-112. A comparison of Xe-139 release data of the two test parameter time frames with the same model from Appendix A applied and compared to a data set that was not part of the model generation process.

Appendix C

The Relationship between A_a and A_v

A_a =activity of isotope in sample volume (Bq/sample)

A_V=activity of isotope entering sample volume per cc (Bq/cc)

To find the Activity in the sample volume, integrate the activity rate (Bq/sec) entering the sample volume from t=0 (when the gas enters) to t=t_{exit} (when the gas leaves).

$$A_a = \int_0^{t_{exit}} A_{sec} \cdot e^{-\lambda t} dt$$

Where:

A_{sec} = activity per second of gas entering sample volume (Bq/sec)

$$A_{sec} = A_v \cdot f \text{ and } t_{exit} = \frac{V_s}{f}$$

Where F =actual capsule flow (cc/s), t = the time fission gas is in the sample trap and Vs is the sample trap volume.

Therefore:

$$A_a = \int_0^{\frac{V_s}{f}} A_v \cdot f \cdot e^{-\lambda t} dt$$

$$A_a = \frac{A_v \cdot f}{\lambda} \left[1 - e^{\frac{-\lambda V_s}{f}} \right]$$

A_a is measured with FPM detectors.

Appendix D

Sample Input Birthrate Files

BY AGR-567 CAPSULE (atoms/sec)

ATR Cycle	Standard Date	Time Step	Step (day)	Capsule no.	Kr-85m (a/sec)	Kr-87 (a/sec)	Kr-88 (a/sec)	Kr-89 (a/sec)	Kr-90 (a/sec)	Xe-131m (a/sec)	Xe-133 (a/sec)	Xe-135 (a/sec)	Xe-135m (a/sec)	Xe-137 (a/sec)	Xe-138 (a/sec)	Xe-139 (a/sec)
168A	04/13/20	1	0.008	1	8.2537E+10	2.5254E+11	3.7461E+11	4.9077E+11	4.7567E+11	1.6237E+13	2.2114E-13	2.7486E+10	3.3824E+10	7.2244E+11	7.5688E+11	5.8945E+11
168A	04/13/20	1	0.008	2	2.4812E+10	7.3957E+10	1.0946E+11	1.4048E+11	1.3577E+11	5.3576E+12	6.7720E-12	1.2527E+10	1.5391E+10	2.5737E+11	2.5803E+11	1.9744E+11
168A	04/13/20	1	0.008	3	1.8839E+10	5.6275E+10	8.3281E+10	1.0705E+11	1.0352E+11	3.9028E+12	4.9187E-12	9.2769E+09	1.1367E+10	1.9394E+11	1.9500E+11	1.4947E+11
168A	04/13/20	1	0.008	4	1.6791E+10	5.0338E+10	7.4558E+10	9.6142E+10	9.2949E+10	3.8427E+12	4.9614E-12	7.8236E+09	9.6411E+09	1.6752E+11	1.6943E+11	1.3005E+11
168A	04/13/20	1	0.008	5	1.8428E+10	5.6462E+10	8.3779E+10	1.0988E+11	1.0649E+11	4.0229E+12	5.5411E-12	5.9498E+09	7.3509E+09	1.5915E+11	1.6723E+11	1.3034E+11
168A	04/14/20	2	1.000	1	4.3520E+12	8.6577E+12	1.2220E+13	1.5300E+13	1.5161E+13	5.3622E+09	7.8593E-12	1.4128E+13	3.4959E+12	2.3671E+13	2.3616E+13	1.8808E+13
168A	04/14/20	2	1.000	2	1.3226E+12	2.5724E+12	3.6196E+12	4.4488E+12	4.3907E+12	2.0362E+09	2.8650E-12	5.2272E+12	1.3779E+12	8.5444E+12	8.1742E+12	6.3910E+12
168A	04/14/20	2	1.000	3	1.0100E+12	1.9682E+12	2.7693E+12	3.4086E+12	3.3666E+12	1.5318E+09	2.1682E-12	3.9523E+12	1.0357E+12	6.4723E+12	6.2090E+12	4.8637E+12
168A	04/14/20	2	1.000	4	9.0188E+11	1.7630E+12	2.4831E+12	3.0652E+12	3.0270E+12	1.3275E+09	1.8739E-12	3.4092E+12	8.8933E+11	5.5991E+12	5.4025E+12	4.2381E+12
168A	04/14/20	2	1.000	5	9.9285E+11	1.9773E+12	2.7920E+12	3.4989E+12	3.4667E+12	1.2168E+09	1.7684E-12	3.1758E+12	7.8383E+11	5.3294E+12	5.3320E+12	4.2491E+12
168A	04/15/20	3	1.000	1	8.6580E+12	1.7204E+13	2.4276E+13	3.0392E+13	3.0116E+13	1.9784E+10	2.5847E-13	3.5163E+13	8.2353E+12	4.7023E+13	4.6913E+13	3.7362E+13
168A	04/15/20	3	1.000	2	2.6504E+12	5.1497E+12	7.2438E+12	8.9035E+12	8.7881E+12	7.5715E+09	9.4369E-12	1.3038E+13	3.2244E+12	1.7094E+13	1.6355E+13	1.2790E+13
168A	04/15/20	3	1.000	3	2.0324E+12	3.9563E+12	5.5649E+12	6.8494E+12	6.7657E+12	5.7253E+09	7.1617E-12	9.8974E+12	2.4360E+12	1.3007E+13	1.2479E+13	9.7762E+12
168A	04/15/20	3	1.000	4	1.8516E+12	3.6160E+12	5.0914E+12	6.2853E+12	6.2075E+12	4.9643E+09	6.2673E-12	8.6736E+12	2.1282E+12	1.1472E+13	1.1072E+13	8.6868E+12
168A	04/15/20	3	1.000	5	2.0705E+12	4.1191E+12	5.8145E+12	7.2865E+12	7.2196E+12	4.5465E+09	5.9865E-12	8.2088E+12	1.9221E+12	1.1096E+13	1.1101E+13	8.8472E+12

Appendix E

Sample FP_PostProc Output Files

Release

Program "FP_	AGR-5/6/7 Cycle 162B or later: capsule 5: Vt / unc (in SCC) = 282 / 23												
SPEC ID	Date Time	elapsed	<flow>	n	36KRM-85	%err	36KR-87	%err	36KR-88	%err	36KR-89	%err	36KR-90
R5200413010	4/13/20 1:08	28800	0.726	-96	1.13E+03	142.8	2.30E+02	474.1	-2.87E+02	625.9	5.78E+02	123.6	-1.43E+05
R5200413090	4/13/20 9:08	28800	0.723	-96	4.01E+02	397.8	-4.61E+02	233.8	-2.33E+02	770	-1.57E+02	524.6	-5.41E+04
R5200413170	4/13/20 17:09	28800	0.725	-96	1.40E+03	122.4	-5.96E+02	190.3	1.57E+03	114.2	1.56E+03	67.9	5.64E+03
R5200414010	4/14/20 1:09	28800	0.763	-96	6.79E+04	7.1	1.00E+05	6.1	1.82E+05	7.6	5.62E+04	12.6	2.20E+05
R5200414090	4/14/20 9:10	28800	0.803	-97	2.78E+06	5.4	2.25E+06	5.3	5.57E+06	5.3	2.54E+05	11.7	9.72E+05
R5200414170	4/14/20 17:10	28800	0.826	-97	1.76E+07	5.3	1.14E+07	5.3	3.22E+07	5.3	6.32E+05	11.4	1.24E+06
R5200415010	4/15/20 1:10	28800	0.839	-97	9.87E+07	5.3	5.96E+07	5.3	1.76E+08	5.3	1.55E+06	11.3	2.42E+06
R5200415090	4/15/20 9:11	15194	0.843	-50	1.11E+08	5.3	6.08E+07	5.3	1.89E+08	5.3	1.38E+06	11.2	1.38E+06
R5200415130	4/15/20 13:25	3600	0.852	-13	1.28E+08	5.3	7.17E+07	5.3	2.19E+08	5.3	1.53E+06	11.2	2.39E+06
R5200415140	4/15/20 14:25	3600	0.847	-13	1.46E+08	5.3	8.15E+07	5.3	2.50E+08	5.3	1.69E+06	11.2	2.82E+06
R5200415150	4/15/20 15:25	3600	0.845	-13	1.33E+08	5.3	7.36E+07	5.3	2.27E+08	5.3	1.56E+06	11.2	4.43E+06
R5200415160	4/15/20 16:26	3600	0.841	-12	1.24E+08	5.3	6.92E+07	5.3	2.13E+08	5.3	1.47E+06	11.3	4.96E+06
R5200415170	4/15/20 17:26	3600	0.837	-12	1.22E+08	5.3	6.86E+07	5.3	2.10E+08	5.3	1.42E+06	11.3	1.44E+06
R5200415180	4/15/20 18:27	3600	0.832	-12	1.14E+08	5.3	6.22E+07	5.3	1.92E+08	5.3	1.27E+06	11.4	4.83E+06
R5200415190	4/15/20 19:27	3600	0.826	-12	1.11E+08	5.3	5.97E+07	5.3	1.88E+08	5.3	1.25E+06	11.5	1.96E+06
R5200415200	4/15/20 20:27	3600	0.822	-12	1.12E+08	5.3	6.02E+07	5.3	1.88E+08	5.3	1.33E+06	11.5	4.92E+06
R5200415210	4/15/20 21:28	3600	0.817	-12	1.01E+08	5.3	5.49E+07	5.3	1.74E+08	5.3	1.25E+06	11.6	2.17E+06
R5200415220	4/15/20 22:28	3600	0.813	-12	9.89E+07	5.3	5.35E+07	5.3	1.67E+08	5.3	1.25E+06	11.6	2.02E+06
R5200415230	4/15/20 23:29	3600	0.809	-12	9.35E+07	5.3	5.10E+07	5.3	1.58E+08	5.3	1.25E+06	11.8	1.06E+06

B_Int

Program "FP	AGR-5/6/7 Cycle 162B or later: capsule 5: Vt / unc (in SCC) = 282 / 23														
SPEC ID	Date Time	elapsed	day	36KRM-85	36KR-87	36KR-88	36KR-89	36KR-90	54XEM-131	54XE-133	54XE-135	54XEM-135	54XE-137	54XE-138	54XE-139
R5200413170	4/13/20 17:09	28800	18366.1	7.63E+11	1.52E+12	2.15E+12	2.70E+12	2.68E+12	9.49E+11	2.66E+12	2.43E+12	6.01E+11	4.11E+12	4.12E+12	3.28E+12
R5200414010	4/14/20 1:09	28800	18366.5	1.22E+12	2.44E+12	3.44E+12	4.31E+12	4.27E+12	1.93E+09	2.67E+12	4.26E+12	1.03E+12	6.57E+12	6.57E+12	5.24E+12
R5200414090	4/14/20 9:10	28800	18366.8	1.58E+12	3.15E+12	4.45E+12	5.58E+12	5.53E+12	3.04E+09	4.08E+12	5.94E+12	1.41E+12	8.49E+12	8.50E+12	6.77E+12
R5200414170	4/14/20 17:10	28800	18367.1	1.94E+12	3.87E+12	5.46E+12	6.84E+12	6.78E+12	4.15E+09	5.49E+12	7.61E+12	1.79E+12	1.04E+13	1.04E+13	8.30E+12
R5200415010	4/15/20 1:10	28800	18367.5	2.07E+12	4.12E+12	5.82E+12	7.29E+12	7.22E+12	5.52E+09	6.75E+12	8.61E+12	2.00E+12	1.11E+13	1.11E+13	8.85E+12
R5200415090	4/15/20 9:11	15194	18367.7	2.07E+12	4.12E+12	5.82E+12	7.29E+12	7.22E+12	6.67E+09	7.66E+12	9.09E+12	2.08E+12	1.11E+13	1.11E+13	8.85E+12
R5200415130	4/15/20 13:25	3600	18367.8	2.07E+12	4.12E+12	5.82E+12	7.29E+12	7.22E+12	7.16E+09	8.05E+12	9.29E+12	2.12E+12	1.11E+13	1.11E+13	8.85E+12
R5200415140	4/15/20 14:25	3600	18367.9	2.07E+12	4.12E+12	5.82E+12	7.29E+12	7.22E+12	7.35E+09	8.20E+12	9.37E+12	2.13E+12	1.11E+13	1.11E+13	8.85E+12
R5200415150	4/15/20 15:25	3600	18367.9	2.07E+12	4.12E+12	5.82E+12	7.29E+12	7.22E+12	7.54E+09	8.34E+12	9.44E+12	2.15E+12	1.11E+13	1.11E+13	8.85E+12
R5200415160	4/15/20 16:26	3600	18368	2.07E+12	4.12E+12	5.82E+12	7.29E+12	7.22E+12	7.73E+09	8.49E+12	9.52E+12	2.16E+12	1.11E+13	1.11E+13	8.85E+12
R5200415170	4/15/20 17:26	3600	18368	2.07E+12	4.12E+12	5.82E+12	7.29E+12	7.22E+12	7.92E+09	8.64E+12	9.60E+12	2.18E+12	1.11E+13	1.11E+13	8.85E+12
R5200415180	4/15/20 18:27	3600	18368	2.07E+12	4.12E+12	5.82E+12	7.29E+12	7.23E+12	8.11E+09	8.79E+12	9.68E+12	2.19E+12	1.11E+13	1.11E+13	8.85E+12
R5200415190	4/15/20 19:27	3600	18368.1	2.07E+12	4.12E+12	5.82E+12	7.29E+12	7.23E+12	8.30E+09	8.94E+12	9.76E+12	2.20E+12	1.11E+13	1.11E+13	8.85E+12
R5200415200	4/15/20 20:27	3600	18368.1	2.08E+12	4.12E+12	5.82E+12	7.29E+12	7.23E+12	8.49E+09	9.09E+12	9.83E+12	2.22E+12	1.11E+13	1.11E+13	8.85E+12
R5200415210	4/15/20 21:28	3600	18368.2	2.08E+12	4.12E+12	5.82E+12	7.29E+12	7.23E+12	8.68E+09	9.24E+12	9.91E+12	2.23E+12	1.11E+13	1.11E+13	8.85E+12
R5200415220	4/15/20 22:28	3600	18368.2	2.08E+12	4.12E+12	5.82E+12	7.29E+12	7.23E+12	8.87E+09	9.39E+12	9.99E+12	2.25E+12	1.11E+13	1.11E+13	8.85E+12
R5200415230	4/15/20 23:29	3600	18368.2	2.08E+12	4.12E+12	5.82E+12	7.29E+12	7.23E+12	9.06E+09	9.54E+12	1.01E+13	2.26E+12	1.11E+13	1.11E+13	8.86E+12
R5200416000	4/16/20 0:29	3600	18368.3	2.08E+12	4.13E+12	5.82E+12	7.30E+12	7.23E+12	9.24E+09	9.61E+12	1.01E+13	2.26E+12	1.11E+13	1.11E+13	8.86E+12

Ratio

Program "FP_Post	AGR-5/6/7 Cycle 162B or later: capsule 5: Vt / unc (in SCC) = 282 / 23												
SPEC ID	Date Time	elapsed	<flow>	n	36KRM-85	%err	36KR-87	%err	36KR-88	%err	36KR-89	%err	36KR-90
R52004131700	4/13/20 17:09	28800	0.725	-96	1.83E-09	122.4	-3.91E-10	190.3	7.31E-10	114.2	5.78E-10	67.9	2.11E-09
R52004140100	4/14/20 1:09	28800	0.763	-96	5.54E-08	7.5	4.11E-08	6.6	5.30E-08	8	1.30E-08	12.8	5.16E-08
R52004140900	4/14/20 9:10	28800	0.803	-97	1.76E-06	5.9	7.13E-07	5.9	1.25E-06	5.9	4.56E-08	11.9	1.76E-07
R52004141700	4/14/20 17:10	28800	0.826	-97	9.06E-06	5.9	2.95E-06	5.8	5.90E-06	5.8	9.24E-08	11.7	1.83E-07
R52004150100	4/15/20 1:10	28800	0.839	-97	4.76E-05	5.9	1.45E-05	5.9	3.02E-05	5.8	2.13E-07	11.5	3.35E-07
R52004150900	4/15/20 9:11	15194	0.843	-50	5.35E-05	5.9	1.48E-05	5.9	3.25E-05	5.8	1.90E-07	11.5	1.91E-07
R52004151300	4/15/20 13:25	3600	0.852	-13	6.19E-05	5.9	1.74E-05	5.9	3.76E-05	5.8	2.10E-07	11.4	3.31E-07
R52004151400	4/15/20 14:25	3600	0.847	-13	7.06E-05	5.9	1.98E-05	5.8	4.30E-05	5.8	2.32E-07	11.5	3.91E-07
R52004151500	4/15/20 15:25	3600	0.845	-13	6.39E-05	5.9	1.78E-05	5.8	3.91E-05	5.8	2.14E-07	11.5	6.13E-07
R52004151600	4/15/20 16:26	3600	0.841	-12	5.96E-05	5.9	1.68E-05	5.8	3.66E-05	5.8	2.02E-07	11.6	6.87E-07
R52004151700	4/15/20 17:26	3600	0.837	-12	5.86E-05	5.9	1.66E-05	5.9	3.62E-05	5.8	1.95E-07	11.6	2.00E-07
R52004151800	4/15/20 18:27	3600	0.832	-12	5.47E-05	5.9	1.51E-05	5.9	3.30E-05	5.8	1.74E-07	11.7	6.69E-07
R52004151900	4/15/20 19:27	3600	0.826	-12	5.33E-05	5.9	1.45E-05	5.9	3.22E-05	5.8	1.72E-07	11.7	2.71E-07
R52004152000	4/15/20 20:27	3600	0.822	-12	5.42E-05	5.9	1.46E-05	5.8	3.23E-05	5.8	1.83E-07	11.8	6.81E-07
R52004152100	4/15/20 21:28	3600	0.817	-12	4.87E-05	5.8	1.33E-05	5.8	2.98E-05	5.8	1.71E-07	11.8	3.00E-07
R52004152200	4/15/20 22:28	3600	0.813	-12	4.76E-05	5.9	1.30E-05	5.9	2.86E-05	5.8	1.71E-07	11.9	2.79E-07
R52004152300	4/15/20 23:29	3600	0.809	-12	4.50E-05	5.9	1.24E-05	5.8	2.72E-05	5.8	1.72E-07	12.1	1.46E-07
R52004160000	4/16/20 0:29	3600	0.805	-12	4.42E-05	5.8	1.21E-05	5.8	2.67E-05	5.8	1.61E-07	12	7.94E-07
R52004160100	4/16/20 1:30	3600	0.803	-13	4.60E-05	5.9	1.26E-05	5.8	2.78E-05	5.8	1.73E-07	12	5.20E-07
R52004160200	4/16/20 2:30	3600	0.8	-13	4.05E-05	5.8	1.12E-05	5.8	2.45E-05	5.8	1.56E-07	12	6.44E-07

Appendix F

FP_PostProc Constants Text File

```
'Decay Constants'
36KRM-85    4.297788E-05   KR 85M
36KR-87     1.514083E-04   KR 87
36KR-88     6.779609E-05   KR 88
36KR-89     3.667445E-03   KR 89
36KR-90     2.144639E-02   KR 90
54XEM-131   6.722421E-07   XE131M
54XE-133    1.530142E-06   XE133
54XE-135    2.106574E-05   XE135
54XEM-135   7.550623E-04   XE135M
54XE-137    3.024202E-03   XE137
54XE-138    8.193229E-04   XE138
54XE-139    1.745963E-02   XE139

'Sample Volume'
58 3

'Birth Percent Uncertainty'
2.5

'I-135 Constants'
lambda          2.931e-5        per sec
br_Xe135M       16.4            percent
```

Appendix G

Sample Flow Data

	Standard_Da	Standard_Da	Capsule_1	Capsule_2	Capsule_3	Capsule_4	Capsule_5
1	12Apr2020:0	12Apr2020:0	-0.018	50.972	46.013	45.722	43.141
2	12Apr2020:0	12Apr2020:0	-0.018	50.987	46	45.735	43.066
3	12Apr2020:0	12Apr2020:0	-0.018	50.968	45.992	45.73	43.09
4	12Apr2020:0	12Apr2020:0	-0.018	50.98	46.008	45.731	43.086
5	12Apr2020:0	12Apr2020:0	-0.018	51.002	46.03	45.753	43.133
6	12Apr2020:0	12Apr2020:0	-0.018	51.013	46.017	45.744	43.131
7	12Apr2020:0	12Apr2020:0	-0.018	51.006	46.039	45.742	43.131
8	12Apr2020:0	12Apr2020:0	-0.018	51.022	46.051	45.767	43.109
9	12Apr2020:0	12Apr2020:0	-0.018	51.042	46.068	45.776	43.18
10	12Apr2020:0	12Apr2020:0	-0.018	51.054	46.068	45.784	43.155
11	12Apr2020:0	12Apr2020:0	-0.018	51.061	46.079	45.785	43.149
12	12Apr2020:0	12Apr2020:0	-0.018	51.051	46.098	45.785	43.18
13	12Apr2020:0	12Apr2020:0	-0.018	51.051	46.094	45.786	43.216
14	12Apr2020:0	12Apr2020:0	-0.018	51.066	46.077	45.785	43.19
15	12Apr2020:0	12Apr2020:0	-0.018	51.058	46.046	45.785	43.153
16	12Apr2020:0	12Apr2020:0	-0.018	51.067	46.061	45.783	43.188
17	12Apr2020:1	12Apr2020:1	-0.018	51.07	46.061	45.773	43.156
18	12Apr2020:1	12Apr2020:1	-0.018	51.06	46.058	45.776	43.184
19	12Apr2020:1	12Apr2020:1	-0.018	51.076	46.059	45.781	43.177
20	12Apr2020:1	12Apr2020:1	-0.018	51.096	46.085	45.79	43.187
21	12Apr2020:1	12Apr2020:1	-0.018	51.084	46.073	45.789	43.149
22	12Apr2020:1	12Apr2020:1	-0.018	51.091	46.082	45.792	43.215
23	12Apr2020:1	12Apr2020:1	-0.018	51.097	46.079	45.792	43.228
24	12Apr2020:1	12Apr2020:1	-0.018	51.107	46.098	45.814	43.186
25	12Apr2020:1	12Apr2020:1	-0.018	51.099	46.109	45.816	43.236
26	12Apr2020:1	12Apr2020:1	-0.018	51.11	46.121	45.818	43.261
27	12Apr2020:1	12Apr2020:1	-0.018	51.126	46.103	45.819	43.255
28	12Apr2020:1	12Apr2020:1	-0.018	51.046	46.067	45.757	43.172
29	12Apr2020:1	12Apr2020:1	-0.018	50.403	45.538	45.169	42.558
30	12Apr2020:1	12Apr2020:1	-0.018	50.129	45.317	44.976	42.335
31	12Apr2020:1	12Apr2020:1	-0.018	50.295	45.432	45.103	42.48
32	12Apr2020:1	12Apr2020:1	-0.018	50.448	45.54	45.246	42.62
33	12Apr2020:1	12Apr2020:1	-0.018	50.597	45.659	45.371	42.765
34	12Apr2020:1	12Apr2020:1	-0.018	50.727	45.778	45.475	42.859
35	12Apr2020:1	12Apr2020:1	-0.018	50.83	45.87	45.571	42.964
36	12Apr2020:1	12Apr2020:1	-0.018	50.909	45.953	45.646	43.061
37	12Apr2020:1	12Apr2020:1	-0.018	50.988	46.001	45.727	43.116
38	12Apr2020:1	12Apr2020:1	-0.018	51.039	46.045	45.76	43.163
39	12Apr2020:1	12Apr2020:1	-0.018	51.084	46.084	45.811	43.2
40	12Apr2020:1	12Apr2020:1	-0.018	51.129	46.109	45.828	43.234
41	12Apr2020:1	12Apr2020:1	-0.018	51.143	46.133	45.85	43.279
42	12Apr2020:1	12Apr2020:1	-0.018	51.183	46.165	45.883	43.281
43	12Apr2020:1	12Apr2020:1	-0.018	51.19	46.166	45.898	43.301

Appendix H

Summary R/B Table for the Fission Gas Isotope for all cycles of the AGR-5/6/7 Irradiation

Isotope	Half-life (min)	Measured R/B			Uncertainty [a] (%)		
		Average	Minimum	Maximum	Average	Minimum	Maximum
Kr-85m	268.7	1.10E-05	2.15E-10	9.81E-04	6.7	5.8	49.5
Kr-88	170.4	4.22E-06	5.60E-10	3.40E-04	6.4	5.8	24.6
Kr-87	76.0	7.80E-06	7.35E-11	7.00E-04	6.7	5.8	46.1
Kr-89	3.2	6.74E-07	5.74E-10	2.86E-05	9.5	5.8	48.4
Kr-90	0.5	1.21E-05	3.02E-09	5.89E-04	32.0	10.6	49.7
Xe-131m	17162.0	2.07E-02	6.14E-06	1.51E+00	40.1	6.4	50.0
Xe-133	7558.9	4.60E-05	4.28E-09	5.62E-03	15.6	5.9	50.0
Xe-135	545.8	3.18E-06	1.78E-11	3.55E-04	6.7	5.8	48.5
Xe-135m	15.3	1.21E-06	6.10E-10	5.53E-05	6.5	5.8	38.6
Xe-138	14.1	2.79E-07	1.61E-10	1.20E-05	8.6	5.8	48.0
Xe-137	3.8	3.57E-07	6.51E-11	1.34E-05	6.3	5.8	47.4
Xe-139	0.7	2.17E-06	3.72E-10	2.31E-04	31.1	8.2	50.0

[a] Only R/B values with uncertainty less than 50% and a standard 8-hour interval are used.